1986

A stochastic analysis of pollutant movement in groundwater

Kevin K. Wolka
Iowa State University

INFORMATION TO USERS

This reproduction was made from a copy of a manuscript sent to us for publication and microfilming. While the most advanced technology has been used to photograph and reproduce this manuscript, the quality of the reproduction is heavily dependent upon the quality of the material submitted. Pages in any manuscript may have indistinct print. In all cases the best available copy has been filmed.

The following explanation of techniques is provided to help clarify notations which may appear on this reproduction.

1. Manuscripts may not always be complete. When it is not possible to obtain missing pages, a note appears to indicate this.

2. When copyrighted materials are removed from the manuscript, a note appears to indicate this.

3. Oversize materials (maps, drawings, and charts) are photographed by sectioning the original, beginning at the upper left hand corner and continuing from left to right in equal sections with small overlaps. Each oversize page is also filmed as one exposure and is available, for an additional charge, as a standard 35mm slide or in black and white paper format.*

4. Most photographs reproduce acceptably on positive microfilm or microfiche but lack clarity on xerographic copies made from the microfilm. For an additional charge, all photographs are available in black and white standard 35mm slide format.*

***For more information about black and white slides or enlarged paper reproductions, please contact the Dissertations Customer Services Department.**

Wolka, Kevin K.

A STOCHASTIC ANALYSIS OF POLLUTANT MOVEMENT IN GROUNDWATER

Iowa State University PH.D. 1986

A stochastic analysis of pollutant movement in groundwater

by

Kevin K. Wolka

A Dissertation Submitted to the
Graduate Faculty in Partial Fulfillment of the
Requirements for the Degree of
DOCTOR OF PHILOSOPHY

Department: Civil Engineering
Major: Water Resources

Approved:

Signature was redacted for privacy.

In Charge of Major Work

Signature was redacted for privacy.

For the Major Department

Signature was redacted for privacy.

For the Graduate College

Iowa State University
Ames, Iowa

1986

TABLE OF CONTENTS

LIST OF TABLES

LIST OF FIGURES

I. INTRODUCTION

Hazardous or toxic chemical spills, leakage from sanitary landfills and underground disposal of waste by injection wells are but a few of the many occurrences which could result in pollution of groundwater systems. Decision makers in groundwater contamination situations often ask the engineer to provide information concerning the effect of these occurrences on groundwater quality in the area surrounding the location of contamination. Such information might include a description of the short and long term effects on the groundwater quality. It might also include the effects on current and future users of the groundwater supply. In this study, the investigation of effects will be limited in scope. Specifically, an investigation will be made into the answers to the two following questions which decision makers often ask of the engineer:

1. Will the pollutant reach a specific location in a groundwater system, and if so, how soon?
2. If the answer to Question 1 above is yes, how long and at what concentration will the pollutant be present at this specified location?

In a recently released report, the U. S. Congress' Office of Technology Assessment (1984) identified four steps required to conduct a risk assessment for groundwater contamination. The four steps are:

1. hazard evaluation - identifying the pollutants and their toxic effects;

2. dose-response assessment - the specification of concentration levels and durations of exposure at which toxic effects occur at a prescribed frequency in a population;
3. exposure assessment - a determination of the magnitude and duration of exposure of a pollutant to a population; and
4. risk characterization - translation of the above three steps into a determination of health risks (presently accomplished by applying factors of safety to the dose-response relationship).

Engineers have traditionally been involved only in Step 3 of the risk assessment process, which corresponds to answering questions #1 and #2 above. Current engineering practice dictates the use of an advective-dispersive mass transport equation in a deterministic model to make an exposure assessment.

This investigation addresses the subject of expanding the exposure assessment step in groundwater contaminant risk assessment. Specific objectives of this investigation are discussed below.

A. Objective #1: Develop a Procedure Containing Stochastic Methods which Introduces Probability into the Determination of the Magnitude and Duration of Exposure of a Pollutant

The advective-dispersive mass transport equation, which determines the magnitude and duration of exposure of a pollutant, uses the best available estimates for the average values of the physical, chemical and

radioactive properties of the pollutant and the porous medium. The engineer arrives at a single deterministic solution with a specific form of the general mass transport equation. Equation I-1, for mass transport in three dimensions through a saturated medium with uniform, steady flow in the x-direction, is given as follows:

$$R_d\frac{\partial C}{\partial t} = D_x\frac{\partial^2 C}{\partial x^2} + D_y\frac{\partial^2 C}{\partial y^2} + D_z\frac{\partial^2 C}{\partial z^2} - V_x\frac{\partial C}{\partial x} - \lambda R_d C \qquad \text{(Eq. I-1)}$$

where,

C = concentration of pollutant as a function of time and space;

D_x = longitudinal dispersion coefficient;

D_y, D_z = transverse dispersion coefficients;

V_x = seepage velocity in the direction of flow along the x-axis;

λ = radioactive decay constant;

R_d = chemical retardation factor, $R_d \geq 1$;

x, y, z = cartesian coordinates; and

t = time.

The average values of the pollutant and porous medium properties introduce error into the deterministic solution. Properties of porous media actually may be quite variable from one location to another in geologic formations. Pollutants entering geologic formations rarely do so at constant rates and concentrations over time or even at the same proportional rate, if there is more than one pollutant present.

Probability will be introduced into the solution procedure in this investigation by describing the variability of pollutant and porous medium properties and solving the mass transport equation numerous times using an equivalent, but unique set of values of the pollutant and porous medium properties. The results will then be expressed as frequency histograms, and probabilities estimated for the solution.

B. Objective #2: Investigate the Effects of Variability in the Hydraulic Conductivity of a Porous Medium on the Magnitude and Duration of Exposure of a Pollutant

Hydraulic conductivity is involved in the determination of seepage velocity according to the following relationship:

$$V = - \frac{K}{n_e} \left(\frac{dh}{dl}\right) \qquad \text{(Eq. I-2)}$$

where,

V = seepage (interstitial) velocity;

K = hydraulic conductivity;

n_e = effective porosity; and

$\left(\frac{dh}{dl}\right)$ = hydraulic gradient.

Hydraulic conductivity is also involved in the determination of the dispersion coefficients because they are a function of the seepage velocity, as shown in Equation I-3 below:

$$D = \alpha V \qquad \text{(Eq. I-3)}$$

where,

D = dispersion coefficient;

α = dispersivity; and

V = seepage velocity.

Consequently, hydraulic conductivity helps in the determination of the magnitude and duration of exposure of the pollutant when the mass transport equation above is applied.

Hydraulic conductivity in a geologic formation may be extremely variable as a function of spatial location. Its quantitative value ranges over ten orders of magnitude in unconsolidated deposits from tight clays to porous gravel. In a specific geologic unit under consideration, the hydraulic conductivity often varies two orders of magnitude; therefore, the uncertainty associated with the spatial variability of hydraulic conductivity could have a significant effect on the estimated magnitude and duration of exposure of the pollutant.

This investigation incorporates the spatial variability of hydraulic conductivity into the advection-dispersion model so as to describe the distribution of occurrence of solutions. The procedure developed in the following chapters does not address the variability associated with other input variables, such as effective porosity or hydraulic gradients, or even the uncertainty associated with field tests for individual measurements of hydraulic conductivity itself.

C. Objective #3: Apply the Procedure and Model Developed from Objectives #1 and #2 above to a Documented Field Situation

Rather than selecting some idealized or hypothetical groundwater contamination event, a well-documented pollutant disposal event was sought in order to verify that the proposed procedure was workable and valid for field conditions. Data were obtained from the Idaho District, United States Geological Survey, for the disposal of radioactive and chemical wastes into the Snake River Plain aquifer on the site of the Idaho National Engineering Laboratory.

A second, synthetic disposal event was also proposed for modeling at this site. The second event would be substantially different in pollutant loading and volume flow rate patterns than the first recorded disposal event. The second disposal event results could then be compared to the results of the first disposal event, looking for similarities and dissimilarities between them.

D. Objective #4: Describe in Statistical Terms the Magnitude and Duration of Exposure Relationship from the Disposal Events

Univariate and multivariate statistical analysis techniques will be used to identify any trends, patterns or relationships in the modeling results. Specifically, probabilistic descriptions of two characteristics of pollutant movement, (1) the time of arrival of the pollutant and (2) the pollutant concentration versus duration of exposure relationship at a specific location, will be examined. The

probabilistic descriptions above provide the answers to questions #1 and #2 posed at the beginning of this chapter.

II. PREVIOUS RESEARCH

This study integrates the findings of research from several diverse but related scientific disciplines. A discussion of previous research initially addresses the hydraulic conductivity property in saturated geologic formations. Hydraulic conductivity is shown to be log-normally distributed and heterogeneous. A computer model is presented which can generate numerous hydraulic conductivity fields, all of which have the same descriptive statistical properties. A groundwater flow-mass transport model takes the hydraulic conductivity fields and generates pollutographs, allowing a time of arrival at a specified location to be calculated and a pollutant concentration versus duration of exposure relationship at a specified location to be formed. Finally, the pertinency of the pollutant concentration versus duration of exposure relationship in groundwater contaminant assessment is addressed.

A. Hydraulic Conductivity--Log-normally Distributed

In the construction of a stochastic model for pollutant transport, the hydraulic conductivity of the medium is assumed to be unknown at a specific location, with a probability density function representing variability from some mean value. Warren and Price (1961), investigating underground petroleum formations using core data and Monte Carlo techniques, concluded that flow behavior was best described by a single value of permeability (hydraulic conductivity) equal to the geometric mean of sample values. This is equivalent to concluding that

the probability of the actual value of hydraulic conductivity at a specific location is log-normally distributed around a mean value. McMillan (1966) also concluded that hydraulic conductivity was log-normally distributed using transmissibility maps of the Los Angeles basin.

Using a finite-element model, Kadi and Brutsaert (1985) investigated unsteady flow through nonuniform aquifers. They also determined that the "effective hydraulic conductivity," an equivalent uniform value which is used to replace hydraulic conductivity values in a nonuniform aquifer, is the geometric mean of sampled hydraulic conductivities. They found that this condition occurs, however, only with long flow times or large aquifers.

B. The Effects of Heterogeneity in Hydraulic Conductivity on Groundwater Flow

The porous medium can therefore be assumed isotropic, but heterogeneous with a mean value of hydraulic conductivity equal to the value used for a homogeneous medium and a variable component specified by a probability density function. Freeze (1975) made this assumption and investigated the uncertainty in hydraulic head estimates from deterministic groundwater flow equations. Using Monte Carlo techniques to model one-dimensional, steady flow in a bounded domain, he found standard deviations of hydraulic head having a relative magnitude of 30% of the head values. These results led Freeze to question the validity of the flow equations used.

Freeze's work created an uproar in groundwater research circles. Subsequent research efforts by Bakr et al. (1978), Dagan (1976) and Gelhar (1976) established that Freeze overestimated the uncertainty in hydraulic head because he assumed that the hydraulic conductivity at any point was uncorrelated with hydraulic conductivity at any other point in the porous medium. Using sophisticated mathematical techniques, these subsequent researchers theorized that the variance of hydraulic head estimates depends on the distance over which hydraulic conductivity is correlated. An order of magnitude reduction in the variance of hydraulic head was obtained by Bakr et al. (1978) for a three-dimensional flow formulation relative to the one-dimensional case of Freeze.

Expanding on the earlier work of Freeze (1975), Smith and Freeze (1979a, 1979b) correlated values of hydraulic conductivity between adjacent points in further analyses of hydraulic head variability. The modeling was accomplished in what they called a "statistically homogeneous" porous medium, i.e., one that has the same expected value at every point in the field and one in which the correlation between two points depends only on the vector between them and not on their absolute position. The correlation effect was obtained by using a "first-order nearest-neighbor model," a linear equation system which makes hydraulic conductivity at a point dependent on adjacent hydraulic conductivity values. Smith and Freeze used this model to generate a selected number of spatially-varying, correlated hydraulic conductivity fields. One

solution was obtained for each field generated. The cumulative results of all generated fields were used to determine a frequency distribution as the solution form. The investigators reached several conclusions from this work as presented below.

1. Uncertainty in hydraulic head predictions depends upon both the heterogeneity in hydraulic conductivity and the nature of the flow system operating within the porous medium.
2. In a bounded field containing nonuniform hydraulic gradients, the uncertainty in hydraulic head increases as the strength and extent of the correlation between neighboring conductivity values increase.
3. Standard deviations in hydraulic head are approximately halved in two-dimensional analysis relative to one-dimensional analysis of bounded domains.
4. In bounded, nonuniform gradient fields, total flux computed with the geometric mean hydraulic conductivity of a heterogeneous porous medium consistently underestimates the flux computed by the stochastic model.
5. Factors in the flow system in addition to correlation distance which influence hydraulic head values were the spatial variation of head gradients, the distance between flow boundaries and the arrangement of statistically homogeneous units within the flow domain.

C. The Turning Bands Method for Developing Random Heterogeneous Hydraulic Conductivity Fields

Mantoglou and Wilson (1982) developed a computer program which can generate a selected number of spatially-varying, correlated hydraulic conductivity fields. Each field may then be used to obtain one problem solution. The cumulative results of all these solutions is in the form of a frequency distribution.

Their model may replace a "first-order nearest-neighbor" solution technique, as used by Smith and Freeze (1979a, 1979b), or some similar matrix solution model in constructing spatially-varying, correlated physical property fields. A major limitation of this model is that the property of the field must be considered to be isotropic. The model cannot generate an anisotropic field. Their investigations concluded that this program was in general both less expensive to run on a computer and more accurate than other methods for isotropic fields.

The program is based on the Turning Bands Method (TBM), a procedure first developed by French engineers in order to maximize underground mining efficiency by recommending which locations were most likely to have higher concentrations of the desired mineral. The mathematical basis for the Turning Bands Method is spectral analysis. It can be used in generating isotropic, but spatially-varied, correlated random fields in two or three dimensions. By using a computerized random number generation procedure, no two fields are exactly alike, but they do have the same descriptive statistical values, i.e., mean, standard deviation

and correlation function for the physical property under study. Figure II-1 shows a typical field map generated by the Turning Bands Method.

A brief summary of the TBM computational process, using the specific example of a two-dimensional, log-normally distributed hydraulic conductivity field, will be discussed below. Given the mean, standard deviation and correlation function, one may compute the logarithm to base 10 of the hydraulic conductivity of a point N in the field, $\log_{10}K_N$, by Equation II-1 below.

$$\log_{10}K_N = \frac{1}{\sqrt{L}} \sum_{i=1}^{L} \log_{10}K_{N_i}(\zeta_{N_i}) \qquad \text{(Eq. II-1)}$$

where,

$\log_{10}K_N$ = logarithm to base 10 of hydraulic conductivity K at point N in the field;

$i = 1, 2, \ldots, L$ = number of TBM line;

$\log_{10}K_N(\zeta_{N_i})$ = fractional value of logarithm to base 10 of hydraulic conductivity K at point N for TBM line i at a distance of ζ_{N_i} from an arbitrarily selected origin in the field.

Figure II-2 is a schematic representation of the components of Equation II-1 above. The distance ζ_{N_i} is obtained by projecting the vector connecting the origin and point N onto TBM line i. The TBM lines radiating from the origin are uniformly distributed at an angle of $2\pi/L$ radians from each adjacent line. The value $\Delta\zeta$ is the discretization distance for computations. Mantoglou and Wilson (1981) recommend that

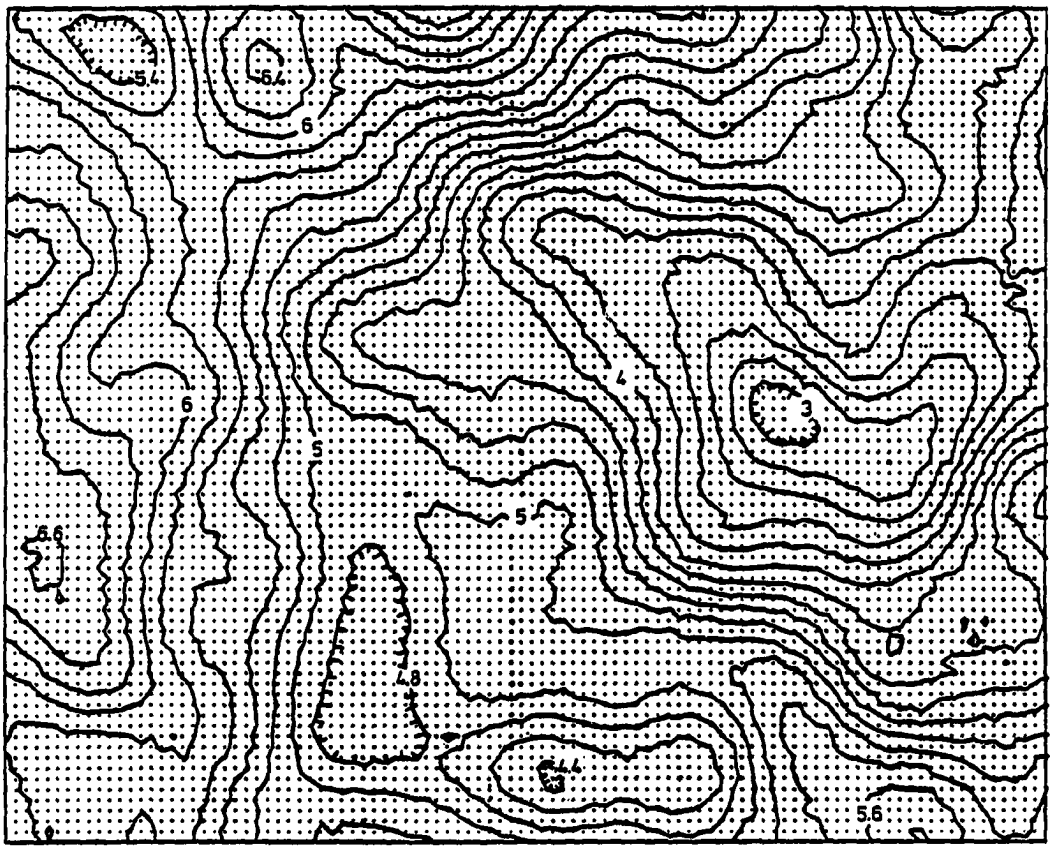

Figure II-1. An example of a random field generated with the TBM (after Mantoglou and Wilson, 1981)

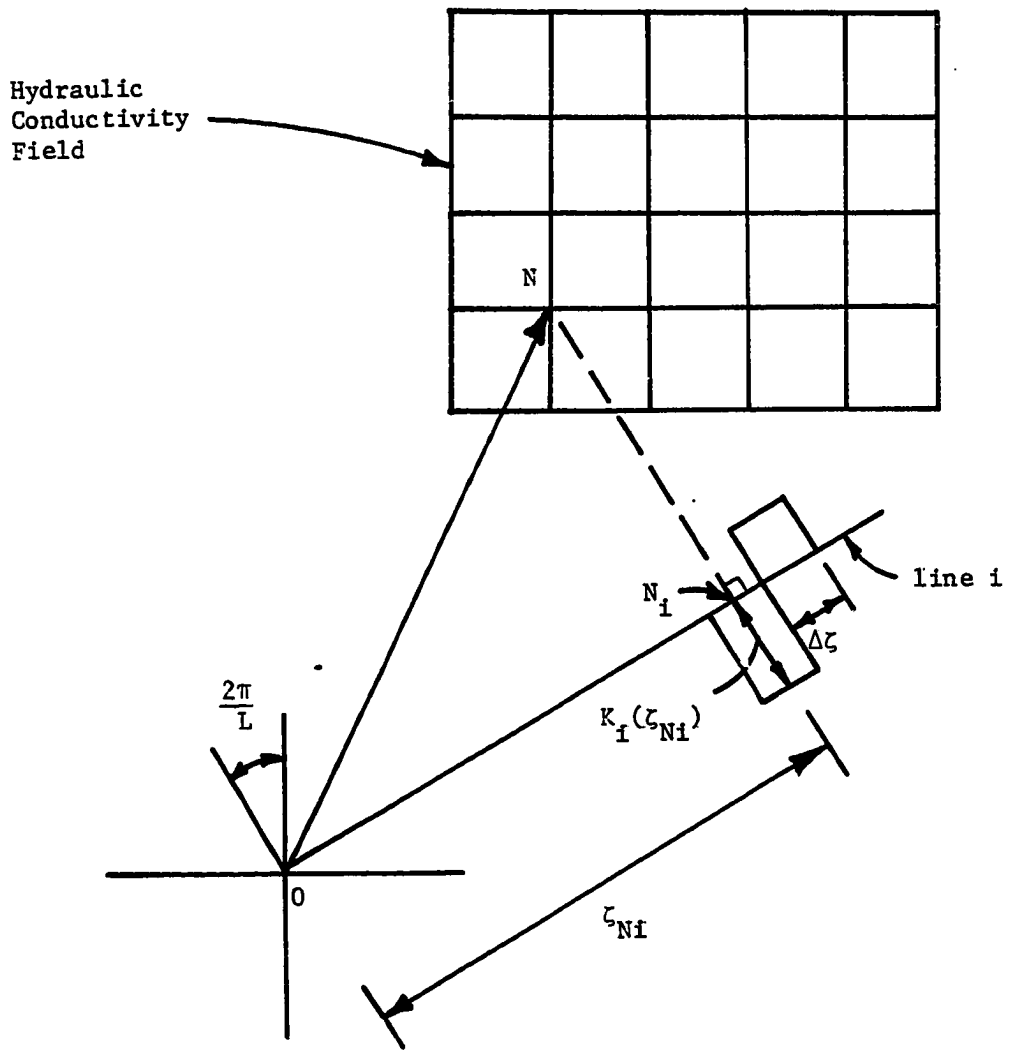

Figure II-2. Schematic representation of the hydraulic conductivity field and the turning bands lines (after Mantoglou and Wilson, 1981)

be less than the grid interval distance between parameter values, i.e., hydraulic conductivity values for obtaining good accuracy with the TBM procedure.

The values of $\log_{10} K_{N_i}(\zeta_{N_i})$ are computed using equations derived by spectral analysis techniques. Two variables, M and Ω, must be specified by the computer program user. The value Ω is the maximum frequency per correlation length over which computations are made. The correlation length, b^{-1}, is the distance over which hydraulic conductivity is correlated and ideally should be larger than the size of the generated field. M is the number of additive terms summed in order to compute $\log_{10} K_{N_i}(\zeta_{N_i})$. The accuracy of the generated hydraulic conductivity field descriptive statistics, when compared to the estimated descriptive statistics input in the TBM program, increases as the values of M increases. When Ω is small, accuracy is good over large distances. When Ω is large, accuracy is good at small distances.

D. The Effects of Heterogeneity in Hydraulic Conductivity on Mass Transport in Groundwater

The earlier work on hydraulic head uncertainty has been a foundation for research into uncertainty in mass transport modeling. In a series of three articles, Smith and Schwarz (1980, 1981a, 1981b) determined that the major cause of dispersion in solute transport in porous media on a macroscopic scale was heterogeneity in hydraulic conductivity, not primarily a mechanical mixing process as represented in the advective-dispersive equation.

In the first paper by Smith and Schwarz (1980), a random walk component was added on to the model of Smith and Freeze (1979b) to simulate mass transport. When a log-normal distribution was assumed for hydraulic conductivity values in a statistically homogeneous porous medium, particle distributions flowing in the porous medium exhibited a non-normal distribution character. The non-normal distributions were concluded to be caused by "preferred" pathways of high conductivity randomly distributed throughout the medium. These "preferred" pathways prevented the particles from undergoing sufficient velocity changes to generate an idealized pattern of particle spreading. The dispersion associated with hydraulic conductivity heterogeneity was determined to be much larger than that with the dispersivity in the mass transport model, which makes estimates of seepage velocities in the porous medium an extremely important factor.

Actual field studies supporting the assertion of Smith and Schwarz that a mechanical mixing type dispersivity is often insignificant are few. Anderson (1984), in a review of the scientific literature addressing the validity of the assumption of dispersion as a mixing process, cites four field investigations where dispersivities were measured. All four measurements indicated that dispersivity increases with distance traveled and does not remain constant, as assumed in the advective-dispersive mass transport model. Anderson concluded that dispersion was not a mixing process in field studies where large distances are traversed by the pollutant.

Smith and Schwarz (1981a) extended their analyses to a variety of different flow configurations. They concluded that factors changing the magnitude and direction of advective transport are most important in determining uncertainties in prediction. These factors include heterogeneity, anisotropy and layering in porous media formations. Those factors changing only the magnitude of velocity are less important in determining uncertainty. Such factors as porosity and chemical retardance fall into this category. The identification of zones of preferential transport appear to be a major requirement for accurate prediction of movement.

Smith and Schwarz (1981b) concluded their analyses by investigating the effect of the amount of field data available on uncertainty in prediction. They concluded that field data significantly decrease uncertainty in transport prediction only in a small area around the location of the data and that considerable data collection is required to significantly decrease prediction uncertainty. They also determined that heterogeneity in hydraulic conductivity is a more important source of uncertainty than errors in estimating the mean and standard deviations of hydraulic conductivity from limited field data.

E. Pollutant Concentration Versus Duration of Exposure

The relevance of the time of arrival of a pollutant to a specified location is self-evident: either the pollutant will arrive or it will not, and if it does, when it will arrive becomes desired information.

However, the relevance of duration of exposure at a given pollutant concentration requires a brief explanation because it is a more complex phenomenon. Several practitioners in water pollution control have expressed ideas concerning the pollutant concentration versus duration of exposure relationship and they are discussed below.

1. Hazard assessment

G. F. Lee et al. (1982) have promoted a "hazard assessment" approach for evaluating the impact of a contaminant on water quality. In this procedure, a concentration versus duration of exposure relationship would be used to define a boundary between safe and unsafe exposures of an organism to a contaminant. Figure II-3 below shows the nature of this relationship. At some point as the duration of exposure decreases, pollutant concentration above the chronic safe concentration may be permitted without creating a hazard. This description of the pollutant concentration versus duration of exposure relationship is presented in a conceptual framework. A more quantitative expression of this relationship is found below in a discussion of toxicity curves.

2. Toxicity curve

A typical toxicity curve might show a graph of median lethal threshold concentration of a pollutant for different periods, or durations, of exposure to an organism. The median lethal threshold concentration for a specified duration of exposure is the pollutant concentration at which 50% of a test organism population dies (Brown,

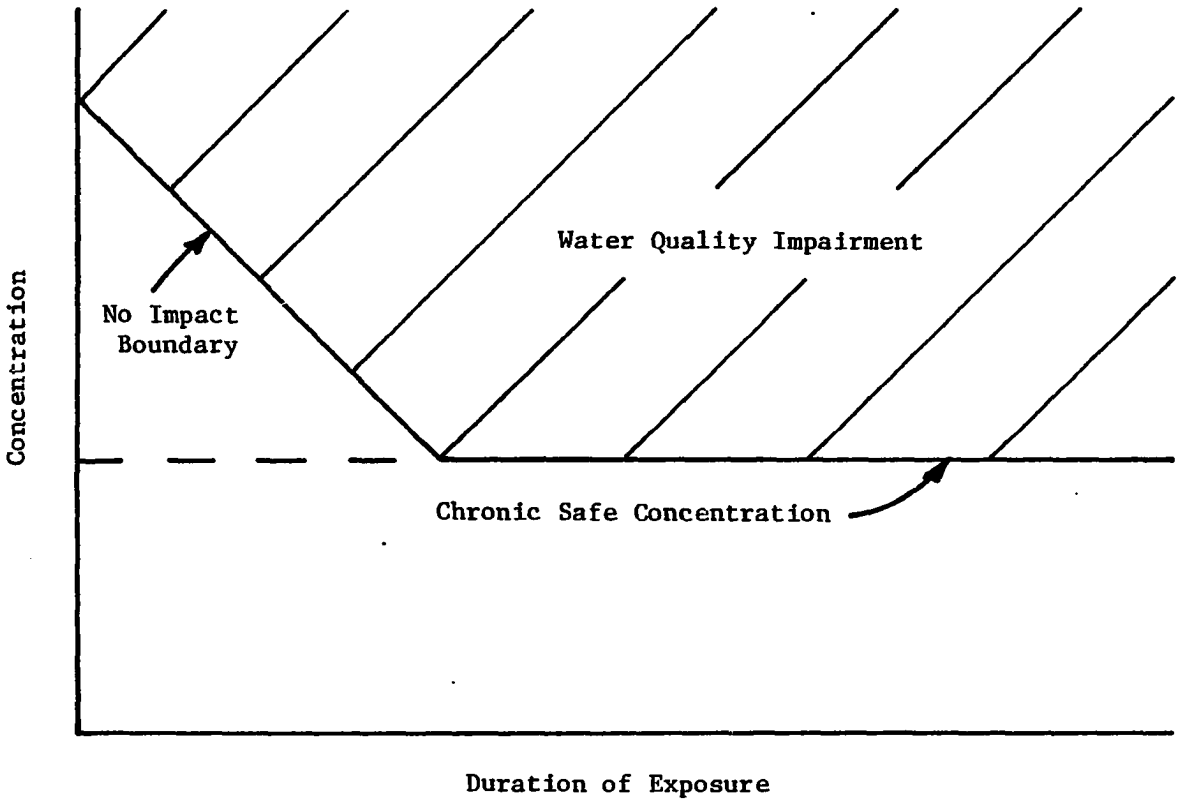

Figure II-3. General case - hazard assessment (after G. F. Lee et al. 1982)

1973). Figure II-4 shows the general shape of a toxicity curve. The toxicity curve shows three things. First, it shows if the curve is asymptotic to the pollutant concentration axis. Second, it describes the range of pollutant concentrations over which a selected proportion of the test organisms has no ability to cope with the pollutant. Last, it shows where the curve is asymptotic to the time axis, the pollutant concentration above which 50% of the test organisms cannot achieve homeostasis with the pollutant. Factors of safety are applied to this concentration in order to establish the "no observed effect level" (NOEL). A toxicity curve is generally downward sloping toward increased duration of exposure.

Toxicity curve analysis usually concentrates on the chronic toxic effects of a pollutant, rather than the behavior due to large concentrations for a short period of time. The definition of acute toxicity generally accepted by toxicologists is an exposure to a toxic substance on one occasion in which the response of an organism is death (Brown, 1980). Sometimes acute toxicity may refer to multiple exposures over a short period of time, usually 24 hours. Occasionally, acute toxicity may refer to the response to exposure, rather than the exposure itself.

For pollutants in water, the test organism often is a fish; whereas mammalian test species, usually mice or rats, probably have biological activity more closely related to humans. Yet, the accuracy of extrapolating toxicity curves of other mammals to humans is also subject

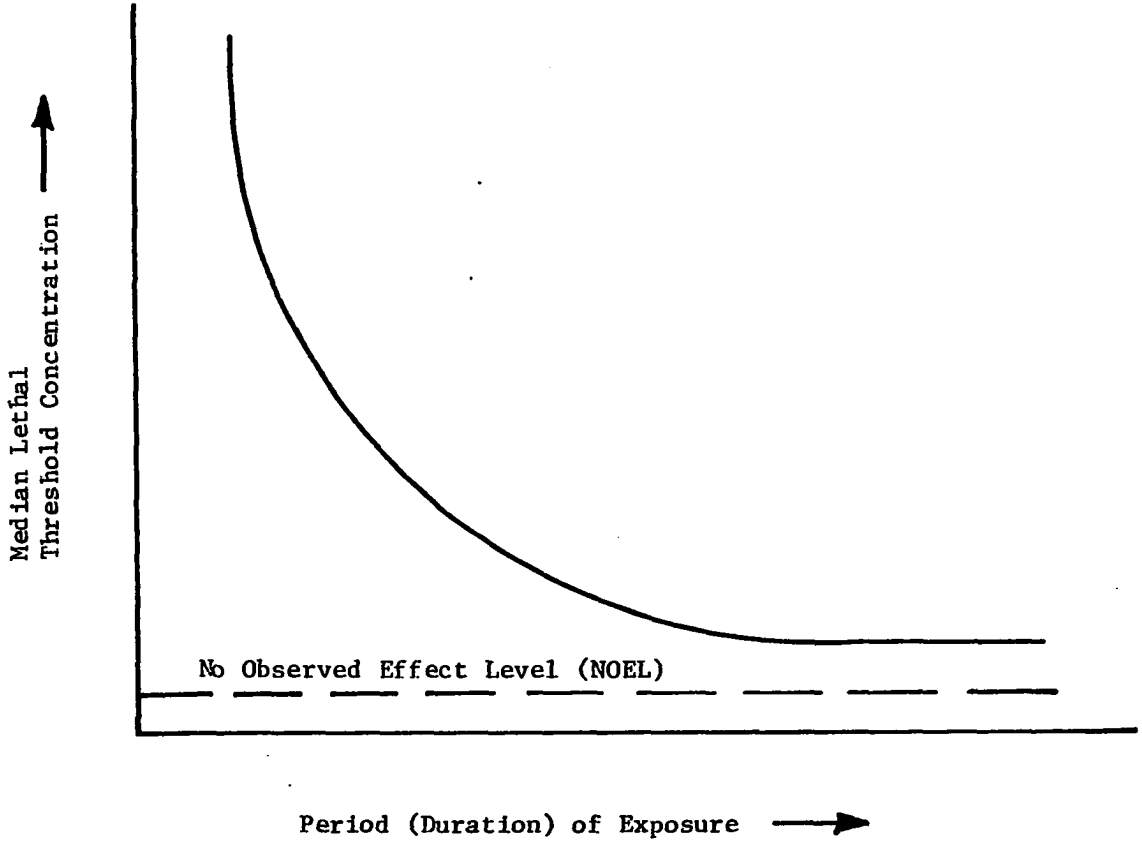

Figure II-4. Toxicity curve

to a large degree of skepticism and uncertainty. The threshold to, or onset of, the occurrence of toxic effects are often difficult to quantify. The threshold concentration depends on the species of the exposed organism, and the type of exposure, e.g., ingestion and absorption through the skin. The threshold concentration may vary even between members of the same species, depending on age, weight, sex, etc.

3. Dose-response relationship

In the Office of Technology Assessment report (1984) previously discussed in Chapter I, Step 2 in the risk assessment procedure is establishing a dose-response relationship. The "no observed effect level" (NOEL) for non-carcinogen pollutants, shown in Figure II-4 above, is a constant concentration below which no adverse responses are observed. This value is the same as the "chronic safe concentration" described by Lee. For carcinogenic pollutants, a relationship between dose and carcinogenic risk is discussed. A "unit risk" is the fraction of test organisms exposed to the carcinogen which develop tumors minus the fraction of a control group of test organisms not exposed to the carcinogen which develop the same type of tumors.

In Step 4 of the Office of Technology Assessment's Risk Assessment procedure, risk characterization, additional factors of safety are used on the NOEL and unit risk to insure that the exposed populations are not significantly at risk. Rodericks and Tardiff (1984) call the use of safety factors "biologically and statistically dubious," and recommend that these arbitrary numbers be stated in explicit terms so that they

are not hidden from decision makers. Nelson (1984) proposed the use of a "pseudo" NOEL which consists of fitting a curve to observed dose-response points. He suggested that some low incidence level, e.g., 1%, be selected as the acceptable level of risk.

4. Risk characterization

Since 1970, a general standard of "unreasonable risk" has been adopted in all federal statutes relating to health and safety. This term has not been rigorously defined by regulating agencies. A close analysis of benefits and costs does not have any significant effect on regulatory decisions, but if the regulatory action is absurd and will make the agency look foolish, it will be abandoned (Hutt, 1984).

In 1981, Executive Order 12291 was signed by President Reagan for the purposes of reducing the burdens of regulation, increasing federal agency accountability, minimizing duplication and conflict in regulation and insuring well-reasoned regulations. Federal agencies not designated by statutes as "independent regulatory agencies" must now employ cost-benefit criteria for the development and issuing of regulations. The United States Environmental Protection Agency (USEPA), which regulates the quality of groundwater, is one of the agencies subject to this Executive Order. No methodology has yet been agreed upon by the USEPA to make the necessary calculations (Zentner, 1984).

5. Proposed pollutant concentration versus duration of exposure relationship

This investigation proposes to present results on pollutant movement and concentration in the format presented below. The modeling results will eventually be compared to and evaluated with the other descriptions of pollutant concentration versus duration of exposure previously discussed.

The following example will describe how concentration versus duration of exposure results might be obtained using an analytic solution to an advective-dispersive model for solute flow in a porous medium. The following assumptions are made:

1. The flow is one dimensional, steady and uniform.
2. The porous medium is homogeneous and isotropic.
3. The mass of the pollutant is an instantaneous slug from a point source.
4. The flow is parallel to the longitudinal axis of dispersion with no transverse dispersion present.
5. The molecular diffusion, chemical retardation and radioactive decay are negligible.

The governing equation of this model is presented below as Equation II-2. The analytic solution is Equation II-3, presented just below Equation II-2.

$$\frac{\partial C}{\partial t} + V_x \frac{\partial C}{\partial x} = D_x \frac{\partial^2 C}{\partial x^2} \qquad \text{(Eq. II-2)}$$

$$\frac{C}{C_o} = \frac{\exp - \dfrac{(x - V_x t)^2}{4D_x t}}{\sqrt{4\pi D_x t}} \qquad \text{(Eq. II-3)}$$

where,

C_o = initial concentration for x = 0, t = 0;

C = concentration for x = x, t = t;

x = flow distance;

t = travel time;

V_x = interstitial velocity (see Eq. I-2); and

D_x = longitudinal coefficient of dispersion (see Eq. I-3).

The results of the analytic solution to the advective-dispersive model allow a pollutant concentration versus time relationship to be developed at a specified location in the path of the dispersing pollutant slug, as shown in Figure II-5 below.

The time of arrival occurs when the pollutant first reaches the specified location. By computing the length of time the concentration at location x equals or exceeds a given concentration amount, a concentration versus duration of exposure relationship is formed, as shown in Figure II-6 below.

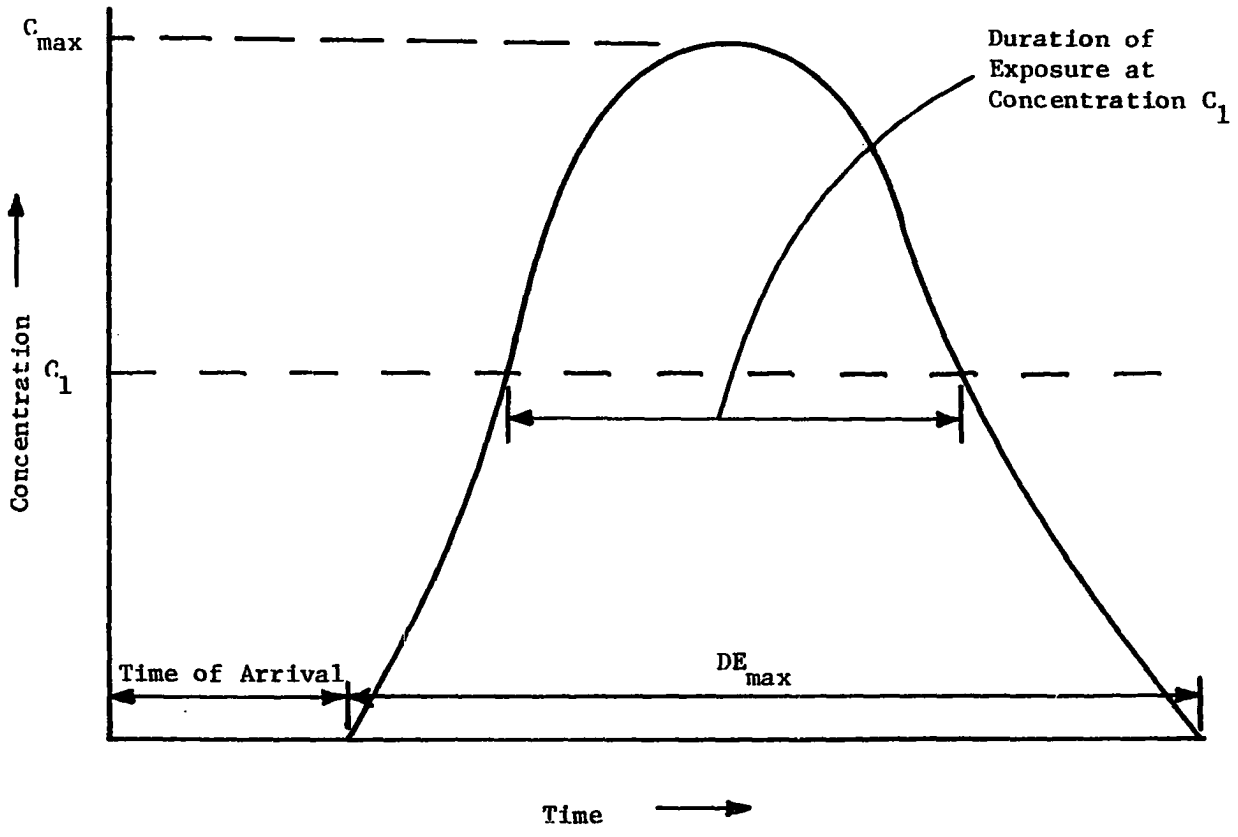

Figure II-5. Pollutant concentration at location X as a function of time

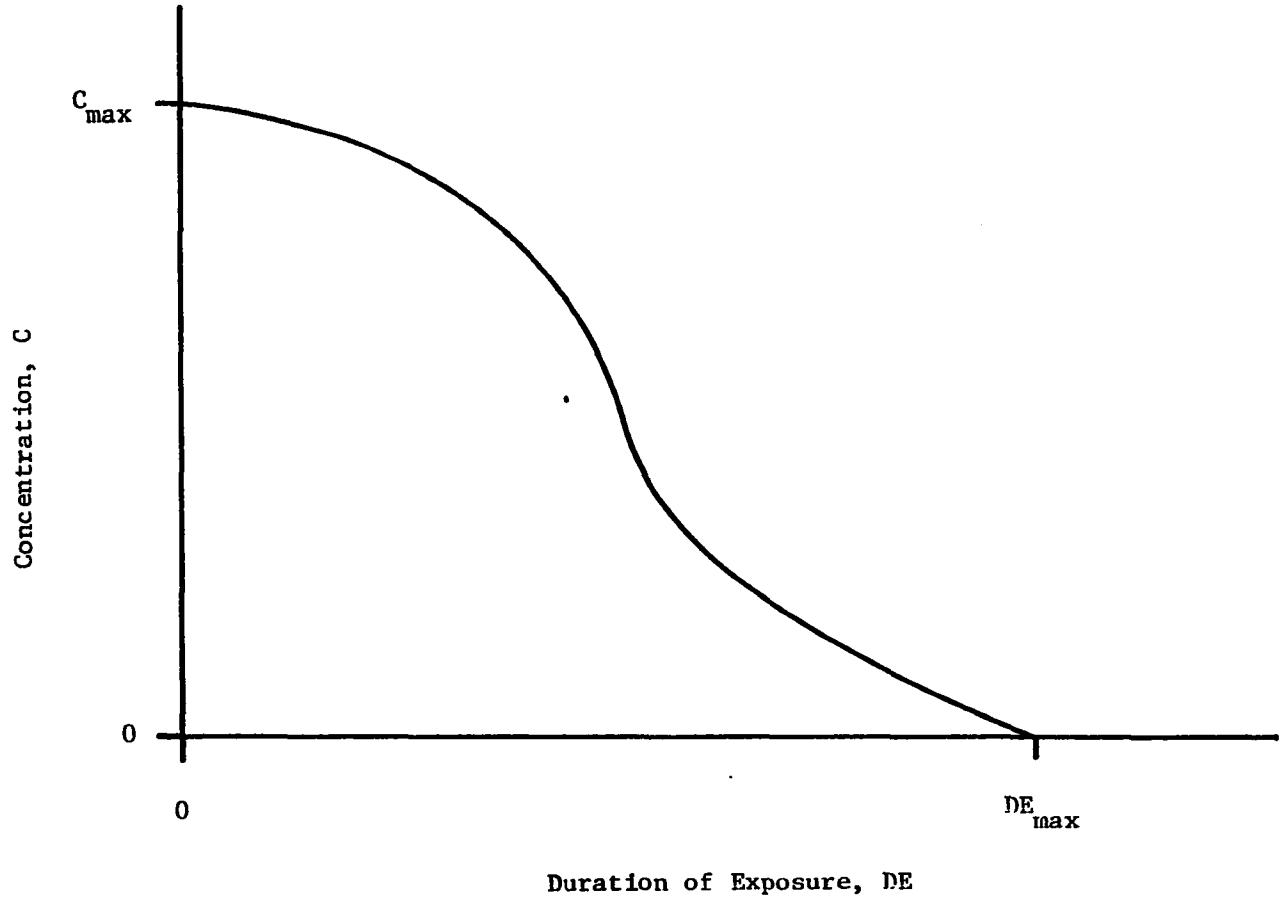

Figure II-6. Pollutant concentration at location X versus duration of exposure

If several of these time of arrival and pollutant concentration versus duration of exposure relationships are generated, frequency distributions of time of arrival and pollutant concentration versus duration of exposure within designated class intervals may be constructed. Probability distributions for time of arrival may be obtained by dividing the frequency in each class by the total frequency in all classes. Pollutant concentration versus duration of exposure frequency distributions may be transformed into probability distributions by dividing the observed frequency in a cell associated with the intersection of two classes by the total frequency in all cells, a normalizing procedure. The pollutant concentration versus duration of exposure probability distribution most resembles the "pseudo" NOEL procedure of Nelson suggested above. The concentrations at selected incidence levels from the toxicity tests could be compared to the exceedance probabilities at those same concentrations. The exceedance probabilities would indicate the risk of exceeding the selected incidence levels.

III. PROPOSED MODEL

A flow diagram of the proposed procedure for obtaining a probability distribution of time of arrival and pollutant concentration versus duration of exposure at a specified location is presented in Figure III-1. This procedure incorporates commercially available computer programs and does not require exhorbitant costs or unusually large amounts of field data.

After determining the descriptive hydraulic conductivity statistics, i.e., mean, standard deviation and correlation function, the Turning Bands Method (TBM) computer program is applied to develop a selected number of spatially-varying, correlated hydraulic conductivity fields. The modeler does not necessarily have to use the same grid network for the TBM program as the groundwater flow-mass transport computer program, but the columns and rows of the two networks should be parallel.

The computer output of the TBM program; other aquifer properties (e.g., groundwater levels, aquifer thickness and effective porosity); and pollutant factors (e.g., retardation factor, radioactive decay rate and location, time and rate of discharge of pollutant into the aquifer) are used as inputs into a groundwater flow-mass transport computer program developed by the Illinois State Water Survey (Prickett and Longquist, 1971; and Prickett et al., 1981). This program is used to model two-dimensional problems with a variety of different boundary conditions. The groundwater flow portion of the program uses a finite-

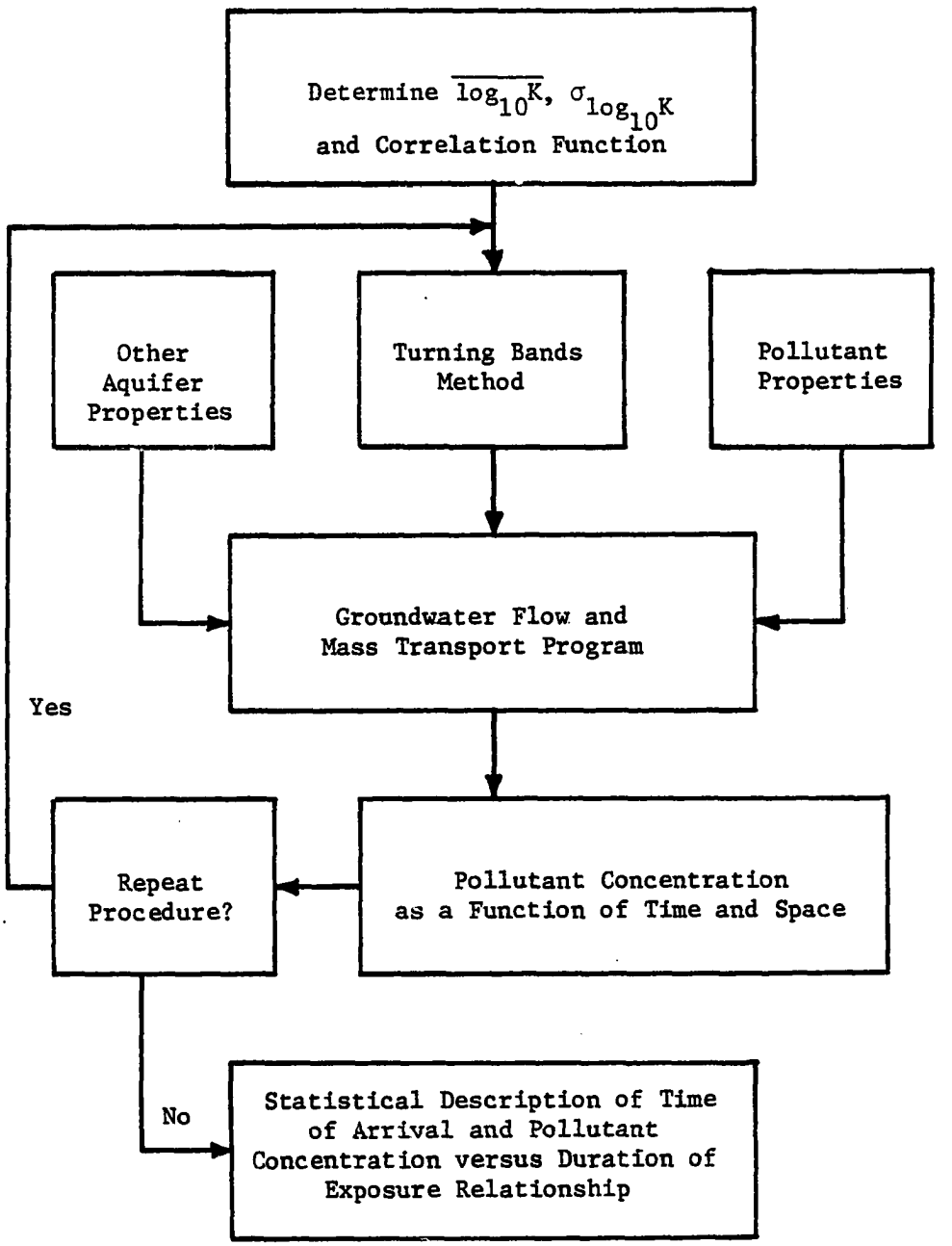

Figure III-1. Proposed model

difference methodology to solve the groundwater flow equations of the grid network for a piezometric head distribution. The head distribution is then used to compute seepage velocities. The mass transport portion of the computer program incorporates the seepage velocities for determining the advection movement of the pollutant and adopts a random walk approach to simulate the dispersion process. The output of the groundwater flow-mass transport program is pollutant concentration as a function of time and space. The groundwater flow-mass transport program is used repeatedly with the different, unique hydraulic conductivity fields developed by the TBM program until a realization is generated for each field. A realization will be defined in this investigation as computation of pollutant concentration as a function of time and space for one hydraulic conductivity field originating from the TBM program. The cumulative output is then a selected number of pollutant concentration maps as a function of time and space. Using the methods described in Chapter II, a time of arrival distribution and a pollutant concentration versus duration of exposure distribution for specified locations are developed.

Lastly, a statistical analysis of the time of arrival and pollutant concentration versus duration of exposure distributions using a standard statistical computer package, SAS (1982a, 1982b), is completed. Typical results of multiple realizations are presented in the format shown by Figures III-2, III-3, and III-4 below. In Figure III-2, the time of arrival of a pollutant at a specified location is expressed as a

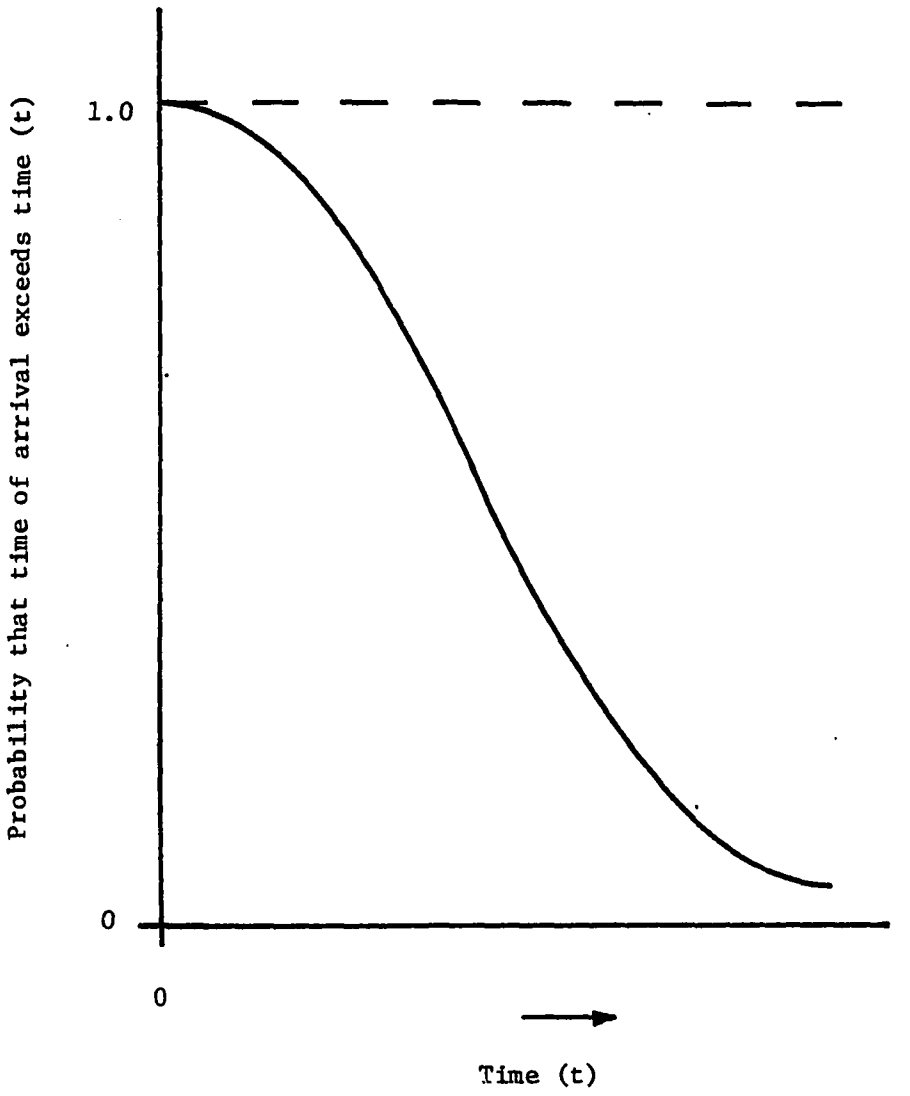

Figure III-2. Time of arrival exceedance probability

cumulative exceedance probability. This plot estimates the probability that the time of arrival will be equal to or greater than a selected time amount. In Figure III-3, the duration of exposure given a pollutant concentration at a specified location is expressed as a conditional probability distribution. In Figure III-4, a pollutant concentration given a duration of exposure at a specified location is expressed as a conditional probability distribution. These plots allow the engineer to give the decision maker an idea of the central value, dispersion, skew and exceedance probability of the resulting distributions. Values from these plots may be compared to the NOEL values established by toxicologists, as discussed in Chapter II.
A joint probability distribution may be computed in order to define the exceedance probabilities for combinations of pollutant concentration and duration of exposure. The joint probability results may be presented in a manner so as to be compared to estimates of acute and chronic concentration limits in order to compute a risk of exceeding the regulatory limits.

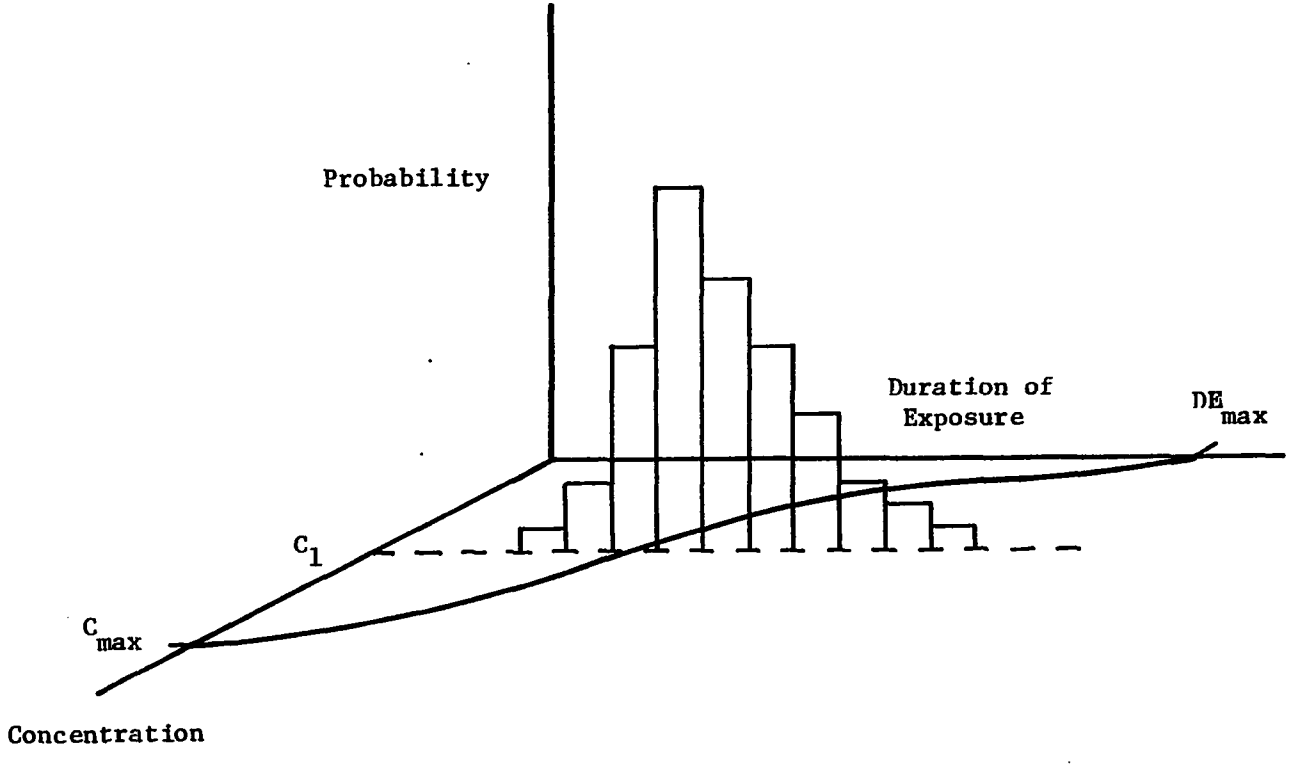

Figure III-3. Conditional probability of duration of exposure given pollutant concentration

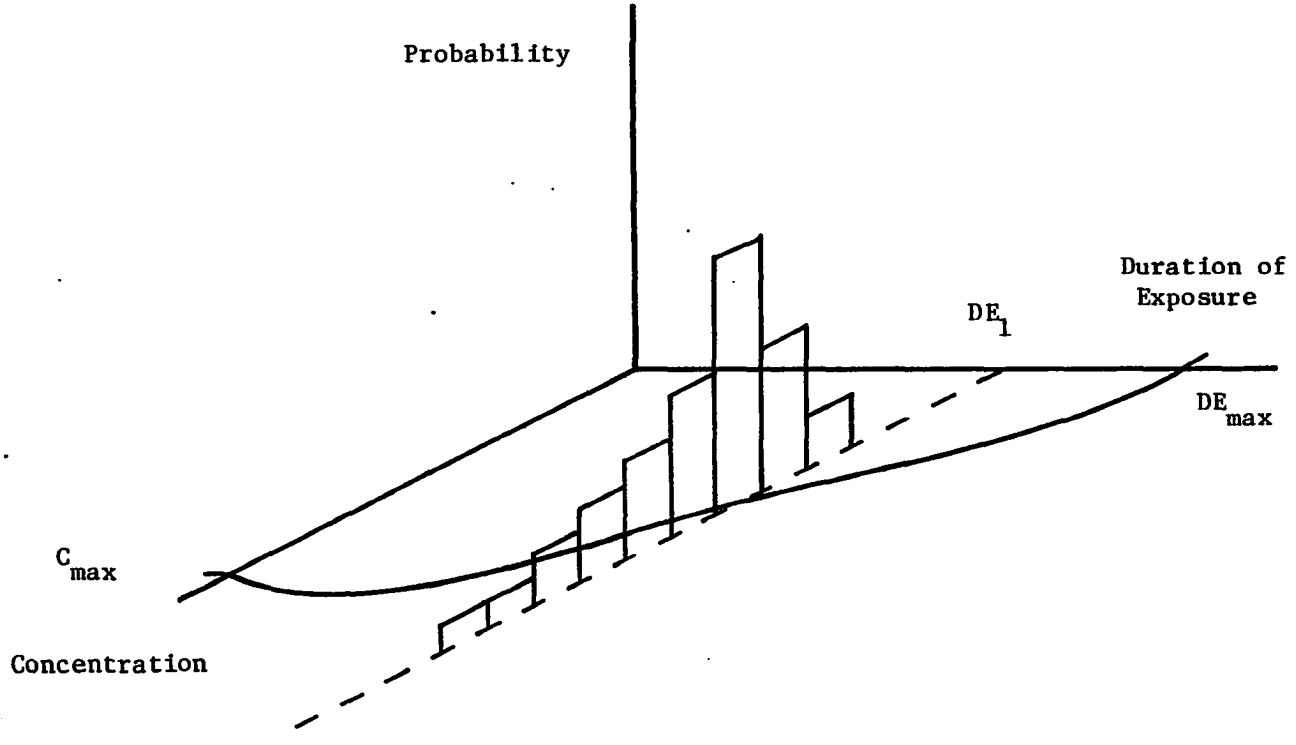

Figure III-4. Conditional probability of pollutant concentration given duration of exposure

IV. CALIBRATING THE PROPOSED MODEL WITH FIELD DATA

Industrial and low-level radioactive nuclear wastes from the Idaho National Engineering Laboratory (INEL), formerly known as the National Reactor Testing Station, have been discharged into the Snake River Plain aquifer since 1952. The Snake River Plain formation is located in southeastern Idaho. The INEL property is located above the middle of the aquifer at the downstream end of the Big Lost River, as shown in Figure IV-1. Wastes from the Test Reactor Area (TRA) and Idaho Chemical Processing Plant (ICPP) enter the aquifer formation through seepage ponds and injection wells. The ICPP primarily discharges tritium, in the form of tritiated water, and sodium chloride through a 600-foot deep injection well. The contaminant data used in this investigation will be limited to tritium concentrations from the ICPP wastes measured in disposal and observation wells.

A. The Snake River Plain Aquifer

Basaltic lava flows and interbedded sediments compose most of the Snake River Plain aquifer. The sediments are primarily silty to sandy alluvial and lacustrine lenses. Rhyollitic ash deposits and ash-flow tuffs can occasionally be found also. These materials constitute the upper 3,000 feet of the aquifer near the INEL site. Below the upper zone of the aquifer, silicic rocks are the predominant formation to a depth of around 10,000 feet below ground surface.

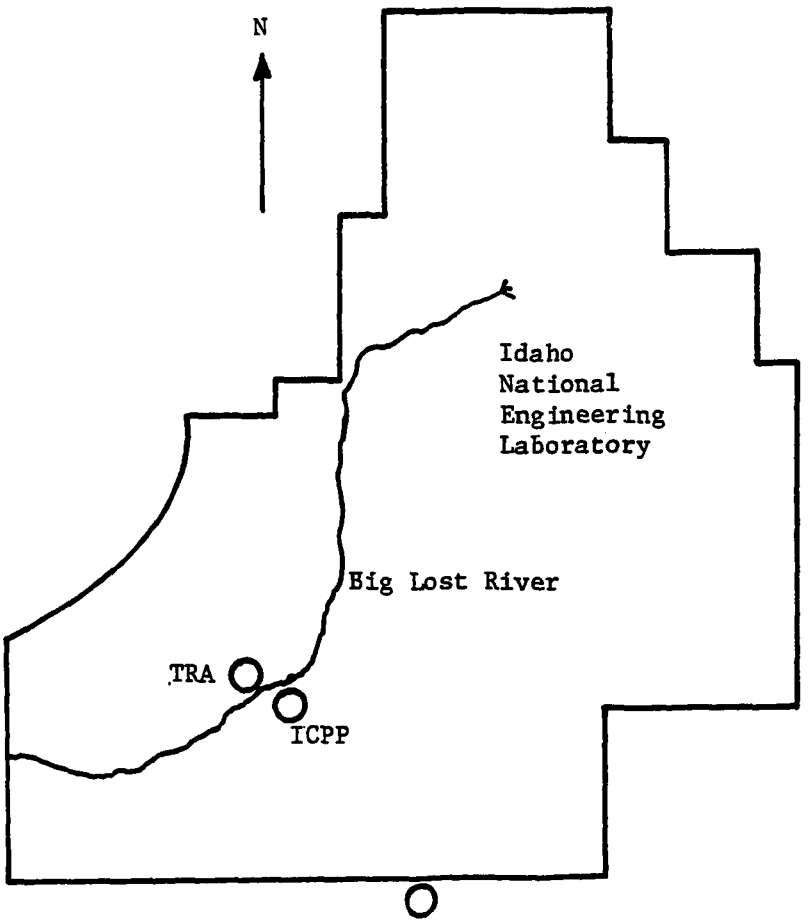

Scale: 1 inch = 8 miles

ICPP - Idaho Chemical Processing Plant
TRA - Test Reactor Area

Figure IV-1. Location map of the Test Reactor Area (TRA) and Idaho Chemical Processing Plant (ICPP) (after Robertson, 1974)

Near the location of the TRA and ICPP disposal areas there are at least six major alternating layers of sediments and basalt in the 3,000-foot upper zone. The basalt is the principal aquifer material. Openings in the basalt transmitting groundwater consist of intercrystalline and intergranular porespace, fractures, cavities, interstitial voids, interflow zones and lava tubes (Lewis and Goldstein, 1982). The variety and degree of interconnection of these openings is quite variable and makes accurate measurements of the transmission characteristics of the aquifer at a specific location quite difficult.

The United States Geological Survey (USGS) has produced a transmissivity map for the Snake River Plain aquifer in and around the INEL, as presented in Figure IV-2. The average thickness of the aquifer layer into which the ICPP discharges is 250 feet.

Measurements of the groundwater level from observation wells in the Snake River Plain in July through October of 1980 indicate that the water table is approximately 400 feet below the ground surface near the TRA and ICPP. They also indicate that the water table slopes generally to the southwest until the groundwater flow is intercepted by the Snake River. The water level of the aquifer under the INEL typically shows only gradual fluctuations due to long term water basin demand-supply inequalities over a time period measured in years. Occasionally, large recharge events from snowmelt flows in the Big Lost River will induce more rapid fluctuations in the groundwater level.

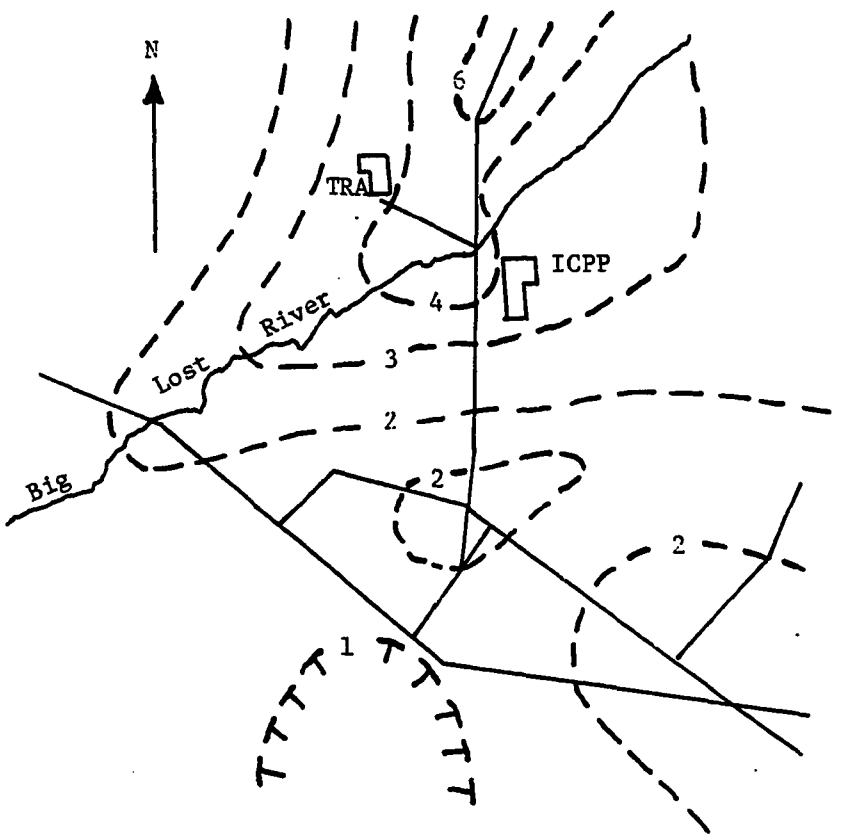

Scale: 1 inch = 2 miles

Idaho National Engineering Laboratory

TRA - Test Reactor Area
ICPP - Idaho Chemical Processing Plant

--1-- Line of equal transmissivity, in feet squared per second; Interval: varies

Figure IV-2. Transmissivity contours for the Snake River Plain aquifer (after Robertson, 1974)

Core samples from test borings in the aquifer have porosities ranging from 12% to 20%. The effective porosity for groundwater movement has been considered to be .10% (Robertson, 1974).

B. The Idaho Chemical Processing Plant (ICPP)

The average yearly discharge of liquid waste from the Idaho Chemical Processing Plant to the Snake River Plain aquifer has been 319 million gallons from 1953 through 1980. Nearly all of the radioactive waste consists of tritium. From 1974 through 1980, the average curie discharge rate of all radioactive isotopes to the injection well was 290 curies per year with an average water volume discharge rate of 377 million gallons per year, which is equivalent to an average concentration of 200 picocuries per milliliter of water. Figure IV-3 shows the extent of the tritium plume on the INEL property in October of 1980. The effect of two different sources of tritium is readily noticeable in the iso-concentration contours. This investigation will limit modeling to the tritium plume area between the ICPP and the Central Facilities Area (CFA).

C. Tritium Field Data

The USGS is presently developing a data base for the observation wells on and around the INEL property site. This investigator has obtained preliminary water level and tritium concentration records for Well #40, Well #37, Well #85 and Well CFA #1, whose locations are shown

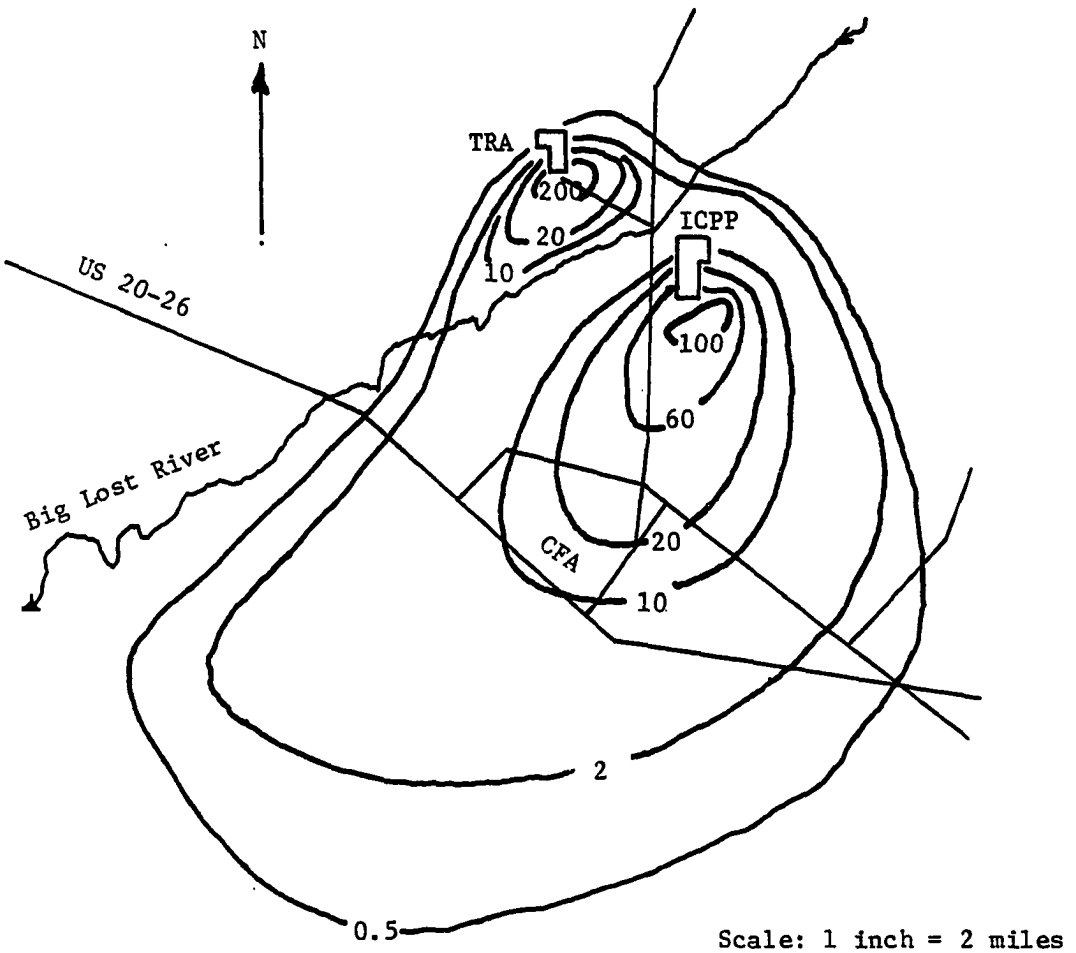

Idaho National Engineering Laboratory

TRA - Test Reactor Area
ICPP - Idaho Chemical Processing Plant
CFA - Central Facilities Area

--2-- Lines of equal tritium concentration, in picocuries per milliliter; Interval: varies

Figure IV-3. Distribution of tritium in the Snake River Plain aquifer, October, 1980 (after Lewis and Goldstein, 1982)

in Figure IV-4. A record of monthly tritium discharges has been published and was available from the current operators of the ICPP, Westinghouse Idaho Nuclear Company (1984). Figure IV-5 shows the ICPP mean monthly service waste volume injection rates in million gallons per day (MGD) and tritium loads in curies from 1976 through 1982. Tritium is a radioactive constituent and decays over time. The half-life of tritium is 12.3 years. Tritium is a relatively conservative constituent in water and typically is not subject to chemical reactions; therefore, the value of the retardation factor, R_d, has been set at 1.0 for this study.

D. Calibration of the Proposed TBM Model with Field Data

Three characteristics of the aquifer hydraulic conductivity field are required by the TBM model. They are the mean value, standard deviation and correlation function. The transmissivity field shown in Figure IV-2 was used for computation of these characteristics.

1. Boundary limits

The boundary limits of the transmissivity field used to define statistical properties were chosen by the following reasoning. The boundary limits need not extend any farther than the limits of the tritium plume, as topological forms of the transmissivity field outside the plume limits have no bearing on previous plume movement. Based on tritium concentration data discussed later in Section E of this chapter, the tritium plume limits for the disposal events used in calibration of

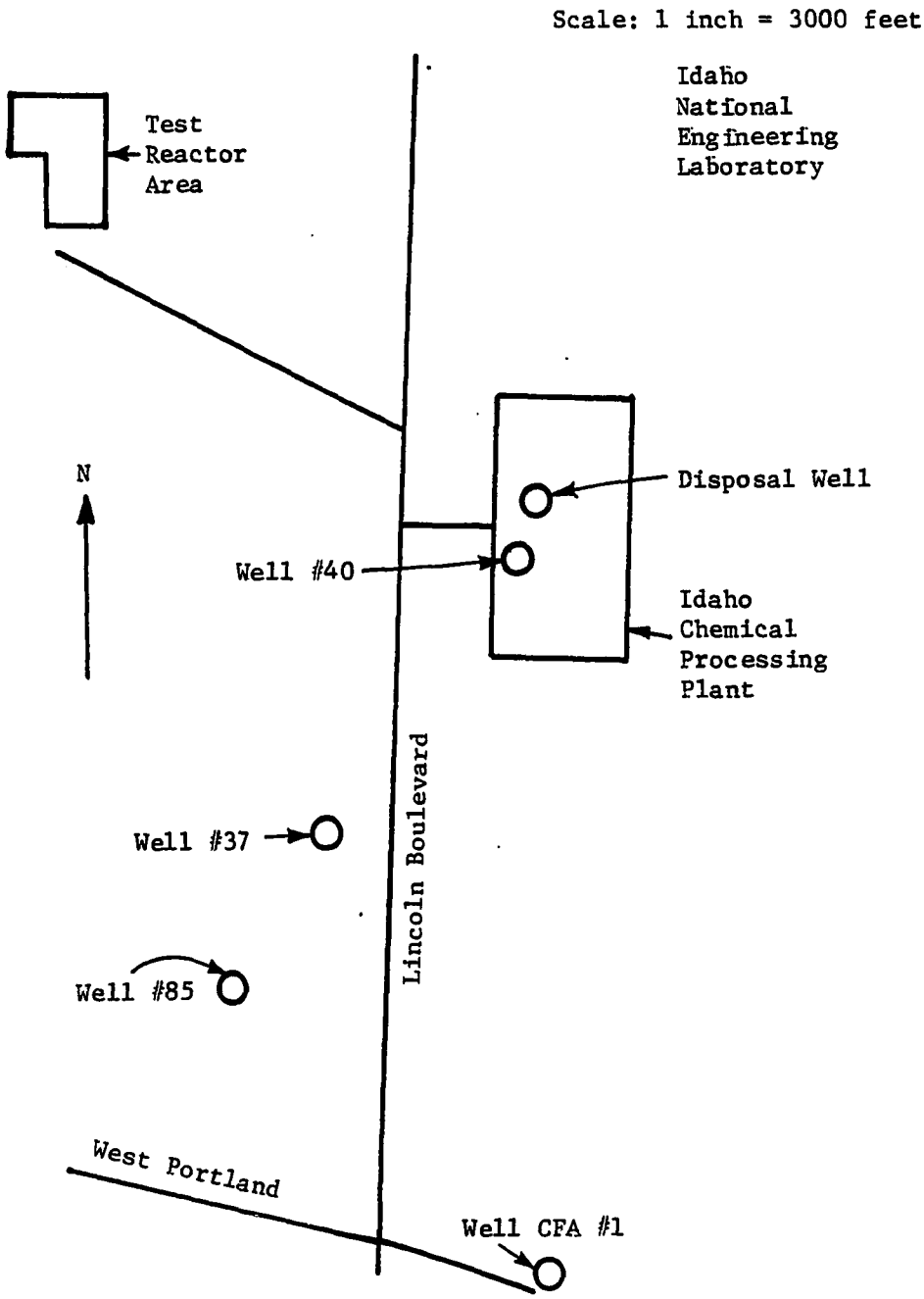

Figure IV-4. Locations of selected wells (after Lewis and Goldstein, 1982)

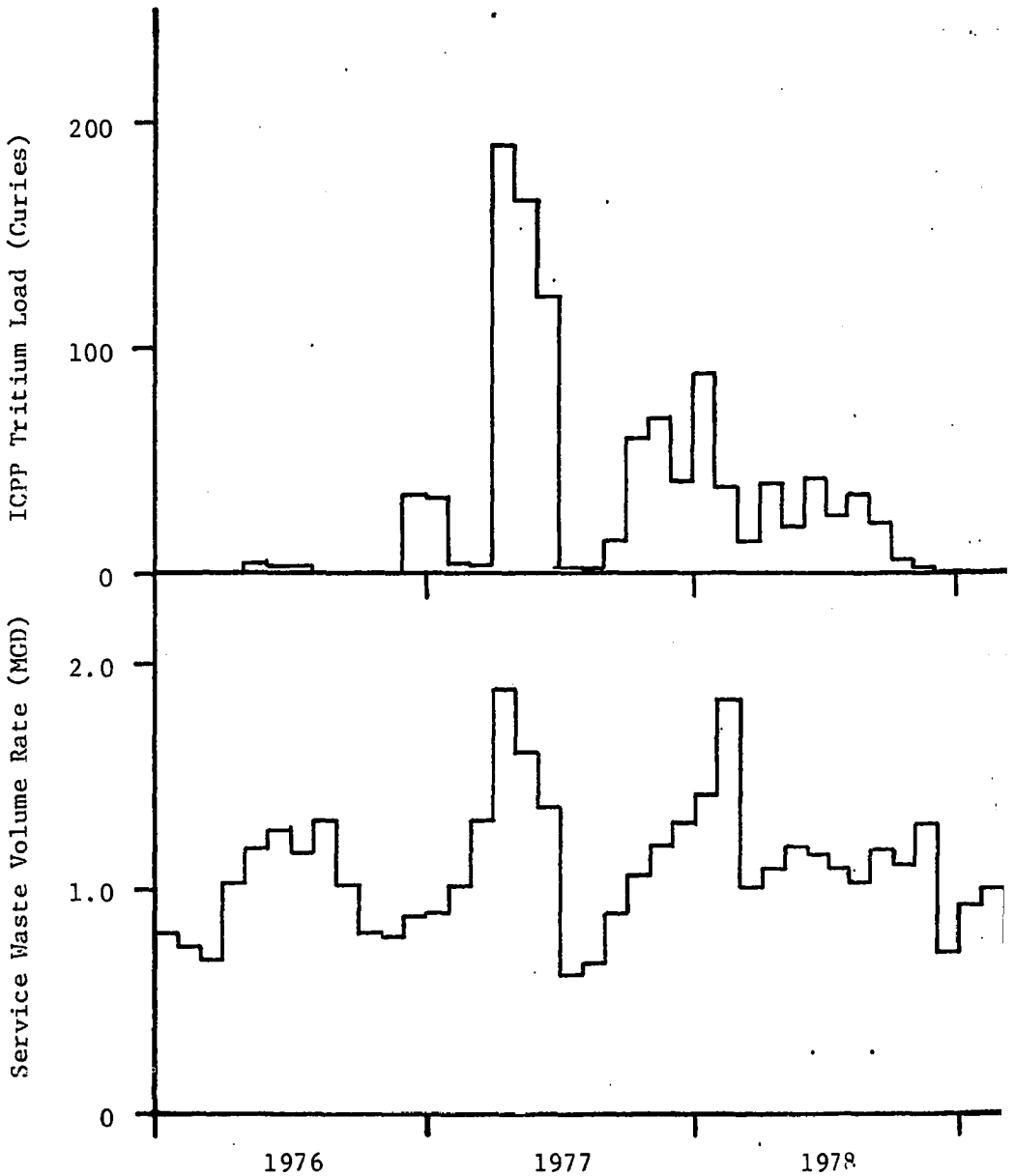

Figure IV-5. ICPP tritium load and service waste volume rate, 197

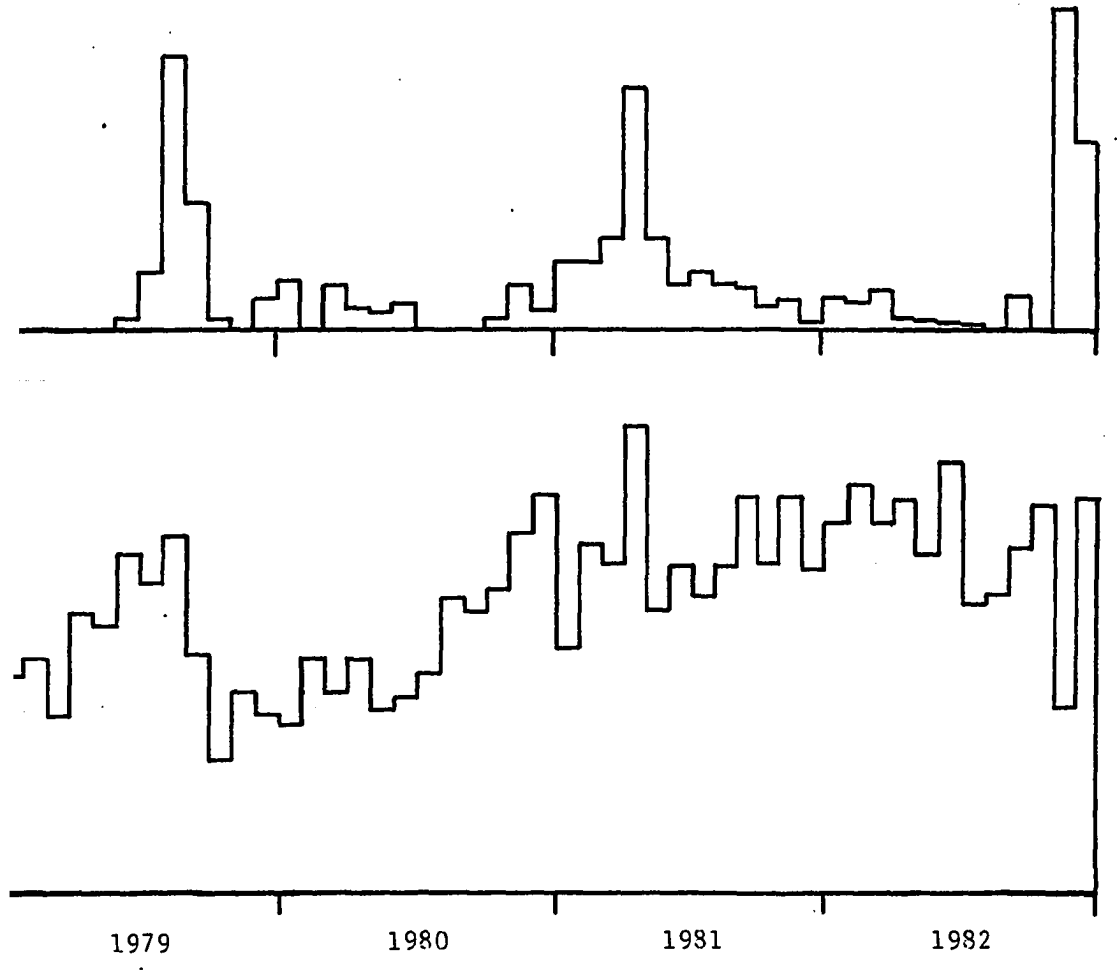

1976-1982

the groundwater flow-mass transport model did not appear to reach or significantly contribute to tritium concentrations at Well #85 or Well CFA #1.

Figure IV-6 shows the boundary limits of the transmissivity field around the disposal well selected for calibration of the TBM model. This area is a 2-1/2 mile square, extending over one mile east and west, less than one mile north and almost two miles south of the disposal well. The large area of the transmissivity field south of the disposal well contains most of the tritium plume.

2. Computation of the mean and standard deviation of the hydraulic conductivity field

Transmissivity values used to determine the mean and standard deviation of the hydraulic conductivity field were obtained by dividing the 2-1/2 mile square into 25 equal size squares, each with 1/2 mile sides, and visually estimating the average transmissivity within each of the small cells. Table IV-1 below contains the estimated transmissivities and hydraulic conductivity for each cell. These transmissivities were then divided by the average thickness of the aquifer, 250 feet, to obtain hydraulic conductivities. These values were then converted from units of feet per second to units of gallons per day per square foot (gpd/ft^2), which are the input units required by the mass transport model. As the hydraulic conductivity field is assumed to be log-normally distributed, the logarithm to base 10 of each hydraulic conductivity was used in computing the mean and standard

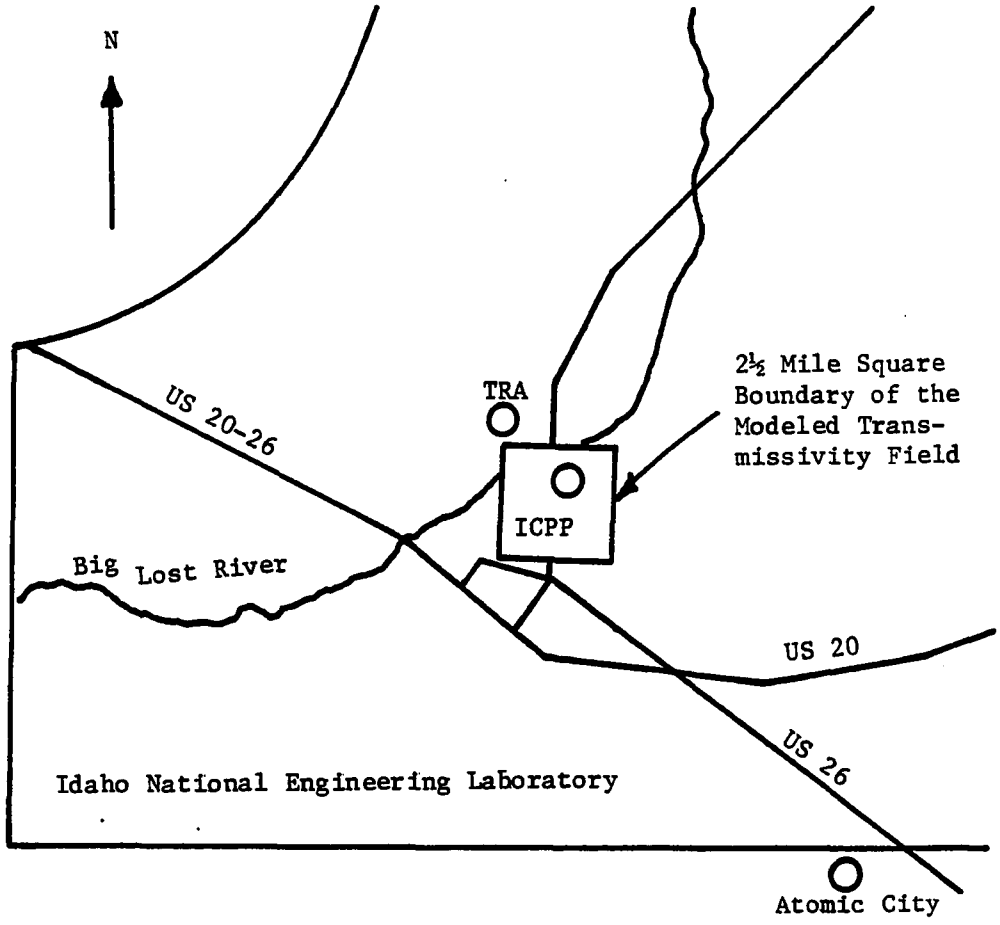

ICPP - Idaho Chemical Processing Plant
TRA - Test Reactor Area

Figure IV-6. Transmissivity field for Turning Bands model

Table IV-1. Individual cell, mean and standard deviation of cell hydraulic conductivities

Cell #	Transmissivity $T(ft^2/sec)$	Hydraulic Conductivity $K(gpd/ft^2)$	$\log_{10}K$	$\log_{10}K - \overline{\log_{10}K}$
(1,1)	4.20	10,857	4.03571	.20312
(1,2)	4.25	10,986	4.04085	.20826
(1,3)	3.95	10,211	4.00906	.17647
(1,4)	3.50	9,048	3.95653	.12394
(1,5)	3.20	8,272	3.91761	.08502
(2,1)	3.75	9,694	3.98649	.15390
(2,2)	3.60	9,306	3.96876	.13617
(2,3)	3.40	8,789	3.94394	.11135
(2,4)	3.10	8,014	3.90382	.07123
(2,5)	2.80	7,238	3.85962	.02703
(3,1)	3.05	7,884	3.89676	.06417
(3,2)	2.70	6,980	3.84382	.01123
(3,3)	2.50	6,463	3.81040	-.02219
(3,4)	2.30	5,946	3.77419	-.05840
(3,5)	2.05	5,299	3.72421	-.10838
(4,1)	2.20	5,687	3.75488	-.07771
(4,2)	2.00	5,170	3.71349	-.11910
(4,3)	2.00	5,170	3.71349	-.11910
(4,4)	1.95	5,041	3.70250	-.13009
(4,5)	1.95	5,041	3.70250	-.13009
(5,1)	1.95	5,041	3.70250	-.13009
(5,2)	2.00	5,170	3.71349	-.11910
(5,3)	2.00	5,170	3.71349	-.11910
(5,4)	2.05	5,299	3.72421	-.10838
(5,5)	1.95	5,041	3.70250	-.13009

$\overline{\log_{10}K} = 3.83259$ $\quad \sigma_{\log_{10}K} = 0.12263$ $\quad K_{\overline{\log_{10}K}} = 6{,}801\ gpd/ft^2$

deviation of the field. The logarithmic mean hydraulic conductivity was 3.83259. The logarithmic standard deviation was 0.12263.

3. Determination of the correlation function of the hydraulic conductivity field

The deviation of the logarithm hydraulic conductivities of each cell from the logarithmic mean hydraulic conductivity is given in Table IV-1 and also illustrated in Figure IV-7 below. These deviations and the distance between the centers of the 25 cells in the field are used to compute the correlation function.

The computation procedure is summarized as follows:

1. Compute the distance between the center of each cell and the center of every other cell in the field. For example, the distance between the center of Cell (1,1) and the center of Cell (2,3) is ($\sqrt{1^2 + 2^2}$ * 1/2 mile =) 1.12 miles.
2. Group those pairs of cells having the same distance and the same directional orientation between them into clusters. Using these criteria, cell pair (1,1) and (1,3) would be in the same cluster as cell pair (2,1) and (2,3), because the distance for each pair is one mile and the directional orientation is within the same row, 1 and 2, respectively. Note that cell pair (1,1) and (1,3) is considered the same as cell pair (1,3) and (1,1), because the mathematical product of their deviations is the same in both cases. No

(1,1) .20312	(1,2) .20826	(1,3) .17647	(1,4) .12394	(1,5) .08502
(2,1) .15390	(2,2) .13617	(2,3) .11135	(2,4) .07123	(2,5) .02703
(3,1) .06417	(3,2) .01123	(3,3) -.02219	(3,4) -.05840	(3,5) -.10838
(4,1) -.07771	(4,2) -.11910	(4,3) -.11910	(4,4) -.13009	(4,5) -.13009
(5,1) -.13009	(5,2) -.11910	(5,3) -.11910	(5,4) -.10838	(5,5) -.13009

0.00000 - Deviations from the mean
(0,0) - Cell # (row, column)

Figure IV-7. Individual cell deviations from the logarithmic mean of hydraulic conductivity

duplication of cell pairs is then necessary in the computations.

3. Compute the correlation coefficient of the deviations from the logarithmic mean for each of the clusters. The equation for the correlation coefficient of the deviations from the logarithmic mean for each cluster is given below by Equation IV-1.

$$r_{xyc} = \frac{\sum_{i=1}^{N_c} (x_i - \bar{x})(y_i - \bar{y})}{\sqrt{\sum_{i=1}^{N_c} (x_i - \bar{x})^2} \sqrt{\sum_{i=1}^{N_c} (y_i - \bar{y})^2}} \qquad \text{(Eq. IV-1)}$$

where,

r_{xyc} = correlation coefficient of cluster c;

$i = 1,2,3\ldots, N_c$, where N_c = total number of cell pairs in cluster c;

x_i = deviation from the logarithmic mean for the cell of the cell pair closest in distance to cell (1,1); note that when both cells of the cell pairs are an equal distance from cell (1,1), the assignment of the cells as either an x_i or y_i cell should be in a sequentially compatible order with the other cell pairs;

$\bar{x} = (\sum_{i=1}^{N_c} x_i)/N_c$ = mean deviation of the x_i's;

y_i = deviation from the logarithmic mean for the cell of the cell pair farthest in distance from cell

(1,1);

$\bar{y} = (\sum_{i=1}^{N_c} y_i)/N_c$ = mean deviation of the y_i's.

In a five-by-five cell matrix, there are 40 different clusters. Table IV-2 identifies each of these clusters by listing a cell pair contained in each distinct cluster and the number of cell pairs in that cluster. The distance and correlation coefficient associated with each cluster are also presented in Table IV-2.

4. Compute average correlation coefficients for distances associated with more than one cluster. Table IV-2 also contains the average correlation coefficients for each distance. The average correlation coefficient for a distance is an approximation for the correlation coefficient of an isotropic field. The TBM model assumes the hydraulic conductivity field is isotropic. A truly isotropic field would have the same correlation coefficient at a given distance between cells, regardless of directional orientation. The different correlation coefficients for the same distance in Table IV-2 shows that the sample field is not truly isotropic; however, the average correlation coefficient does show a trend, when graphed against distance, as in Figure IV-8 below. This plot shows that the average correlation coefficient, in general, decreases as the distance between cell pairs increases.

Table IV-2. Hydraulic conductivity correlation coefficients

Cluster #	Sample Cell Pair	# of Cell Pairs	Distance Between Cells, Miles	Correlation Coefficient, r	Average Correlation Coefficient, $\bar{r}$
1	(1,1),(1,2)	20	0.50	0.986	
2	(1,1),(2,1)	20	0.50	0.901	0.944
3	(1,1),(2,2)	16	0.71	0.849	
4	(1,2),(2,1)	16	0.71	0.936	0.893
5	(1,1),(1,3)	15	1.00	0.969	
6	(1,1),(3,1)	15	1.00	0.712	0.841
7	(1,1),(2,3)	12	1.12	0.803	
8	(1,1),(3,2)	12	1.12	0.666	
9	(1,3),(2,1)	12	1.12	0.958	
10	(1,2),(3,1)	12	1.12	0.751	0.795
11	(1,1),(3,3)	9	1.41	0.603	
12	(1,3),(3,1)	9	1.41	0.790	0.697
13	(1,1),(1,4)	10	1.50	0.946	
14	(1,1),(4,1)	10	1.50	0.455	0.701
15	(1,1),(2,4)	8	1.58	0.750	
16	(1,1),(4,2)	8	1.58	0.159	
17	(1,4),(2,1)	8	1.58	0.983	
18	(1,2),(4,1)	8	1.58	0.433	0.581
19	(1,1),(3,4)	6	1.80	0.512	
20	(1,1),(4,3)	6	1.80	-0.191	
21	(1,4),(3,1)	6	1.80	0.809	
22	(1,3),(4,1)	6	1.80	0.658	0.447
23	(1,1),(1,5)	5	2.00	0.906	
24	(1,1),(5,1)	5	2.00	-0.022	0.442
25	(1,1),(2,5)	4	2.06	0.711	
26	(1,1),(5,2)	4	2.06	0.563	
27	(1,5),(2,1)	4	2.06	0.995	
28	(1,2),(5,1)	4	2.06	-0.919	0.338
29	(1,1),(4,4)	4	2.12	-0.399	
30	(1,5),(4,2)	4	2.12	0.726	0.164
31	(1,1),(3,5)	3	2.24	0.771	
32	(1,1),(5,3)	3	2.24	0.934	
33	(1,5),(3,1)	3	2.24	0.884	
34	(1,3),(5,1)	3	2.24	-0.906	0.421
35	(1,1),(4,5)	2	2.50	0.000	
36	(1,1),(5,4)	2	2.50	-1.000	
37	(1,5),(4,1)	2	2.50	1.000	
38	(1,4),(5,1)	2	2.50	-1.000	—[a]
39	(1,1),(5,5)	1	2.83	0.000	
40	(1,5),(5,1)	1	2.83	0.000	—[a]

[a] Sample size too small.

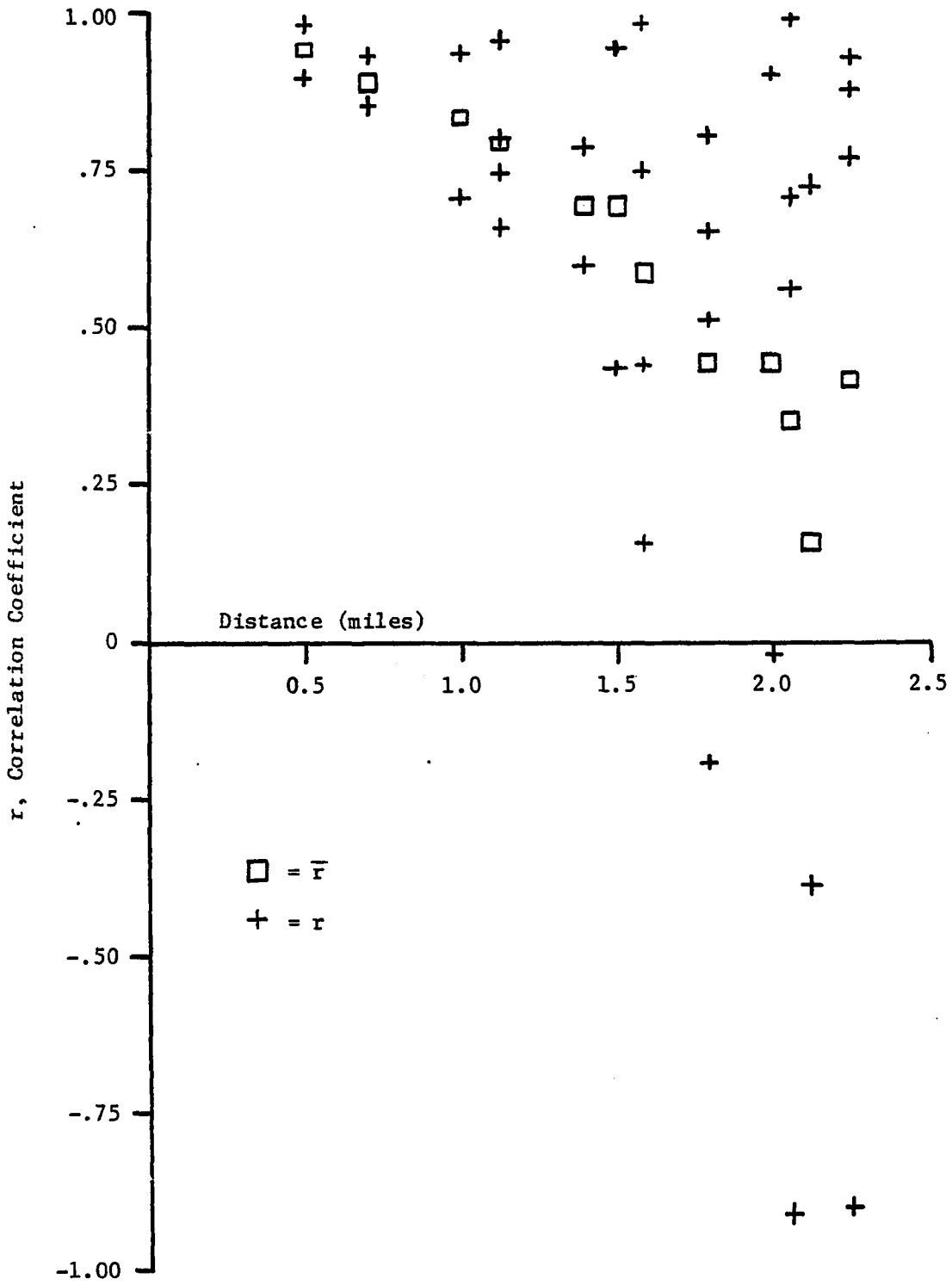

Figure IV-8. Hydraulic conductivity correlation coefficient versus distance

5. Determine the correlation function. Several mathematical equations are able to represent a decreasing function that starts with a value of 1.0. In this investigation, a negative double exponential function has been chosen to represent the correlation function. This function is given by Equation IV-2 below:

$$r = e^{-b^2 d^2} \qquad \text{(Eq. IV-2)}$$

where,

r = average correlation coefficient;

b = the inverse of the correlation length, miles^{-1}; and

d = distance between cell pairs, miles.

The value of b was determined by a least squares analysis. First, Equation IV-2 was transformed by taking the natural logarithm of both sides of the equation. The transformed equation is linear when the natural logarithm of r is graphed versus d^2. This is a straight line which goes through the origin with a slope of $-b^2$. Figure IV-9 is a plot of the natural logarithm of the average correlation coefficient computed previously versus the corresponding d^2. Because the straight line is forced to go through the origin, the value of the slope, $-b^2$, is simply the sum of the natural

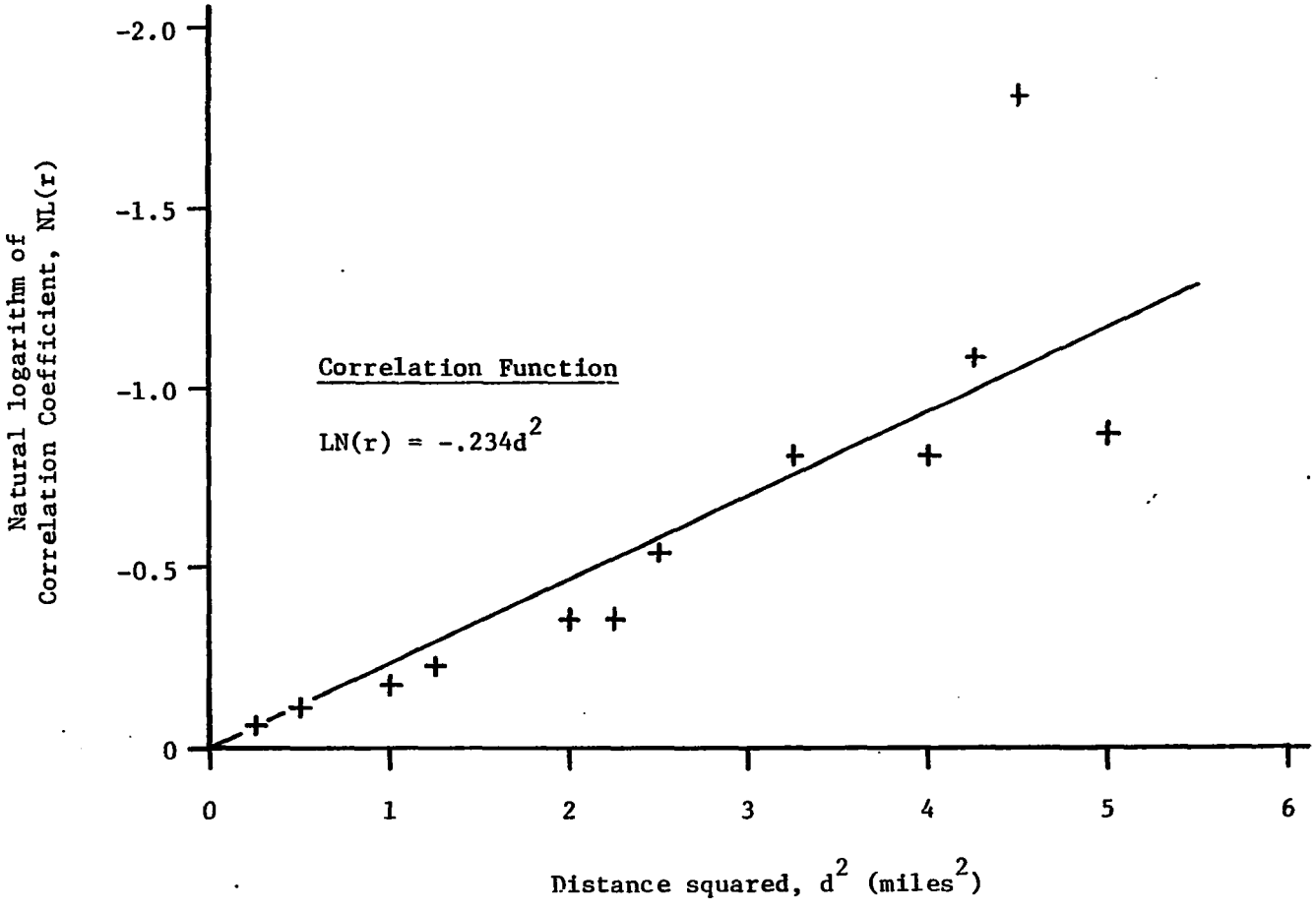

Figure IV-9. Natural logarithm of hydraulic conductivity correlation coefficient versus distance squared

logarithms divided by the sum of the d^2 terms. The value of $-b^2$ was computed to be -0.234, which gives a b value of 0.484. Figure IV-10 shows a plot of the selected correlation function, using r and d^2 as the axes. This particular mathematical function was selected primarily because of its close fit to computed values of r for small values of d^2. The values of r for small values of d^2 were considered to have more validity than those with large values of d^2 because their sample size was larger.

The value of the correlation length, 1/b, the length over which hydraulic conductivity is correlated, is 2.07 miles. This is slightly less than the length of the groundwater field, 2.5 miles. Ideally, the correlation length should be greater than the length of the generated field because the accuracy of the correlation function decreases with distances greater than the correlation length. As will be seen in Chapter V, the pollutant never moves more than one mile in the modeled disposal events; therefore, the accuracy of the correlation function at large distances is not an important factor in the results.

E. Calibration of the Groundwater Flow-Mass Transport Model with Field Data

The tritium concentrations and groundwater levels collected by the USGS in and around the INEL property from observation wells were used to

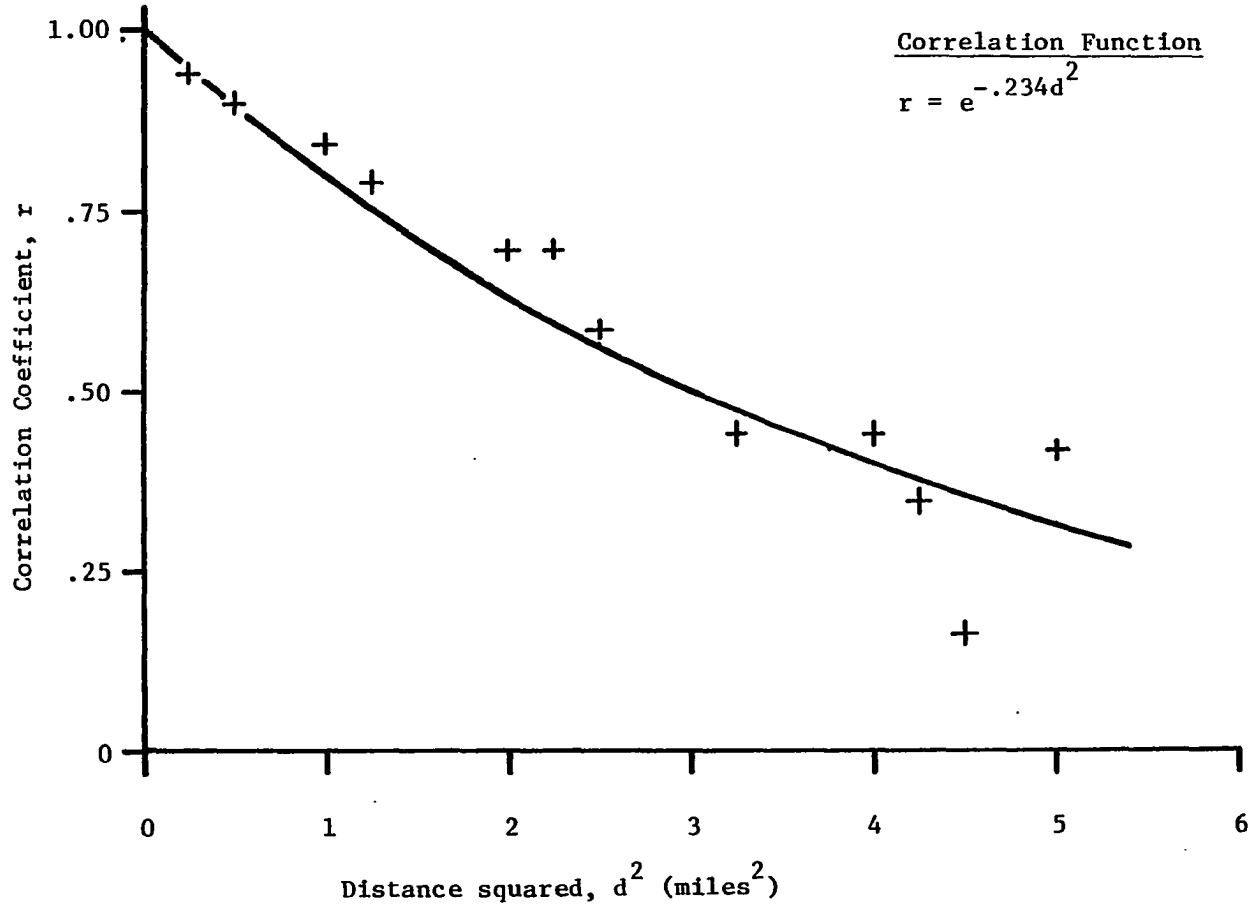

Figure IV-10. Hydraulic conductivity correlation coefficient versus distance squared

determine the time and space boundary limits for the groundwater flow and mass transport model. Other input parameters to the model, such as the grid interval distance and computational time increment, are then chosen after the boundary limits have been selected.

1. Spatial and temporal boundary limits

Figure IV-11 presents the observed tritium concentrations at Well #40, Well #37, Well #85 and Well CFA #1 from 1976 through 1982. These observation points may be connected in order to provide a relatively straight linear path for examining the change in tritium concentration over time. The ICPP monthly tritium waste load concentrations are also presented in this figure. These values were obtained by dividing the monthly waste loads by the monthly volume flow rates shown in Figure IV-5.

One may observe that the peak tritium concentrations at Well #40, the observation well closest to the disposal well, are somewhat smaller and occur slightly later than the peak concentrations at the disposal well. This relationship between concentration rates at these two wells was expected and is consistent with a dispersing constituent plume. The tritium concentration data from Well #37 shows three flattened peaks, but whether these peak concentrations are necessarily causally correlated with the ICPP disposal events between 1976 and 1982 or are caused by movement of the larger plume from disposal events prior to 1976 is not evident from Figure IV-11 alone. The observed tritium

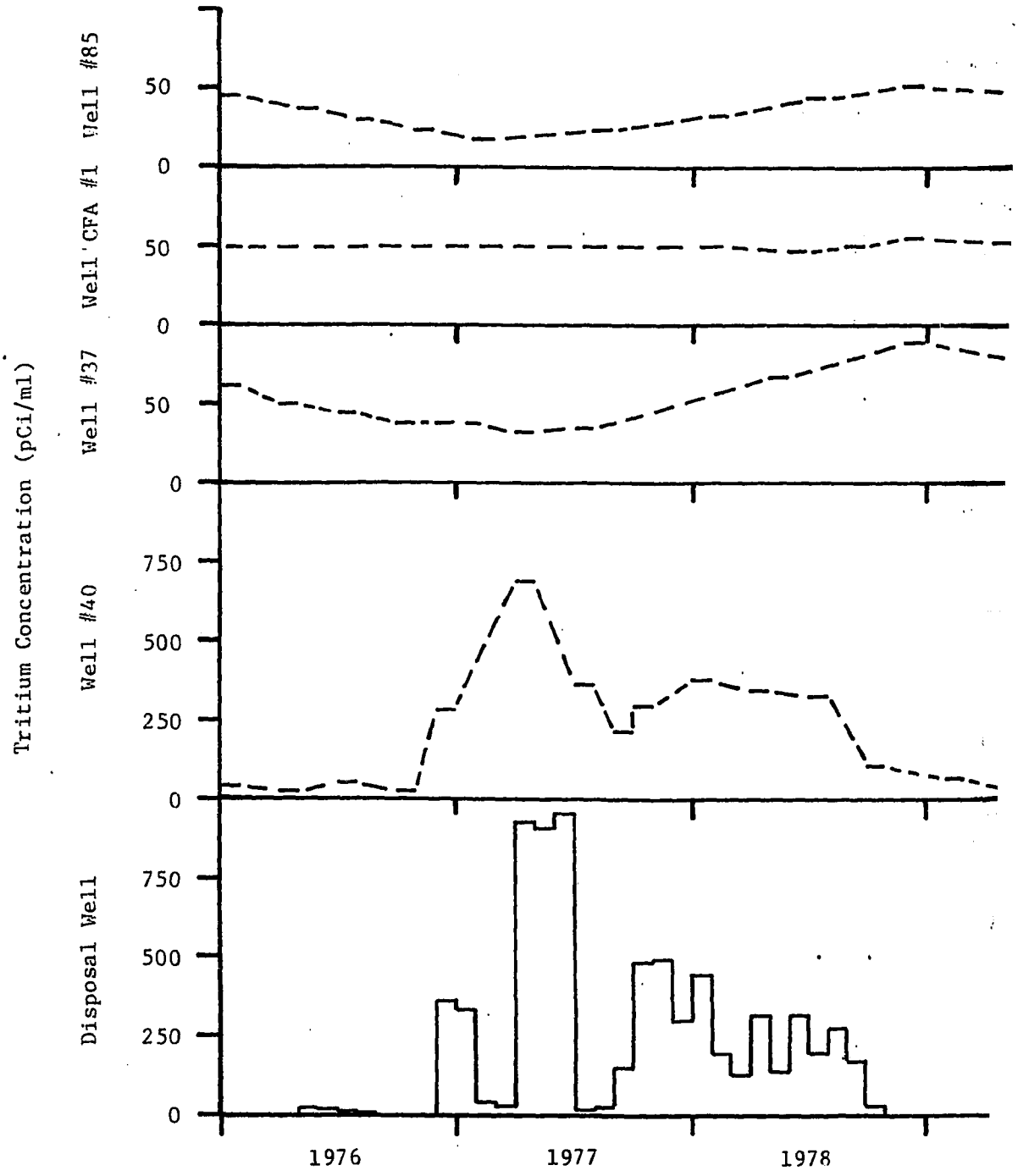

Figure IV-11. Tritium concentration, 1976-1982

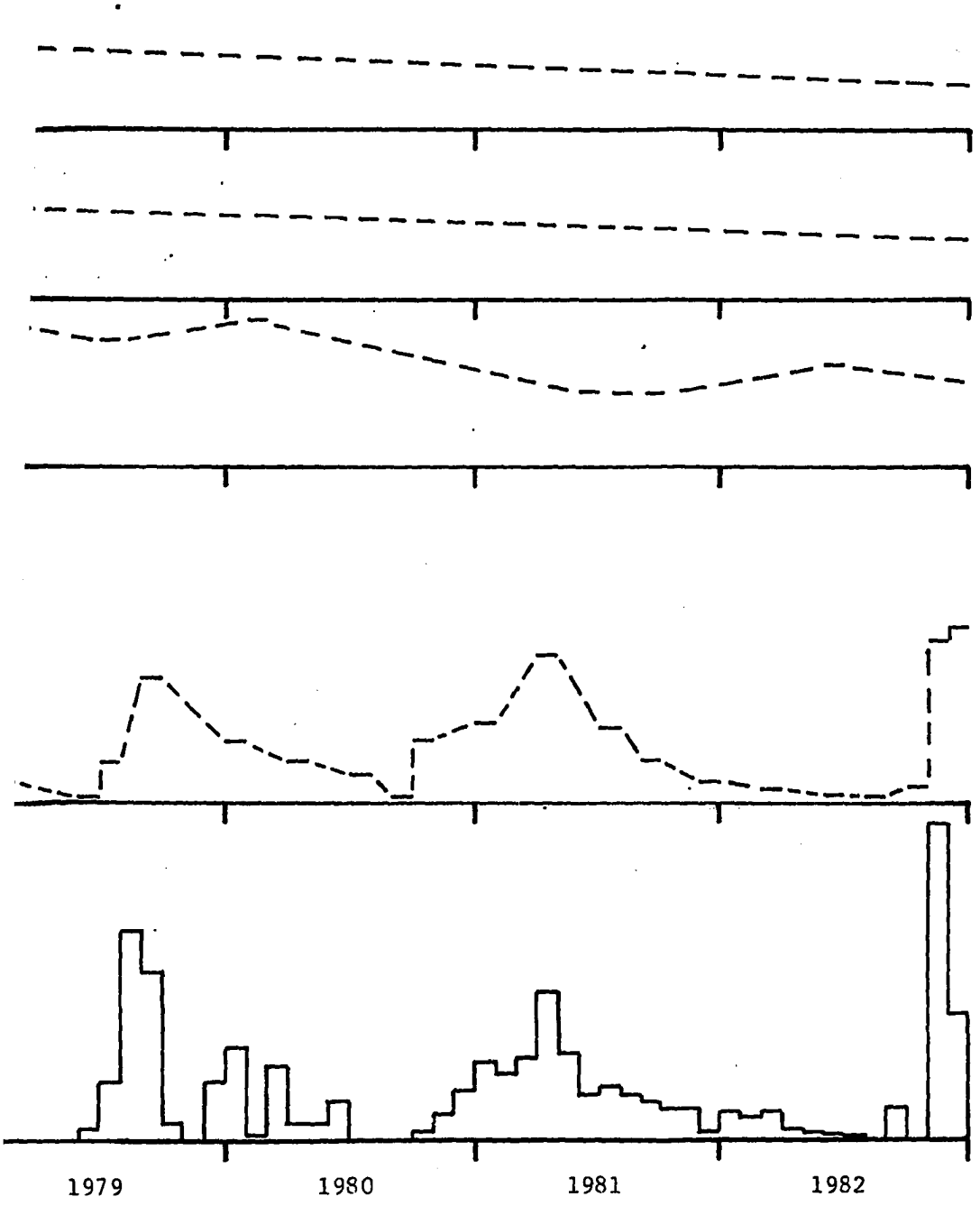
1979
1980
1981
1982
Time

concentrations at Well #85 and Well CFA #1 indicate fairly constant behavior. As these two wells are the farthest from the disposal well, the conclusion was made that the tritium disposed between 1976 and 1982 either had not yet reached these wells or, if it had, the concentration rate was so small as to be inconsequential. Therefore, the spatial area selected for calibration contained only the disposal well, Well #40 and Well #37 within its boundaries.

Groundwater elevations were available for Well #40, Well #37 and Well #85 from 1976 through 1982 and are plotted in Figure IV-12 below. The groundwater table at all three wells show a general decline during 1976, 1977 and 1978. From 1979 through 1982, the regional water table is relatively stable and could be considered to be in a steady-state condition during the two tritium disposal events in 1979-80 and 1981-82. If steady-state regional groundwater flow conditions are assumed, the proposed model is greatly simplified compared to unsteady flow conditions.

Therefore, a decision was made to use the tritium disposal events from 1979 through 1982 for the calibration of the groundwater flow-mass transport model. This time period was also selected because it was the only occasion that steady-state regional groundwater conditions coincided with accurate waste flow rate and tritium loadings data from the Westinghouse Idaho Nuclear Company. This time period also contained two major disposal sequences. By trying to match two pollutograph

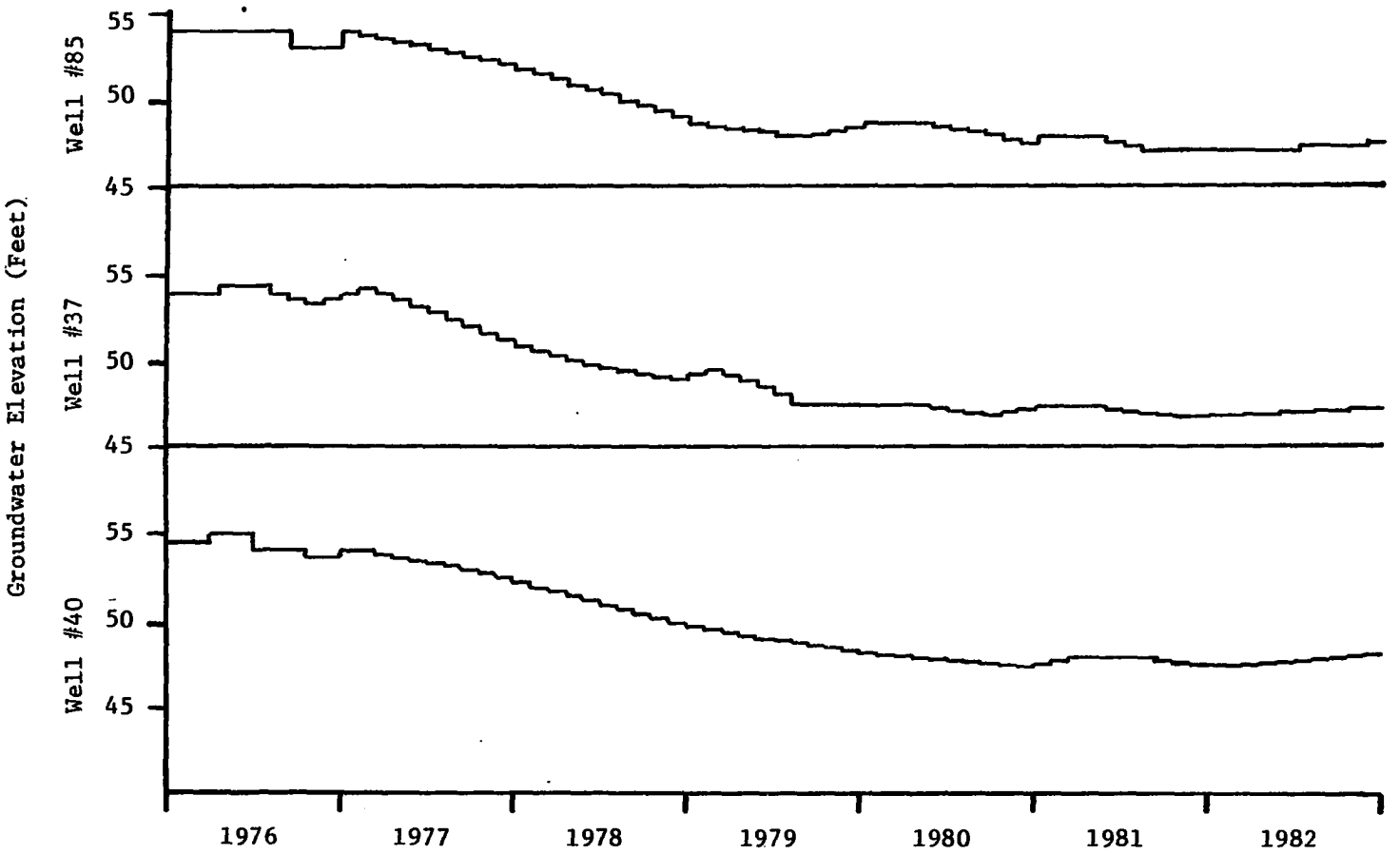

Figure IV-12. Groundwater elevations, 1976-1982

peaks, the calibrated model will have less chance of its parameters being skewed by a single pollutograph peak. By using the most accurate pollutant data and a relatively simple hydrologic situation for calibration purposes, this investigator hoped to be able to simulate quite closely the observed pollutographs at Well #40 and Well #37.

2. Determination of grid interval, computational time increment and other input parameters to the model

A grid network was developed for the model which included the disposal well, Well #40 and Well #37 within its boundaries. Figure IV-13 shows the layout of the network. There are 20 rows and 20 columns in the network, with a grid interval of 660 feet. The total network area is 6.25 square miles, a square with 2.5 miles as the boundary length of all sides. The actual transmissivity values of the Snake River Plain aquifer at each nodal point were used for the calibration process because they increased the accuracy of the calibrated results. The actual transmissivity values were obtained from the transmissivity map developed by the USGS, which has been discussed previously.

The computational time increment was selected to be 30 days or approximately one month. Because the tritium disposal loads and waste volume flow rates were published as monthly values, the 30-day time increment was a choice of convenience. As 30 days is not exactly one month, one might be concerned about observed and computed tritium values being slightly out of synchronization. With a modeling time span of four years, there would be 17 days difference between observed and

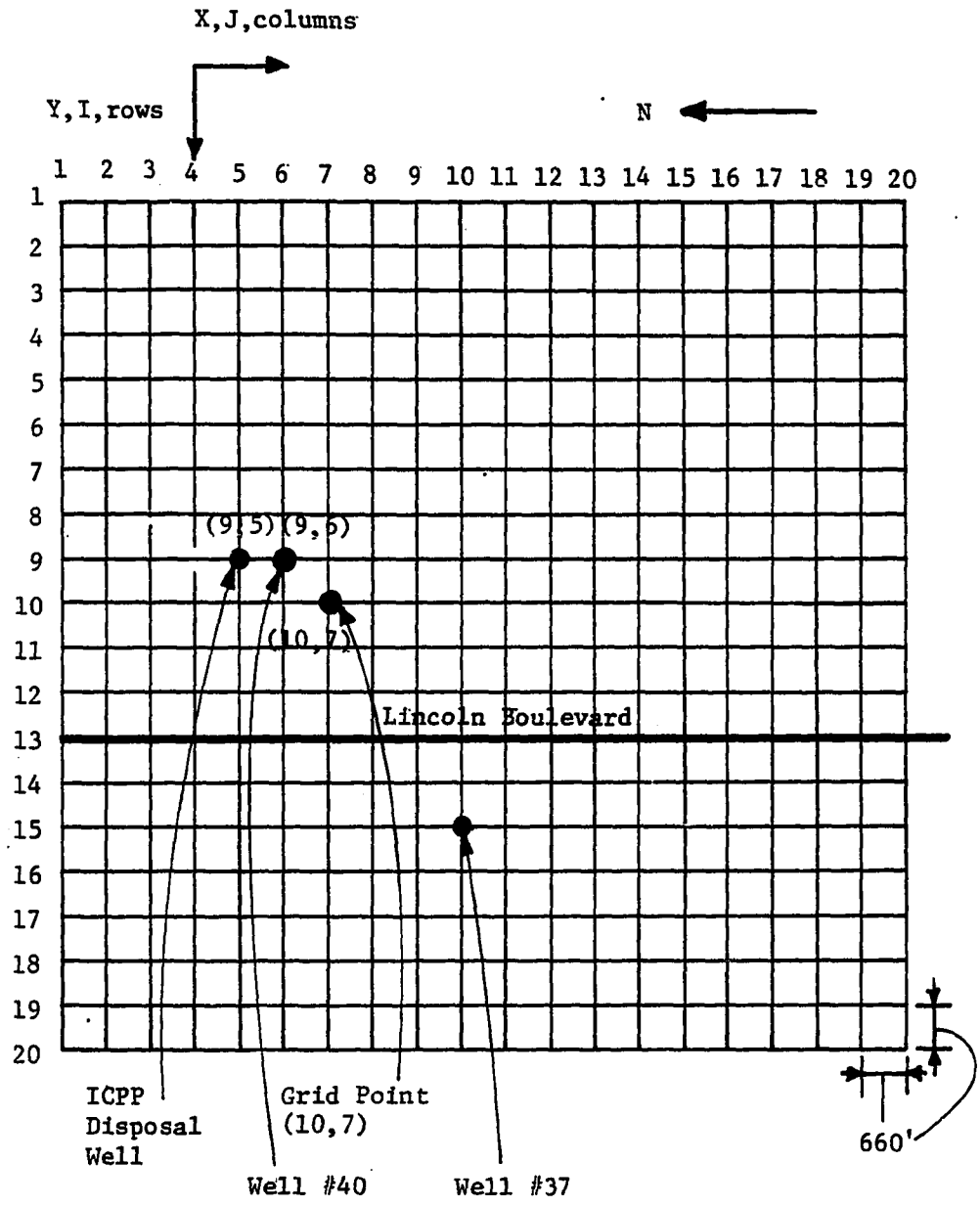

Figure IV-13. Grid network layout

computed values. Given the level of precision acceptable in this kind of modeling and that the computed values were for 30 day increments, this effect was considered to be negligible.

Other input parameters to the model considered the disposal well to be a point source input and the aquifer to be a constant thickness of 250 feet with an effective porosity of 0.10.

3. Determination of hydraulic gradients

In the general case, the hydraulic gradients of an aquifer vary with unsteady flow conditions. As discussed in Chapter III previously, a finite-difference computer algorithm may be used to determine the hydraulic head distribution as a function of time for unsteady flow conditions. Because the hydraulic head distribution during the time of the calibrated disposal event could be identified with steady-flow conditions, the use of the finite-difference computer subroutine became unnecessary. A simpler method to compute hydraulic gradients was adopted instead.

The hydraulic head distribution was determined by estimating a regional hydraulic gradient for the area containing the tritium disposal plume with a plane surface. On top of the plane surface, a cone of impression around the disposal well was superimposed on the plane representing the regional hydraulic gradient in order to represent the effect of the flow volume of tritium waste on the hydraulic head distribution. Through a process of trial and error in calibration runs, values were selected for the regional hydraulic gradient plane and the

waste flow volume cone of impression which were modified from initially selected amounts. The initial values were modified in order to increase the accuracy of simulating the observed pollutographs. The following discussion describes how the regional hydraulic gradient and cone of impression were modified.

As described previously, groundwater level information was available for Well #40, Well #37 and Well #85. Using the three average water table elevations of the wells from 1979 through 1982 the equation of a plane surface through these points was computed. The resulting plane surface had a gradient of 0.0000909 ft/ft in a direction parallel to Lincoln Boulevard between the TRA area and the ICPP area shown in Figure IV-4. The gradient of the groundwater surface perpendicular to Lincoln Boulevard was 0.0000455 ft/ft. Initially, this plane surface was adopted as the regional hydraulic gradient. The selected regional hydraulic gradient after the calibration process was the same as the initial assumption for the gradient perpendicular to Lincoln Boulevard, but was increased by one third to a value of 0.000121 ft/ft in the direction parallel to Lincoln Boulevard in order to increase the calibration accuracy.

It was decided that initially the representation of the cone of impression around the disposal well would be simple and would increase in complexity only if an increase in accuracy in simulating the observed pollutograph was obtained. At first, the calibration process used a cone of impression for the node representing the disposal well equal to

a steady-state value 1.0 foot of head increase and no head increases at all other nodes. The one foot value is approximately the height of the cone of impression for the average flow rate from the disposal well between 1976 and 1982 using a 12-inch well diameter, the actual transmissivity at the disposal well and a cone of impression extending 10,000 feet from the disposal well. The 10,000-foot cone of impression is recommended as a starting value by the Illinois State Water Survey in their groundwater flow-mass transport model. Eventually, the accuracy of the computed pollutographs, when compared to the observed tritium concentrations at Well #40, was significantly increased by using "semi-steady state" head increase values at and around the disposal well. The selected head increases were developed using a modified Theim equation for equilibrium groundwater flow conditions as shown in Equation IV-3 below:

$$z_{ijt} = \frac{q_t \ln(r_o/r_{ij})}{2\pi T} \qquad \text{(Eq. IV-3)}$$

where,

z_{ijt} = height of cone of impression at node (i,j) for time period t;

q_t = injection volume flow rate for time period t;

ln = natural logarithm;

r_o = distance from the disposal well to the location where the head increase equals zero;

r_{ij} = distance from the disposal well to node (i,j);

π = 3.14....;

T = the average transmissivity of the four transmissivity values between the disposal well and adjacent nodes.

The height of the cone of impression on top of the regional piezometric head at a specific location varies as a function of the term (r_o/r_{ij}). Various sets of values of (r_o/r_{ij}) were used in the calibration runs. The final, selected set of values for (r_o/r_{ij}) in the calibration process assumed that $(r_o/r_{\text{disposal well}})$ was 20,000. This value is equivalent to having a 12-inch diameter injection well and a cone of impression extending 10,000 feet from the disposal well. Even though the transmissivity near the disposal well is somewhat larger than the average transmissivity of the modeling field, the use of this value had a negligible effect on the accuracy of the computation of head increases at nodes further removed from the disposal well. The selected head increases were recomputed at 30 day intervals in order to be compatible with the monthly flow rates from the disposal well. The head increases during the 1979-82 time period generally ranged from 0.5 feet to 1.5 feet at the disposal well for the selected $(r_o/r_{\text{disposal well}})$ value of 20,000. No attempt was made to determine hydraulic head distributions and hydraulic gradients using the assumption of the more complex unsteady state analysis because the calibration results using the "semi-steady state" were considered to be adequate.

4. Determination of longitudinal and transverse dispersivities

Initially, longitudinal and transverse dispersivities used by the Idaho District USGS in previous studies of the tritium plume were used

in the calibration process. After correcting for different directional alignments in the USGS's and this investigation's modeling grids, the initial longitudinal dispersivity, α_L, was computed to be 412.5 feet and the initial transverse dispersivity, α_T, was computed to be 350 feet. The results using these dispersivities, the modified Theim equation heads, the regional hydraulic gradients and the logarithmic mean hydraulic conductivity at all nodes are presented in Figure IV-14. The logarithmic mean hydraulic conductivity was used to be consistent with the input parameter values of the previous USGS studies. One observes that the shape of the computed pollutograph at Well #40 is radically different than that observed. This observation does not mean that the USGS model is necessarily inaccurate. The USGS reports do indicate an accurate description of the tritium plume movement over a much longer time period and larger area than addressed in this investigation. This observation indicates only that the dispersivities used by the USGS should not be used for modeling short periods of time at locations close to the disposal well. By calibration runs using various similar ratios of longitudinal and transverse dispersivities, dispersivity values of α_L = 8.25 feet and α_T = 7.00 feet were selected. Each of these dispersivities is fifty times smaller than its USGS counterpart.

5. Calibration of the tritium disposal events from 1979 to 1982

Figure IV-15 shows three pollutographs at Well #40 developed with the selected parameters of the groundwater flow-mass transport model chosen in the calibration process. The selected parameters are

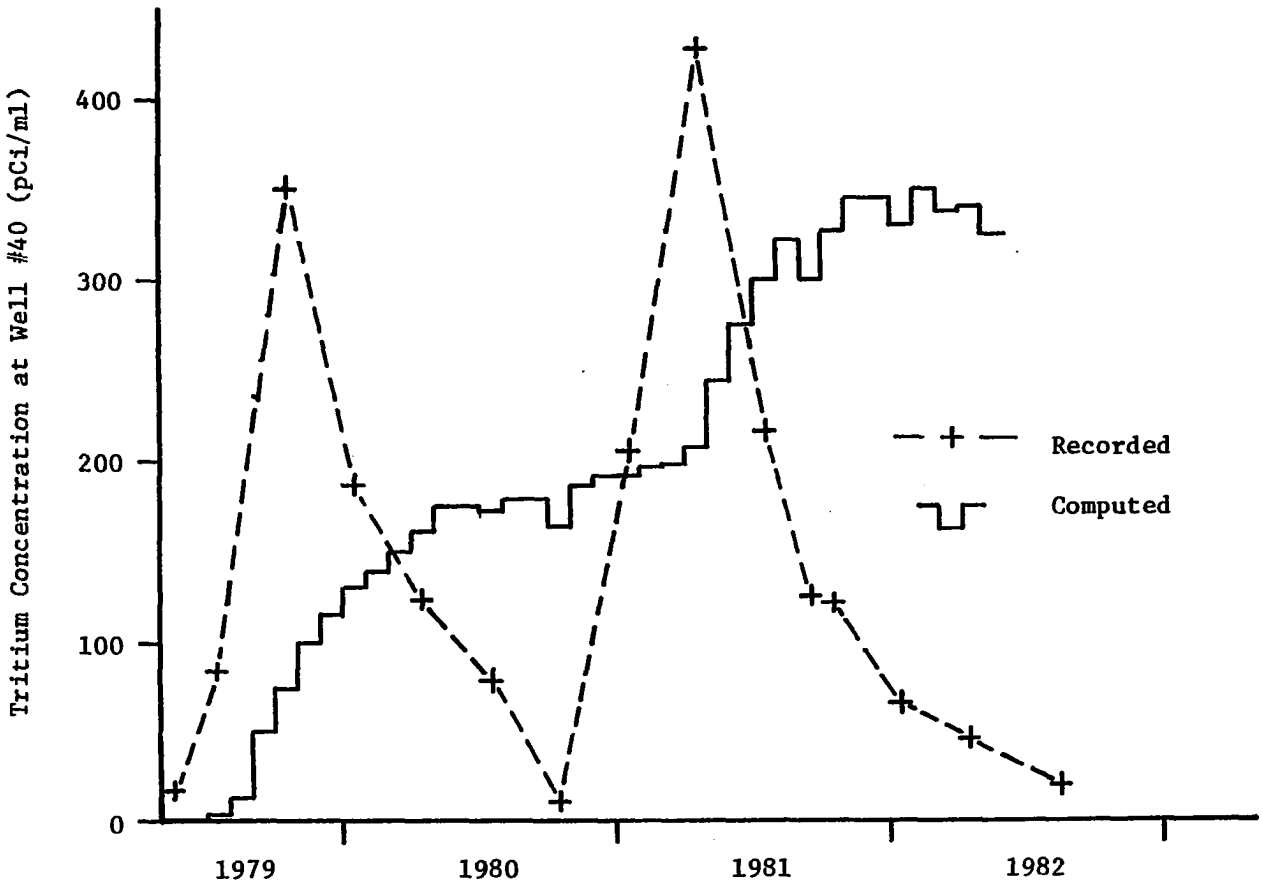

Figure IV-14. Pollutograph using α_L = 412.5 feet and α_T = 350 feet

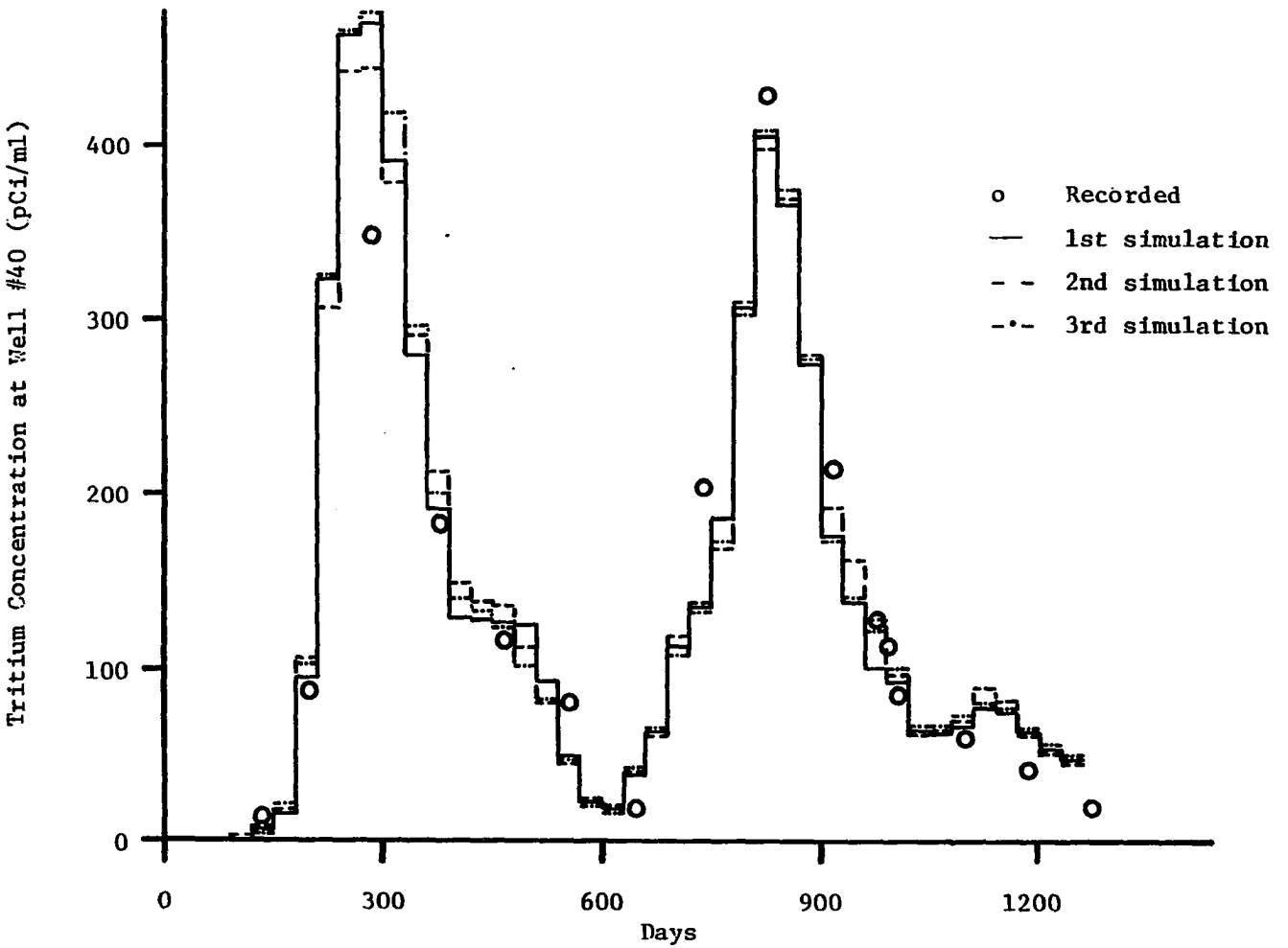

Figure IV-15. Tritium pollutograph at Well #40, 1976-1982

summarized in Table IV-3 below. Because the mass transport portion of the model uses a random number generator in the dispersion simulation procedure, each simulation for a given set of input parameters is unique; however, the difference between simulations is relatively minor compared to the difference in simulated pollutographs caused by modifications of other input parameters.

The actual hydraulic conductivities between each pair of nodes were selected instead of the logarithmic mean hydraulic conductivity, and selected dispersivities 50 times smaller than the USGS values were also used. This selection would be consistent and tend to substantiate Smith and Schwartz's contention that field dispersion is primarily due to variability in hydraulic conductivity rather than large values of dispersivity in the aquifer.

No calibration results were obtained at Well #37. In nearly all of the calibration runs, tritium from the 1979-82 disposal events never reached the location of Well #37; therefore, a tentative conclusion has been reached that the peaks in Well #37 from 1979-82 were due to previous disposal events.

Table IV-3. Groundwater flow-mass transport parameters selected by the calibration process

Parameter	Value	Unit
Grid Rows	20	-
Grid Columns	20	-
Grid Interval	660	feet
Time Interval	30	days
Time Duration	1979-1982	years
Transmissivity	Actual values at each node	gpd/ft
Regional Hydraulic Gradient		
N-S direction	.000121	ft/ft
E-W direction	.0000455	ft/ft
Height of cone of impression due to modified Theim equation	Varies with time and location	ft
$(r_o/r_{\text{disposal well}})$	20,000	ft/ft
Longitudinal dispersivity, α_L	8.25	feet
Transverse dispersivity, α_T	7.00	feet

V. MULTIPLE REALIZATIONS OF A DISPOSAL EVENT

The 1979-1980 tritium disposal event was selected for development of probability distributions for time of arrival and tritium concentration versus duration of exposure. This disposal event is the first of two major disposal sequences for the 1979-1982 time period used in the calibration process. A disposal event not involved in the calibration process was not selected for the development of probability distribution. The accuracy of the tritium loadings before 1976 was suspect and outside of the 1979-1982 time period, the regional groundwater system was not under steady state conditions. Only this one recorded disposal event was selected in order to simplify the analysis and minimize computation costs.

A. Selection of Input Parameter Values

Tables V-1 and V-2 summarize the input parameter values for the TBM model and transport model, respectively. Table V-3 lists the monthly tritium loads and injection flow rates used by the transport model. A discussion of the reasoning for using the selected values follows.

1. Selection of TBM grid interval

Initially, multiple realizations using a 20 row-by-20 column grid were proposed for both the Turning Bands Method and the groundwater flow-mass transport model. After examining the first few realization results of the TBM model, which generated hydraulic conductivity fields

Table V-1. TBM model input parameter values

Parameter	Symbol	Value	Units
Number of realizations	NS	Varies, typically 10	-
Maximum distance in x-direction	XMAX	2.4583[a]	miles
Maximum distance in y-direction	YMAX	2.4583[a]	miles
Number of rows	NX	60	-
Number of columns	NY	60	-
Mean log of hydraulic conductivity	AM	3.83259	(gpd/ft^2)
Standard deviation of hydraulic conductivity	S	0.12263	(gpd/ft^2)
Inverse of the correlation length of the double exponential function	BI	0.484	$miles^{-1}$
Number of TBM lines	L	16	-
Maximum normalized discretization distance	DS	0.015	-
Number of additive terms	MMAX	40	-
Maximum frequency per correlation length	OMMAX	16.0	$miles^{-1}$

[a] $XMAX = YMAX = \frac{\text{Field Distance}}{\text{Number of rows (or columns)}} = \text{Number of grid intervals}$

$= \frac{2.50 \text{ miles}}{60} \times 59 = 2.4583 \text{ miles}.$

Table V-2. Groundwater flow-mass transport model input parameter values

Parameter	Symbol	Value	Units
Number of time increments	NSTEPS	1[a]	-
Time increment	DELTA	10^{10}[a]	Days
Allowable error in computed head	ERROR	0.1[a]	Ft
Number of particle movement time steps per time increment	NPITS	30	-
Number of pumps	NPUMP	1	-
Number of time increments per pumpage change	NSP	1	-
Number of rates in pumpage schedule	NRT	30	-
Total number of columns, I	NC	20	-
Total number of rows, J	NR	20	-
Column number of pump	IP	5	-
Row number of pump	JP	9	-
Column grid interval	DELX	660	Ft
Row grid interval	DELY	660	Ft
Time increment particles are allowed to move	DELP	30	Days
Total pollutant load	PL	331.9	Curies
Maximum number of particles	MAXP	1125	-
Particle mass	PM	0.3	Curies/ Particle
Longitudinal dispersivity	DISPL	8.25	Ft
Transverse dispersivity	DISPT	7.00	Ft
Elevation of bottom of aquifer	BOT	-242.0	Ft
Hydraulic head elevation for row J and column I	H(I,J)	Varies[b]	Ft
Theim equation head for column I, row J	Z(I,J,T)	Varies[c]	Ft
Effective porosity	EPOR	0.1	-
Actual porosity	APOR	0.1	-
Storage factor for water table aquifer	SF2	10^{30}[d]	Gal/Ft

[a] These values produce a steady-state head distribution.

[b] $H(I,J) = 8.85 + (.03 \times I) - (.08 \times J) + Z(I,J,T)$.

[c] This value changes with the change in volume flow rate for each 30 day time increment.

[d] This value maintains a constant head.

Table V-3. Monthly tritium loads and injection flow rates, 1979-1980

Time	Load (Curies)	Flow Rate (MGD)
1979 May	0	0
June	5.5	1.46
July	25.2	1.33
Aug	117.0	1.54
Sept	55.6	1.02
Oct	5.5	0.56
Nov	0.3	0.86
Dec	13.4	0.77
1980 Jan	23.0	0.72
Feb	1.0	1.00
Mar	21.3	0.86
Apr	10.0	0.99
May	7.9	0.78
June	11.5	0.83
July	0.5	0.95
Aug	0.3	1.25
Sept	0.9	1.19
Oct	4.8	1.29
Nov	20.0	1.55
Dec	8.2	1.70
TOTAL	331.9	

with standard deviations of the logarithm values only 25% of that desired, it was decided that the 400 nodes in the grid were insufficient. The developers of the TBM model had noted in their investigations that accuracy in obtaining the desired standard deviation increased as the number of nodes increased. A few trials with a 40 row-by-40 column grid (330-foot intervals) increased generated standard deviations by about 100%, but still resulted in unacceptably low standard deviations. The final, selected grid contained 60 rows by 60 columns (220-foot intervals) with a 900% increase in the number of nodes, from 400 to 3,600.

This selected grid generated standard deviations consistently above 0.10, compared to a desired standard deviation of 0.12. Increasing the grid size beyond 3,600 nodes was rejected because the increase in computational costs was not considered to be worthwhile for additional accuracy. For example, a 80 row-by-80 columnn grid would contain 6,400 nodes, almost double that of the 60 x 60 grid, but could be expected only to increase the generated standard deviations by 10%.

The difference in the grid interval between the TBM model, 220-foot interval, and the transport model, 660-foot interval, was reconciled by using hydraulic conductivities from every third row and column from the TBM output as input to the transport model. For example, the value for (row 1, column 1) in the TBM output would become the value of (row 1, column 1) in the transport model input. The values of (row 4, column 1) and (row 1, column 4) in the TBM output would become the transport input

values for (row 2, column 1) and (row 1, column 2), respectively. The logarithmic means of hydraulic conductivity for the 20 x 20 grids of realizations were within 0.1% of that of the corresponding 60 x 60 grid values. The logarithmic standard deviations of the 20 x 20 grids of realizations were also close to the corresponding 60 x 60 grid values. Correlation coefficients of the 20 x 20 grids and 60 x 60 grids contained similar boundaries over a large range of distances. Based on these observations, this systematic sampling procedure was assumed not to be significantly biased.

2. Selection of other TBM parameter values

The maximum normalized discretization distance was selected to be 0.015. The TBM model developers recommend that the discretization distance, $\Delta\zeta$, which is the maximum normalized discretization distance divided by the inverse of the correlation length, b, be less than the grid interval. In this case, the grid interval, 0.0417 miles, is greater than the discretization distance, (0.015/0.484 =) 0.0310 miles.

The number of additive terms, M, was selected to be 40 and maximum frequency per correlation length, Ω, was 16.0b. The developers of the TBM models recommend using M = 100 and Ω = 40.0b in order to insure good results for all situations. The smaller values used in this study were limited by a computer system constraint of $e^{\pm 75}$. Using M = 100 and Ω = 40b with a double exponential correlation function caused a computed value of e^{-400}, beyond the computer system limits. The error associated

with M = 40 and Ω = 16b increases when the distance between grid points decreases. At a distance of zero, the computed correlation coefficient is within approximately 10% of the theoretical correlation coefficient. This level of accuracy is similar to the accuracy of the reported transmissivities of the Snake River Plain aquifer and is considered sufficient for the objectives of this study.

3. Selection of the parameter values for the transport model

The parameter values listed in Tables V-2 and V-3 for the transport model remained constant for all realizations. There is some variation in the transport model results due to the random walk process; however, these variations are minor compared to the variations due to different hydraulic conductivity fields. Figure V-1 shows the pollutographs associated with three of the generated hydraulic conductivity fields. As can be visually observed, the pollutographs due to hydraulic conductivity fields vary considerably more than the variation due to the random walk process, shown in Figure IV-15.

B. Multiple Realization Results

One hundred realizations of the 1979-1980 tritium disposal sequence were generated. The logarithmic mean hydraulic conductivity of the 100 fields was 3.82766, 0.1% less than the estimated field value of 3.83259. The logarithmic standard deviation was 0.10584, approximately 14% less than the estimated value of 0.12263. The frequency distributions of

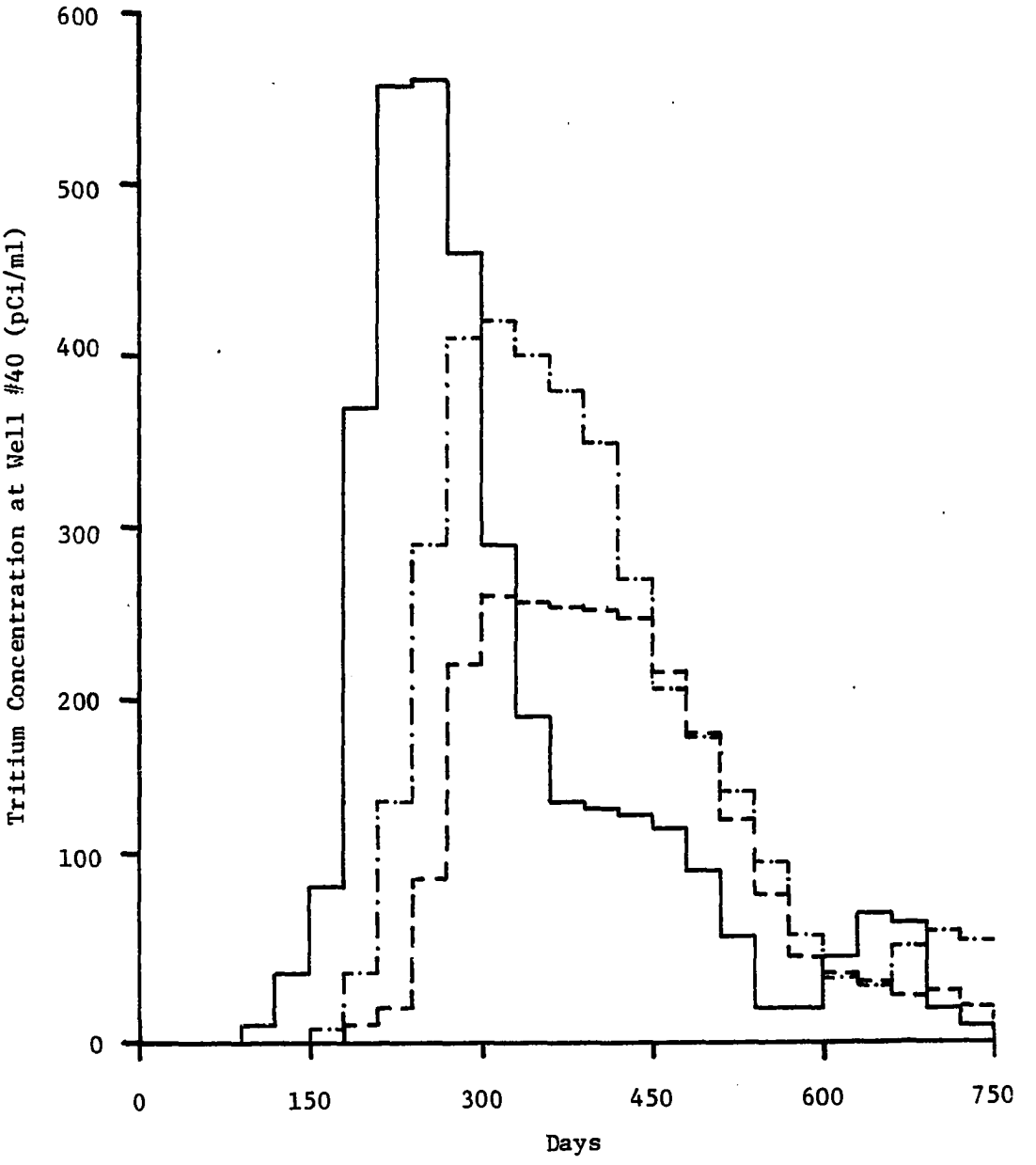

Figure V-1. Pollutographs for three hydraulic conductivity field realizations

time of arrival and tritium concentration versus duration of exposure for 100 realizations were tabulated and are presented in the following sections. Statistical tests were then performed on these frequency distributions in order to systematically describe the results and determine probabilities of occurrence.

1. Time of arrival distributions

Figures V-2 and V-3 show the frequency distributions for time of arrival at Well #40 and Grid Point (10,7), respectively. The time of arrival at Well #40 ranged from 90 to 270 days for the 100 realizations. At Grid Point (10,7) the time of arrival ranged between 210 days and above. In one realization, the tritium travels to the side of and never reaches Well #40 or the Grid Point. During 19 realizations, the tritium did not reach Grid Point (10,7) within 900 days. Table V-4 summarizes the statistical properties of these frequency distributions and shows the cumulative exceedance probability of time of arrival at Well #40 and Grid Point (10,7).

Table V-5 compares the actual observed cumulative exceedance probability for time of arrival to a theoretical cumulative exceedance probability. The theoretical values are obtained by assuming a Pearson Type III distribution. The mathematical form of the Pearson Type III distribution is given below:

$$X = \overline{X} + K\sigma \qquad \text{(Eq. V-1)}$$

where,

X = time of arrival in days for exceedance probability p;

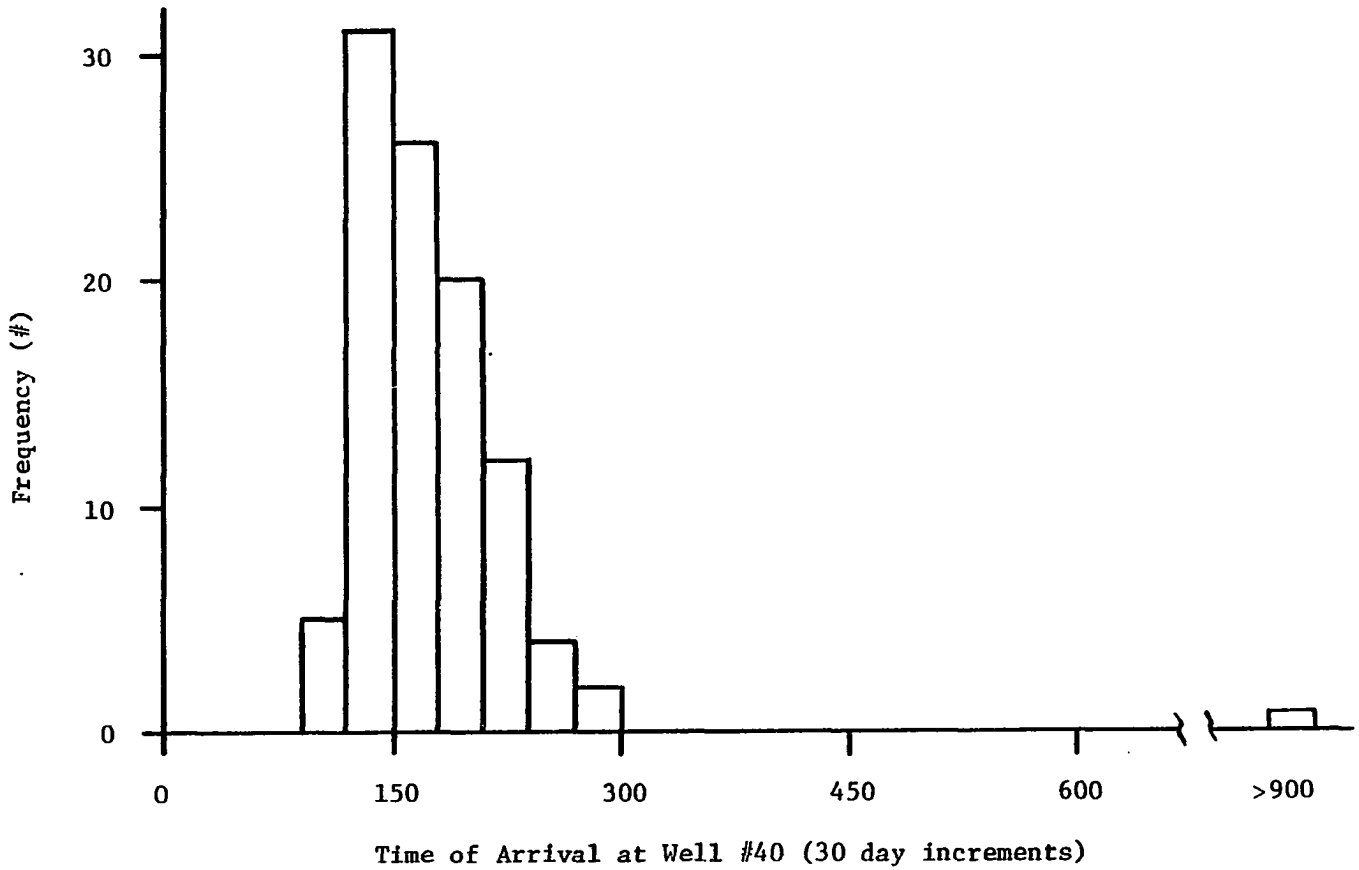

Figure V-2. Frequency of time of arrival at Well #40, 660 feet downstream of the disposal well, for 100 realizations

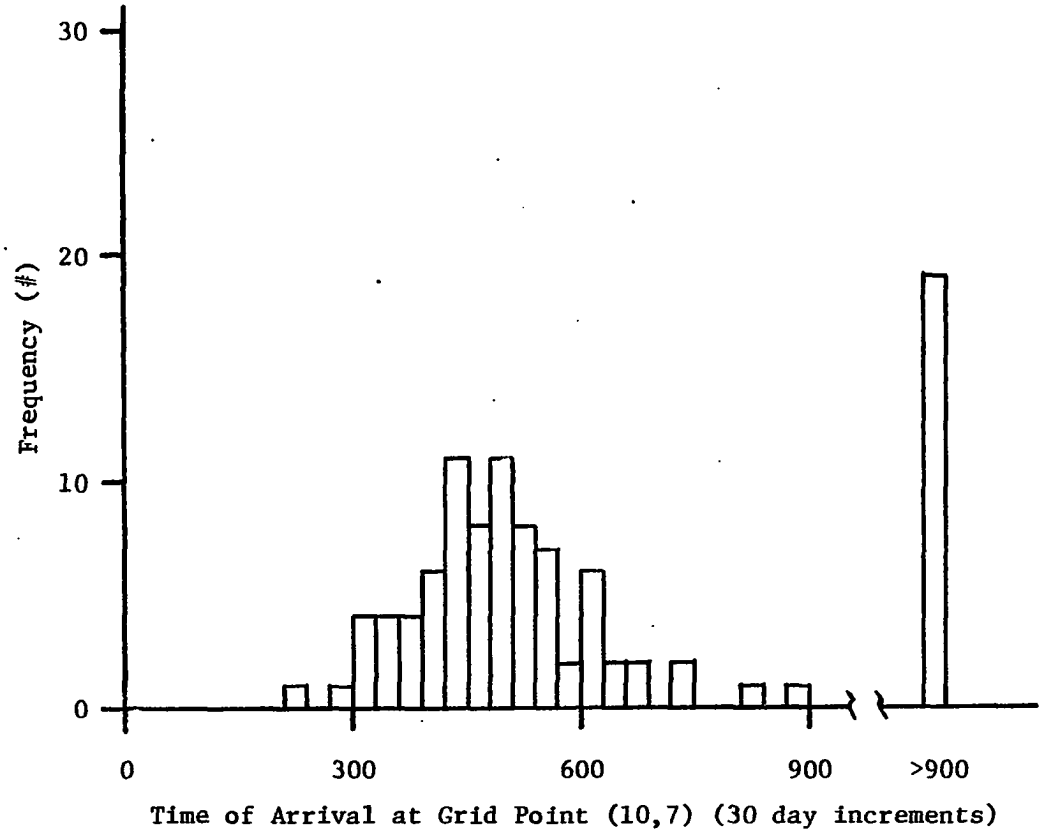

Figure V-3. Frequency of time of arrival at Grid Point (10,7), 1476 feet downstream of the disposal well, for 100 realizations

Table V-4. Frequency and probability distributions for time of arrival

Well #40	Time of Arrival (Days)	Cumulative Exceedance Probability (%)
Sample Size: 99[a]	90	100.0
	120	94.9
Mean: 172 days	150	63.6
Median: 150-180 days	180	38.4
Mode: 120-150 days	210	18.2
	240	6.1
Range: 90-300 days	270	2.0
Standard Deviation: 41 days	300	0.0
Skew: 0.63		

Grid Point (10,7)	Time of Arrival (Days)	Cumulative Exceedance Probability (%)
Sample Size: 81[b]	210	100.0
	240	98.8
Mean: 491 days	270	98.8
Median: 480-510 days	300	97.5
Mode: 420-450 days and	330	93.6
480-510 days	360	87.7
	390	82.7
Range: 210-900 days	420	75.3
Standard Deviation: 118 days	450	61.7
	480	51.9
Skew: 0.69	510	38.3
	540	28.4
	570	19.8
	600	17.3
	630	9.9
	660	7.4
	690	4.9
	720	4.9
	750	2.5
	780	2.5
	810	2.5
	840	1.2
	870	1.2
	900	0.0

[a] For 1 realization the time of arrival exceeded 900 days and no exact time of arrival was obtained.

[b] For 19 realizations the time of arrival exceeded 900 days and no exact time of arrival was obtained.

Table V-5. Comparison of actual and theoretical cumulative exceedance probabilities at Well #40 and Grid Point (10,7)

Exceedance Probability for Sample Size = 99 (%)	Time of Arrival Days (Days)			
	Well #40			
	K	Theoretical	Actual	% Error
1	2.8	290	285	1.8
10	1.3	225	230	-2.2
20	0.80	205	210	-2.4
50	-0.10	170	165	3.0
80	-0.86	140	135	3.8
99	-1.9	95	95	0.0
Exceedance Probability for Sample Size = 81 (%)	**Grid Point (10,7)**			
	K	Theoretical	Actual	% Error
1	2.8	820	875	-6.3
10	1.3	640	630	1.6
20	0.79	580	570	1.8
50	-0.11	480	485	-1.0
80	-0.86	390	400	-2.5
99	-1.8	280	280	0

$\bar{X}$ = sample mean time of arrival in days;

σ = sample standard deviation of time of arrival in days; and

K = fitting parameter for skew g and exceedance probability p.

The K values were obtained from a table presented by Linsley, Kohler and Paulhus (1982). The Pearson Type III distribution fit the recorded exceedance probabilities quite well. The errors between the actual and the theoretical value were all less than 10%.

2. Joint and marginal distributions of pollutant concentrations and duration of exposure

Table V-6 shows the joint and marginal frequency distributions of tritium concentrations and duration of exposure at Well #40. The tritium concentration values have been categorized using 50 pCi/ml class widths from zero to 700 pCi/ml. The duration of exposure values have been categorized using 60 day class widths from zero to 960 days. The boundary of occurrence for combinations of tritium concentration and duration of exposure is quite evident upon observing this table. The maximum tritium concentration observed is less than 700 pCi/ml. The maximum duration of exposure is less than 960 days. At large values of tritium concentration or duration of exposure, the frequency is small. At intermediate values of pairs of tritium concentration and duration of exposure, the frequency is also small, e.g., at a tritium concentration of 300-350 pCi/ml and a duration of exposure of 360-420 days the frequency is zero. The most frequent occurrences take place with

Table V-6. Joint and marginal frequency distributions of tritium concentrati

		Duration of							
		0-60	60-120	120-180	180-240	240-300	300-360	360-420	420-480
Tritium Concentration (pCi/ml)	0-50		1		1	1	3	7	2
	50-100	2	2	1	2	4	14	18	16
	100-150		2	1	7	1	21	36	3
	150-200			8	17	9	39	8	
	200-250		4	13	18	22	20	2	
	250-300		6	17	22	20	10	1	
	300-350		10	18	26	11	6		
	350-400	1	9	20	23	7	1		
	400-450		12	23	16	6			
	450-500	2	13	26	6	4			
	500-550	3	18	19	8				
	550-600	5	22	10	4				
	600-650	5	6	5	1				
	650-700	2	4						
Marginal Frequency Distribution of Duration of Exposure		20	109	161	151	95	114	72	21

ation and duration of exposure at Well #40

of Exposure (Days)									Marginal Frequency Distribution of Tritium Concentration
0	480-540	540-600	600-660	660-720	720-780	780-840	840-900	900-960	
2	7	8	24	19	7	4	6	6	96
16	6	18	8	1					92
3	3	2							86
	1								82
									79
									76
									71
									61
									57
									51
									48
									41
									17
									6
									Total Frequency
21	17	28	32	20	7	4	6	6	863

Joint Frequency Distribution of Tritium Concentration and Duration of Exposure

intermediate values of tritium concentration and low values of duration of exposures or low values of tritium concentration and intermediate values of duration of exposure. At low values of both tritium concentration and duration of exposure, the frequency of occurrence again is small.

Table V-7 presents the joint and marginal probability of distributions of tritium concentration and duration of exposure. The joint probabilities are obtained by dividing the frequency of occurrence in each cell by the total frequency of occurrence. The marginal probability distributions are obtained by summing the joint probabilities for each row and column.

Table V-8 presents the statistical characteristics of both marginal probability distributions. Both distributions are positively skewed with mean, median and mode values much closer to the lower end of the range than the higher end. Table V-8 also contains the marginal cumulative exceedance probability distributions of tritium concentration and duration of exposure. The actual probabilities are compared to theoretical values using the Pearson Type III distribution. The errors associated with the Pearson Type III distribution are considerably higher for the marginal distributions than were observed with the time of arrival distributions. Four out of the ten errors computed are above 10%, although a compensating factor is that the absolute errors are not large at large exceedance probabilities. Overall, the Pearson Type III distribution does not fit the marginal distributions as well as the time of arrival distributions.

Table V-7. Joint and marginal probability distributions of tritium concent

		Duration of							
		0-60	60-120	120-180	180-240	240-300	300-360	360-420	420-480
Tritium Concentration (pCi/ml)	0-50		.001		.001	.001	.003	.008	.002
	50-100	.002	.002	.001	.002	.005	.016	.021	.019
	100-150		.002	.001	.008	.013	.024	.042	.003
	150-200			.009	.020	.010	.045	.009	
	200-250		.005	.015	.021	.025	.023	.002	
	250-300		.007	.020	.025	.023	.012	.001	
	300-350		.012	.021	.030	.013	.007		
	350-400	.001	.010	.023	.027	.008	.001		
	400-450		.014	.027	.019	.007			
	450-500	.002	.015	.030	.007	.005			
	500-550	.003	.021	.022	.009				
	550-600	.006	.025	.012	.005				
	600-650	.006	.007	.006	.001				
	650-700	.002	.005						
Marginal Probabilities of Duration of Exposure		.022	.126	.187	.175	.110	.131	.083	.02

:entration and duration of exposure at Well #40

ı of Exposure (Days)								Marginal Probabilities of Tritium Concentration
)- 480	480- 540	540- 600	600- 660	660- 720	720- 780	780- 840	840- 900	900- 960	
002	.008	.009	.028	:022	.008	.005	.007	.007	.110
019	.007	.021	.009	.001					.106
003	.003	.002							.098
	.001								.094
									.091
									.088
									.083
									.070
									.067
									.059
									.055
									.048
									.020
									.007
.024	.019	.032	.037	.023	.008	.005	.007	.007	Total Probability .996

Joint Probabilities of Tritium Concentration and Duration of Exposure

Table V-8. Marginal probability distributions at Well #40

Statistic	Duration of Exposure (days)	Tritium Concentration (pCi/ml)	Cumulative Exceedance Probability (%)	Tritium Concentration (pCi/ml)				Duration of Exposure (days)			
				K	Theo.	Act.	% E	K	Theo.	Act.	% E
Mean	284	268									
Median	180-240	150-200									
Mode	120-180	0-50	1	2.6	720	640	12.5	3.2	860	840	2.4
Range	0-960	0-700	10	1.3	500	530	-5.7	1.3	520	550	-5.5
Standard			20	.82	410	440	-6.8	.73	420	390	7.7
Deviation	181	175	50	-.06	260	220	18	-.20	250	210	19
Skew	1.2	0.35	80	-.85	120	90	33	-.84	130	140	-7.1

Marginal Cumulative Exceedance Probability
Distribution of Tritium Concentration (%)
Tritium Concentration (pCi/ml)

0-50	50-100	100-150	150-200	200-250	250-300	300-350	350-400	400-450	450-500	500-550	550-600	600-650	650-700	700-750
99.6	88.6	78.0	68.2	58.8	49.7	40.9	32.6	25.6	18.9	13.0	7.5	2.7	0.7	0.0

Marginal Cumulative Exceedance Probability
Distribution of Duration of Exposure (%)
Duration of Exposure (days)

0-60	60-120	120-180	180-240	240-300	300-360	360-420	420-480	480-540	540-600	600-660	660-720	720-780	780-840	840-900	900-960	960-1020
99.6	97.4	84.8	66.1	48.6	37.6	24.5	16.2	13.8	11.9	8.7	5.0	2.7	1.9	1.4	0.7	0.0

A detailed discussion of fitting the actual joint probability distribution of tritium concentration and duration of exposure to a mathematical relationship is contained in a later section of this chapter.

3. Conditional distributions of pollutant concentration and duration of exposure

Tables V-9 and V-11 contain conditional probability distributions for tritium concentration and duration of exposure, respectively. The conditional probability of each cell is obtained by dividing the joint probability of the cell by the marginal probability of its row or column, whichever is applicable.

Tables V-10 and V-12 summarize the statistical properties of the conditional probability distributions of tritium concentration and duration of exposure, respectively. Some general comments about these distributions can be made. As tritium concentration increases, the mean and standard deviation of duration of exposure decreases. As duration of exposure increases, the mean and standard deviation of tritium concentration decreases. This relationship was expected, given the general shape of the pollutographs for the disposal event.

At both low concentrations and short durations of exposure, the skews of the distributions are highly negative. As concentration reaches its largest values and duration of exposure reaches its longest values, the skews have become positive.

Table V-9. Conditional probability distributions of tritium concentration gi

Tritium Concentration (pCi/ml)	Duration of Exposu								
	0-60	60-120	120-180	180-240	240-300	300-360	360-420	420-480	480-540
0-50		.008		.006	.009	.023	.096	.083	.421
50-100	.091	.016	.005	.011	.045	.122	.253	.792	.368
100-150		.016	.005	.046	.118	.183	.506	.125	.158
150-200			.048	.114	.091	.344	.108		.053
200-250		.040	.080	.120	.227	.176	.024		
250-300		.056	.107	.143	.209	.092	.012		
300-350		.095	.112	.171	.118	.053			
350-400	.045	.079	.123	.154	.073	.008			
400-450		.111	.144	.109	.064				
450-500	.091	.119	.160	.040	.045				
500-550	.136	.167	.118	.051					
550-600	.272	.198	.064	.029					
600-650	.272	.056	.032	.006					
650-700	.091	.040							
ΣP	0.998	1.001	0.998	1.000	0.999	1.001	0.999	1.000	1.000

ion given specified duration of exposure classes at Well #40

Exposure (Days)							
480-540	540-600	600-660	660-720	720-780	780-840	840-900	900-960
.421	.281	.757	.957	1.000	1.000	1.000	1.000
.368	.656	.243	.043				
.158	.063						
.053							
1.000	1.000	1.000	1.000	1.000	1.000	1.000	1.000

Table V-10. Statistical summary of conditional probability distributions of tritium concentration at Well #40

Tritium Concentration Statistic	Duration of Exposure (days)[a]											
	0-60	60-120	120-180	180-240	240-300	300-360	360-420	420-480	480-540	540-600	600-660	660-720
Mean (pCi/ml)	527	455	396	319	257	178	112	77	67	64	37	27
Median (pCi/ml)	550-600	450-500	400-450	300-350	250-300	150-200	100-150	50-100	50-100	50-100	0-50	0-50
Mode (pCi/ml)	550-600 & 600-650	500-550	450-500	300-350	200-250	150-200	100-150	50-100	0-50	50-100	0-50	0-50
Range (pCi/ml)	50-700	0-700	50-650	0-650	0-500	0-400	0-300	0-150	0-200	0-150	0-100	0-100
Standard Deviation (pCi/ml)	159	138	121	118	102	71	47	23	44	27	21	10
Skew	-2.0	-.79	-.19	.19	.19	.26	.35	.17	.78	-.09	1.2	4.5

[a]Duration of exposure classes from 720-960 days contained values only in the tritium concentration class of 0-50 pCi/ml.

Table V-11. Conditional probability distributions of duration of exposure

		Duration of Expo								
		0–60	60–120	120–180	180–240	240–300	300–360	360–420	420–480	480–54
Tritium Concentration (pCi/ml)	0–50		.009		.009	.009	.027	.073	.018	.07
	50–100	.019	.019	.009	.019	.047	.151	.198	.179	.06
	100–150		.020	.010	.082	.133	.245	.429	.031	.03
	150–200			.096	.213	.106	.479	.096		.01
	200–250		.055	.165	.231	.275	.253	.022		
	250–300		.080	.227	.284	.261	.136	.011		
	300–350		.145	.253	.361	.157	.084			
	350–400	.014	.143	.329	.386	.114	.014			
	400–450		.209	.403	.284	.104				
	450–500	.034	.254	.508	.119	.085				
	500–550	.055	.382	.400	.164					
	550–600	.127	.521	.250	.104					
	600–650	.300	.350	.300	.050					
	650–700	.286	.714							

sure given specified tritium concentration classes at Well #40

Exposure (Days)								
480-540	540-600	600-660	660-720	720-780	780-840	840-900	900-960	ΣP
.073	.082	.255	.200	.073	.045	.064	.064	1.001
.066	.198	.085	.009					0.999
.031	.020							1.001
.011								1.001
								1.001
								0.999
								1.000
								1.000
								1.000
								1.000
								1.001
								1.002
								1.000
								1.000

Table V-12. Statistical summary of conditional probability distributions of duration of exposure at Well #40

Duration of Exposure Statistic	Tritium Concentration (pCi/ml)													
	0-50	50-100	100-150	150-200	200-250	250-300	300-350	350-400	400-450	450-500	500-550	550-600	600-650	650-700
Mean (days)	639	435	345	289	244	221	197	179	167	148	130	110	96	73
Median (days)	600-660	420-480	360-420	300-360	240-300	180-240	180-240	180-240	120-180	120-180	120-180	60-120	60-120	60-120
Mode (days)	600-660	360-420 & 540-600	360-420	300-360	240-300	180-240	180-240	180-240	120-180	120-180	120-180	60-120	60-120	60-120
Range (days)	60-960	0-720	60-600	120-540	60-420	60-420	60-360	0-360	60-300	0-300	0-240	0-240	0-240	0-120
Standard Deviation (days)	163	135	84	74	75	72	69	58	55	55	49	50	53	27
Skew	-.50	-.63	-.39	-.26	-.28	.01	.18	-.05	.24	.46	.05	.43	.23	-.95

This relationship might be explained by looking at the tritium loading sequence in Table V-3. The loading took place over approximately 600 days. Regardless of how fast or slow the tritium moved through the aquifer, one would expect the plume to have a duration of exposure heavily influenced by the 600 day loading duration. The duration of exposure at low concentrations falls below 600 days only when the central area of the plume occasionally bypasses Well #40. The duration of exposure does not usually last much longer than the 600 day loading duration. This phenomenon would explain negative skews at low tritium concentration. The positive skews at high concentration may be caused because the duration of exposure is small near the peak of the pollutograph. A minimum value boundary of zero for duration of exposure on the low end combined with an unbounded maximum value make an ideal situation for a positive skew at high concentrations.

Negative skew values for tritium concentrations at short durations of exposure may be also explained by looking at the tritium loading sequence. The extremely large loading value in August, 1979, approximately 35% of the total loading, causes the peak tritium concentration to be large in most realizations. The longitudinal and transverse dispersivities are small and Well #40 is close to the disposal well. The only opportunity for the peak tritium concentrations to be small is when the central area of the plume occasionally bypasses Well #40. The maximum tritium concentration is limited by the tritium

concentration during the peak loading rate at the disposal well. The positive skews at high durations of exposure again may be explained by the minimum boundary value of zero for tritium concentration. There is no boundary value for the maximum tritium concentration at long durations of exposure.

Tables V-13 and V-14 show the conditional cumulative exceedance probability distributions for tritium concentration and duration of exposure. The actual probabilities are compared to the theoretical probabilities of Pearson Type III distributions in Tables V-15 and V-16. The errors between the actual and theoretical values are consistently below 10% except for very high exceedance probabilities and long durations of exposure. The large relative errors at high exceedance probabilities and long durations of exposure are compensated somewhat by the fact that the absolute errors are small. In general, the relative errors for the conditional distributions are significantly smaller than the relative errors for the marginal distributions and slightly larger than the relative errors for the time of arrival distributions. It was expected that the conditional distributions would have smaller relative errors than the marginal distributions because the conditional distributions represent the probability associated with one-dimensional slices of the joint probability surface, whereas the marginal distributions represent an average probability computed over several slices.

Table V-13. Conditional cumulative exceedance probability distribut

Tritium Concentration (pCi/ml)	Duration of							
	0-60	60-120	120-180	180-240	240-300	300-360	360-420	420-480
0-50	.998	1.001	.998	1.000	.999	1.001	.999	1.000
50-100	.998	.993	.998	.994	.990	.978	.903	.917
100-150	.907	.977	.993	.983	.945	.856	.650	.125
150-200	.907	.961	.988	.937	.827	.673	.144	
200-250	.907	.961	.940	.823	.736	.329	.036	
250-300	.907	.921	.860	.703	.509	.153	.012	
300-350	.907	.865	.753	.560	.300	.061		
350-400	.907	.770	.641	.389	.182	.008		
400-450	.862	.691	.518	.235	.109			
450-500	.862	.580	.374	.126	.045			
500-550	.771	.461	.214	.086				
550-600	.635	.294	.096	.035				
600-650	.363	.096	.032	.006				
650-700	.091	.040						

ibutions of tritium concentration at Well #40

n of Exposure (Days)								
0-480	480-540	540-600	600-660	660-720	720-780	780-840	840-900	900-960
000	1.000	1.000	1.000	1.000	1.000	1.000	1.000	1.000
917	.579	.719	.243	.043				
125	.211	.063						
	.053							

Table V-14. Conditional cumulative exceedance probability distributi

Tritium Concentration (pCi/ml)	Duration of							
	0-60	60-120	120-180	180-240	240-300	300-360	360-420	420-480
0-50	1.001	1.001	.992	.992	.983	.974	.947	.874
50-100	.999	.980	.961	.952	.933	.886	.735	.537
100-150	1.001	1.001	.981	.971	.889	.756	.511	.082
150-200	1.001	1.001	1.001	.905	.692	.586	.107	.011
200-250	1.001	1.001	.946	.781	.550	.275	.022	
250-300	.999	.999	.919	.692	.408	.147	.011	
300-350	1.001	1.001	.855	.602	.241	.084		
350-400	1.000	.986	.843	.514	.128	.014		
400-450	1.000	1.000	.791	.388	.104			
450-500	1.000	.966	.712	.204	.085			
500-550	1.001	.946	.564	.164				
550-600	1.002	.875	.354	.104				
600-650	1.000	.700	.350	.050				
650-700	1.000	.714						

ibutions of duration of exposure at Well #40

n of Exposure (Days)								
0-480	480-540	540-600	600-660	660-720	720-780	780-840	840-900	900-960
.874	.856	.783	.701	.446	.246	.173	.128	.064
.537	.358	.292	.094	.009				
.082	.051	.020						
.011	.011							

Table V-15. Conditional cumulative exceedance probability of tritium concentrati

	Duration of Expo							
Cumulative Exceedance Probability (%)	0-60				60-120			
	K	Theo.	Act.	% E	K	Theo.	Act.	% E
1	.99	680	690	-1.4	1.7	690	690	0
10	.90	670	650	3.1	1.2	620	600	3.3
20	.78	650	630	3.2	.86	570	580	-1.7
50	.31	580	580	0	.13	470	480	-2.1
80	-.61	430	480	-10	-.78	350	330	6.1
99	-3.6	-	60	-	-2.9	50	50	0
Cumulative Exceedance Probability (%)	240-300				300-360			
	K	Theo.	Act.	% E	K	Theo.	Act.	% E
1	2.5	510	490	4.1	2.5	360	350	2.9
10	1.3	390	410	-4.9	1.3	270	280	-3.6
20	.83	300	340	-12	.82	240	240	0
50	-.03	250	250	0	-.04	180	180	0
80	-.85	170	160	6.3	-.85	120	120	0
99	-2.2	30	50	-40	-2.1	30	20	50
Cumulative Exceedance Probability (%)	480-540				540-600			
	K	Theo.	Act.	% E	K	Theo.	Act.	% E
1	2.9	190	190	0	2.3	130	140	-7.1
10	1.3	120	130	-7.7	1.3	100	100	0
20	.78	100	100	0	.85	90	90	0
50	-.13	60	60	0	.02	60	70	-14
80	-.86	30	20	50	-.84	40	40	0
99	-1.7	-	0	-	-2.4	0	0	0

ration at Well #40 using the Pearson Type III distribution

Exposure (days)

	120-180				180-240			
E	K	Theo.	Act.	% E	K	Theo.	Act.	% E
	2.2	660	640	3.1	2.5	610	590	3.4
3	1.3	550	550	0	1.3	470	480	-2.1
7	.85	500	510	-2.0	.83	420	420	0
1	.03	400	410	-2.4	-.03	320	320	0
1	-.83	300	280	7.1	-.85	220	210	4.8
	-2.5	90	150	-40	-2.2	60	70	-14

	360-420				420-480			
E	K	Theo.	Act.	% E	K	Theo.	Act.	% E
9	2.6	230	250	-8.0	2.5	130	150	-13
6	1.3	170	170	0	1.3	110	110	0
)	.82	150	140	7.1	.83	100	90	11
)	-.06	110	100	10.0	-.03	80	80	0
)	-.85	70	70	0	-.85	60	60	0
)	-2.1	10	0	-	-2.2	30	10	200

	600-660				660-720			
E	K	Theo.	Act.	% E	K	Theo.	Act.	% E
.1	3.1	100	100	0	4.3	70	90	-22
0	1.3	60	80	-25	1.0	40	50	-20
0	.73	50	60	-17	.2	30	40	-25
4	-.20	30	30	0	-.50	20	30	-33
0	-.84	20	10	100	-.50	20	10	100
0	-1.4	10	0	-	-.60	20	0	-

Table V-16. Conditional cumulative exceedance probability of duration of exp

											Tritium Conc
Cumulative Exceedance Probability (%)	0-50				50-100				100-		
	K	Theo.	Act.	% E	K	Theo.	Act.	% E	K	Theo.	
1	2.0	970	950	2.1	1.9	690	660	4.5	2.0	600	
10	1.2	830	840	-1.1	1.2	600	600	0	1.2	450	
20	.86	780	730	6.8	.86	550	540	1.9	.86	420	
50	.08	650	650	0	.10	450	430	4.7	.07	350	
80	-.81	510	530	-3.8	-.80	330	340	-3.0	-.82	280	
99	-2.7	200	130	54	-2.8	60	30	100	-2.6	130	
Cumulative Exceedance Probability (%)	250-300				300-350				350		
	K	Theo.	Act.	% E	K	Theo.	Act.	% E	K	Theo.	
1	2.3	390	360	8.3	2.5	370	350	5.7	2.2	310	
10	1.3	310	320	-3.1	1.3	290	290	0	1.3	250	
20	.84	280	290	-3.4	.83	250	260	-3.8	.85	230	
50	0	220	220	0	-.03	190	200	-5.0	.02	180	
80	-.84	160	150	6.7	-.85	140	100	40	-.84	130	
99	-2.3	60	70	-14	-2.2	50	60	-17	-2.4	40	
Cumulative Exceedance Probability (%)	500-550				550-600				600		
	K	Theo.	Act.	% E	K	Theo.	Act.	% E	K	Theo.	
1	2.7	260	240	8.3	2.6	240	230	4.3	2.5	230	
10	1.3	190	200	-5.0	1.3	180	180	0	1.3	160	
20	.81	170	170	0	.81	150	160	-6.3	.83	140	
50	-.07	130	130	0	-.07	110	100	10	-.04	90	
80	-.86	90	80	13	-.86	70	70	0	-.85	50	
99	-2.0	30	10	200	-2.0	10	0	-	-2.2	-	

f exposure at Well #40 using the Pearson Type III distribution

Concentration (pCi/ml)

100-150				150-200				200-250			
heo.	Act.	% E	K	Theo.	Act.	% E	K	Theo.	Act.	% E
600	570	5.3	2.1	440	420	4.8	2.1	400	390	2.6
450	420	7.1	1.3	390	360	8.3	1.2	330	350	-5.7
420	410	2.4	.85	350	350	0	.85	310	300	3.3
350	360	-2.8	.05	290	310	-6.5	.05	250	250	0
280	280	0	-.83	230	210	9.5	-.83	180	170	5.9
130	90	44	-2.5	100	120	-17	-2.5	60	70	-14

350-400				400-450				450-500			
heo.	Act.	% E	K	Theo.	Act.	% E	K	Theo.	Act.	% E
310	320	3.1	2.5	300	290	3.4	2.7	300	290	3.4
250	260	-3.8	1.3	240	240	0	1.3	220	230	-4.3
230	230	0	2.5	210	220	-4.5	.81	190	190	5.5
180	180	0	-.04	160	160	0	-.07	140	140	0
130	130	0	-.85	120	120	0	-.86	100	100	0
40	40	0	-2.2	50	60	-17	-2.0	40	20	100

600-650				650-700			
heo.	Act.	% E	K	Theo.	Act.	% E
230	230	0	1.6	120	120	0
160	170	-5.9	1.1	100	110	-9.1
140	150	-6.7	.85	100	100	0
90	100	-10	.15	80	80	0
50	40	25	-.76	50	50	0
-	0	-	-3.0	-	0	-

It is expected that the pollutant concentration associated with a 1% incidence level of a "pseudo" NOEL, the proposal of Nelson discussed in Chapter II, may be associated with large conditional cumulative exceedance probability values of a pollutant in some instances. Although this is the precise area of the probability distributions having the largest relative error in this investigation, the absolute error is not much larger than the absolute error of smaller cumulative exceedance probabilities in this investigation. The error at high exceedance probabilities might be reduced somewhat if the number of realizations were increased above the 100 realizations used in this investigation.

4. Joint probability distribution of tritium concentration and duration of exposure

Table V-17 shows the joint cumulative exceedance probability distribution of tritium concentration and duration of exposure. This joint distribution differs from the previously discussed marginal and conditional distributions because it is a bivariate, instead of univariate, distribution.

The fitting of a mathematical equation to this bivariate distribution is a complicated process in comparison to the fitting of a univariate distribution. Hoaglin (1977) describes a procedure which can be used to fit a bivariate distribution to a mathematical equation by direct approximations. The direct approximations approach uses

Table V-17. Joint cumulative exceedance probability distribution of tritium con

Tritium Concentration (pCi/ml)	Duration of Exposure									
	0-60	60-120	120-180	180-240	240-300	300-360	360-420	420-480	480-540	54
0-50	.996	.974	.848	.661	.486	.376	.245	.162	.138	.
50-100	.925	.913	.788	.601	.427	.268	.140	.065	.043	.
100-150	.780	.760	.637	.451	.279	.175	.063	.009	.006	.
150-200	.682	.662	.541	.356	.192	.101	.013	.001	.001	
200-250	.588	.568	.447	.271	.127	.046	.003			
250-300	.490	.470	.361	.200	.077	.021	.001			
300-350	.409	.389	.280	.139	.041	.008				
350-400	.326	.306	.209	.089	.021	.001				
400-450	.256	.237	.150	.053	.012					
450-500	.189	.170	.097	.027	.005					
500-550	.130	.113	.055	.015						
550-600	.075	.061	.024	.006						
600-650	.027	.019	.007	.001						
650-700	.007	.005								

n concentration and duration of exposure at Well #40

ure (Days)						
540-600	600-660	660-720	720-780	780-840	840-900	900-960
.119	.087	.050	.027	.019	.014	.007
.033	.010	.001				
.002						

techniques of exploratory data analysis, which will be described below in more detail. A simple mathematical function of each of the two parameters under consideration, i.e., tritium concentration and duration of exposure, is developed in this procedure. The two functions are then added together to form the bivariate probability estimate.

Because it was desired to have the resulting mathematical equation yield estimated exceedance probabilities in the range of zero to one (0-1), the logit transformation was performed on the joint cumulative exceedance probabilities, as shown in Equation V-2 below:

$$\theta_{ij} = \ln \left(\frac{P_{ij}}{1 - P_{ij}}\right) \qquad \text{(Eq. V-2)}$$

where,

P_{ij} = joint cumulative exceedance probability for ith level of tritium concentration and jth level of duration of exposure (note that i=1 for tritium concentrations between 0 and 50 pCi/ml, i=2 between 50 and 100 pCi/ml, etc., that j=1 for durations of exposure between 0 and 60 days, j=2 between 60 and 120 days, etc., and that minimum numeric values of tritium concentration and duration of exposure within each cell level are used for the equation fitting process);

ln = natural logarithm; and

θ_{ij} = logit of P_{ij} $(0 \leq \theta_{ij} \leq 1)$.

The first step will then be to use the logit as the dependent variable in the analysis, replacing the joint cumulative exceedance probability.

In many of the (i,j) cells, the observed joint cumulative exceedance probability is zero due to the error associated with a finite

sample size (number) of realizations. Because the natural logarithm of zero is undefined, the cells containing zero probability have not been included in the fitting process.

The second step is to decide if an additive model can separate the effects of tritium concentration and duration of exposure on the logit of the observed joint cumulative exceedance probabilities. The additive model is presented in Equation V-3 below:

$$\theta_{ij} = CVAL + RE_i + CE_j + \varepsilon_{ij} \qquad \text{(Eq. V-3)}$$

where,

θ_{ij} = the logit of the ith level of tritium concentration and the jth level of duration of exposure;

CVAL = the common effect of the joint distribution;

RE_i = the row effect for tritium concentration;

CE_j = the column effect for duration of exposure; and

ε_{ij} = residual of the ith level of tritium concentration and the jth level of duration of exposure.

By defining the common row and column effects above in a specific manner, one may impose a set of parameter restrictions in order to obtain a solution for the equation fitting process. The second step includes defining the common, row and column effects by the specifications that $\hat{RE}_I = 0$ and $\hat{CE}_J = 0$. Thus, $\hat{RE}_i$ estimates the difference between the average effect of the ith and Ith (largest) level

of tritium concentration, averaging across the level of duration of exposure; $\hat{CE}_j$ estimates the differences between the average effect of jth and Jth (largest) levels of duration of exposure; and $\hat{CVAL}$ estimates the effect of the (Ith, Jth) level of concentration and duration of exposure, respectively. Using a linear regression procedure, the squares of the residuals of the additive model due to the observed common, row and column effects are minimized in order to obtain the predicted common, row and column effects of the joint distribution, which are represented by Equations V-4a, 4b, and 4c below.

$$\hat{RE}_i = \bar{\theta}_i - \bar{\theta}_I \qquad \text{(Eq. V-4a)}$$

$$\hat{CE}_j = \bar{\theta}_j - \bar{\theta}_J \qquad \text{(Eq. V-4b)}$$

$$\hat{CVAL} = \theta_{I,J} \qquad \text{(Eq. V-4c)}$$

where,

$\bar{\Theta}_i$ = 1,2,...,I - the average logit value of the ith level of tritium concentration;

$\bar{\Theta}_j$ = 1,2,...,J - the average logit value of the jth level of duration of exposure; and

$\Theta_{I,J}$ = the logit value of the Ith level of tritium concentration and Jth level of duration of exposure.

Table V-18 below shows estimated values of the common, row and column effects using the linear regression procedure on the additive model.

Table V-18. Row, column and common effects

Parameter		Estimated Value
Common Effect (Intercept)		-14.18586165
Row Effects (Concentration)	**i=**	**Estimated Value**
0	1	9.23104113
50	2	7.87739976
100	3	6.77590546
150	4	5.95704821
200	5	5.69946316
250	6	5.12643542
300	7	4.85273958
350	8	4.12098082
400	9	4.04520369
450	10	3.46789046
500	11	3.10013379
550	12	2.33219013
600	13	1.00003457
650	14	0.00000000
Column Effects (Duration of Exposure)	**j=**	**Estimated Value**
0	1	9.20137486
60	2	8.92222310
120	3	8.15841832
180	4	7.07103605
240	5	6.08579170
300	6	4.99958714
360	7	3.62749412
420	8	2.74605657
480	9	2.48767866
540	10	2.36033581
600	11	2.15866739
660	12	0.70604432
720	13	1.37027330
780	14	1.01068703
840	15	0.70022149
900	16	0.00000000

A diagnostic plot developed by Tukey (1970) is used to examine the residuals of the additive model. The residuals of the additive model are plotted against comparison values in the third step of the analysis. Comparison values are computed by Equation V-5 below:

$$CV_{ij} = \frac{\hat{RE}_i \times \hat{CE}_{ij}}{\hat{CVAL}} \qquad \text{(Eq. V-5)}$$

where,

CV_{ij} = comparison value for ith level of tritium concentration and jth level of duration of exposure.

If the plot of the residuals versus comparison values shows a consistent linear relationship with slope m, a transformation of the logit to the power (1-m) is suggested for the additive model. After several attempts to significantly decrease the residuals of the additive model with such transformations proved ineffective, the search for a transformation of the logit value was abandoned for the sake of model simplicity.

The fourth step in this process is to determine the form of a tritium concentration and a duration of exposure function in the additive model. By fitting the predicted row effects of tritium concentration versus the tritium concentration levels and also the predicted column effects of duration of exposure versus the duration of exposure levels, the type of mathematical functions for tritium concentration and duration of exposure may be estimated. After investigating several types of functions, it was decided that linear

functions of tritium concentration and duration of exposure were the best combination of simplicity and accuracy. These estimated linear functions are given by Equations V-6a and V-6b below:

$$\hat{RE}_i = 8.410171 - .011902\ (CONC)_i \qquad \text{(Eq. V-6a)}$$

$$\hat{CE}_j = 8.601411 - .010558\ (DUREXP)_j \qquad \text{(Eq. V-6b)}$$

where,

$(CONC)_i$ = lower bound of tritium concentration for the ith level (pCi/ml); and

$(DUREXP)_j$ = lower bound of duration of exposure for the jth level (days).

Combining Equations V-3, V-6a, V-6b and the common effect from Table V-18 above and rounding off coefficients to two significant digits, Equation V-7 will predict logit values as follows:

$$\hat{\theta}_{ij} = 2.8 - .012\ (CONC)_i - .011\ (DUREXP)_j$$

where,

$\hat{\theta}_{ij}$ = predicted logit for the ith level of tritium concentration and jth level of duration of exposure.

Predicted logit values may then be transformed back to probabilities by Equation V-8 below:

$$\hat{P}_{ij} = \frac{\exp\ (\hat{\theta}_{ij})}{1 + \exp\ (\hat{\theta}_{ij})} \qquad \text{(Eq. V-8)}$$

where,

$\hat{P}_{ij}$ = predicted cumulative exceedance probability of the ith level of tritium concentration and the jth level of duration of exposure; and

exp = 2.718... = exponential.

Table X-1 in the appendix lists the observed and predicted joint cumulative exceedance probability values for each tritium concentration-duration of exposure cell. It also gives the residual (observed less predicted) probability values for each cell. The prediction equation generally underestimates the joint probability for combinations of small values of both tritium concentration and duration of exposure. The prediction equation also tends to overestimate the joint probability for combinations of large values of both tritium concentration and duration of exposure. These areas of systematic error are due to the inadequacies of the selected simple mathematical functions in the fitting process. The trade-off for simple mathematics is increased error.

Some of the error in the prediction equation is due to the irregularity of the observed joint probability values. Such irregularly could be reduced by increasing the number of realizations used to determine the probability values. Increasing the number of realizations would also decrease the number of zero probability cells and likely increase the fit of the prediction equation.

C. Multiple Realizations of a Synthetic Disposal Event

A synthetic disposal event was modeled in order to compare the results of two different tritium loading and waste volume flow rates. The tritium load and waste volume flow rates of the synthetic disposal event are given in Table V-19. The total tritium load for the synthetic disposal event, 287 curies, is slightly less than the total loading for the recorded disposal event, 332 curies. The average loading rate for the synthetic disposal event is 48 curies per 30 day period versus 17 curies per 30 day period for the recorded disposal event. The synthetic disposal event also has only 30% of the loading time of the recorded disposal event. An additional 100 hydraulic conductivity fields, with a mean logarithmic value of 3.826907 and a standard deviation of the logarithm values of 0.106717, were generated with the TBM procedure. These descriptive statistics are very close to those of the first 100 fields generated. All other input parameters to the mass transport model are identical in value to those of the recorded disposal event.

Figure V-4 shows the frequency distribution of time of arrival at Grid Point (10,7) for 100 realizations. The frequency distribution is similar in general shape to the frequency distribution of the recorded disposal event, but is considerably more dispersed. For 19 of 100 realizations of the recorded disposal event, the time of arrival exceeded 900 days at Grid Point (10,7), whereas the synthetic disposal event had 33 of 100 realizations with the time of arrival at Grid Point (10,7) exceeding 900 days. The median value of the synthetic disposal

Table V-19. Tritium load and waste volume flow rate for a synthetic disposal event

Time (Days)	Tritium Load (Curies)	Volume Flow Rate (MGD)
0-30	250	0.5
30-60	5	1.0
60-90	1	2.0
90-120	1	2.0
120-150	5	1.0
150-180	25	0.5
	Total: 287	

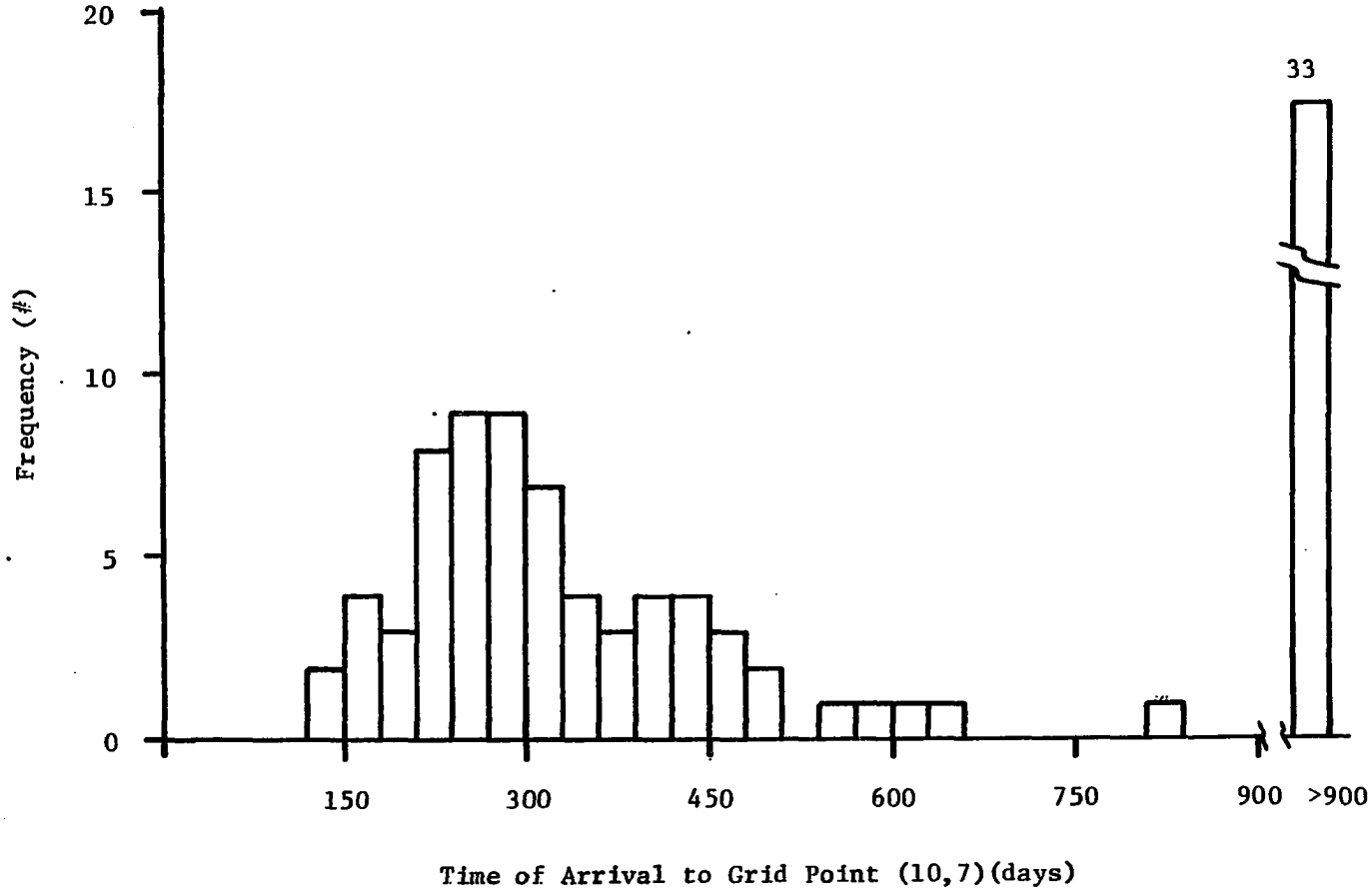

Figure V-4. Frequency distribution of time of arrival at Grid Point (10,7) for 100 realizations of a synthetic disposal event

event was 390-420 days, which also was less than the 480-510 days median value for the recorded disposal event.

Table V-20 shows the joint probability distribution of tritium concentration and duration of exposure of the synthetic disposal event. The shape of the joint probability surface for the synthetic disposal event is similar to the shape of the joint probability surface for the recorded disposal event, but the extremes of the pollutographs of the synthetic disposal event are much greater than those of the recorded disposal event. The maximum tritium concentration and maximum duration of exposure of the synthetic disposal event are considerably larger than the maximum values of the recorded disposal events, even though the total load of the synthetic disposal event was slightly less than that of the recorded disposal event.

These observations are consistent with a conclusion that the results of the synthetic disposal events are more dispersed than the results of the recorded disposal event. This dispersion of results appears to be caused by the different pattern of tritium loading and waste volume rates. As the total load for the synthetic disposal event is similar to the total load of the recorded event, the difference is suspected to be caused by the loading rate pattern and short time of disposal. The large loading rate causes high concentrations to be injected. The high volume rates in the middle of the disposal event cause large seepage velocities after injection of the high concentration loads. The large seepage velocities and short time of disposal appear

Table V-20. Joint probability distribution of tritium concentration and duratio

		Tritium Conc									
		0-2	2-4	4-6	6-8	8-10	10-12	12-14	14-16	16-18	1
Duration of Exposure (Days)	0-60	.009	.015	.024	.027	0	.005	0	0	0	
	60-120	.011	.033	.060	.032	.012	.006	.009	.009	.009	.
	120-180	.018	.056	.056	.014	.003	.006	.005	.011	.012	.
	180-240	.042	.058	.021	.011	.012	.009	.008	.0015		
	240-300	.055	.021	.008	.003						
	300-360	.046	.006								
	360-420	.015	.0015								
	420-480	.009									
	480-540	.006									
	540-600	.006									
	600-660	.003									
	660-720	.003									
	720-780	.003									
	780-840	.005									
	840-900	.006									
	900-960	.006									
	960-1020	.006									
	1020-1080	.003									
	1080-1140	.003									
	1140-1200	.003									
	1200-1260	.003									
	1260-1320	.0015									
	Σ P										
	Σ P	.263	.191	.169	.087	.027	.026	.022	.022	.021	

tion of exposure at Well #40 for a synthetic disposal event

oncentration (100 pCi/ml)

18-20	20-22	22-24	24-26	26-28	28-30	30-32	32-34	34-36	36-38	Σ P
0	.0015	.005	.006	.009	.011	.012	.011	.011	.0015	.149
.009	.008	.008	.009	.009	.009	.006	.006			.245
.012	.012	.009	.006	.003						.223
										.163
										.087
										.052
										.017
										.009
										.006
										.006
										.003
										.003
										.003
										.005
										.006
										.006
										.006
										.003
										.003
										.003
										.003
										.002
										1.003
.021	.022	.022	.021	.021	.020	.018	.017	.011	.002	1.003

to cause the load to be more concentrated for the synthetic disposal event than the recorded disposal event. Because the waste load is more concentrated in space, the central area of the plume of the synthetic disposal event has a tendency to either pass through the location of Well #40 at high concentrations or bypass Well #40 at low concentrations more often than the central area of the plume of the recorded disposal event, resulting in a more dispersed and a greater ranging joint probability surface for the synthetic disposal event.

VI. POLLUTANT MOVEMENT, TOXICITY STUDIES AND BENEFIT-COST ANALYSES

The joint probability distribution of pollutant concentration versus duration of exposure and a toxicity study are two components which may be used to make benefit-cost analyses of groundwater contamination events. The general procedure for this process is outlined below.

A. Joint Probability of Pollutant Concentration and Duration of Exposure

In Chapter V, a process for determining the predicted joint cumulative exceedance probability of the ith level of pollutant concentration and the jth level of duration of exposure, $\hat{P}_{ij}$, was presented. The predicted joint probability of any (i,j) level may be computed by the equation given below:

$$\hat{p}_{ij} = \hat{P}_{ij} + \hat{P}_{i+1,j+1} - \hat{P}_{i+1,j} - \hat{P}_{i,j+1} \qquad \text{(Eq. VI-1)}$$

where,

$i = 1,2,\ldots,I$ = ith level of pollutant concentration;

$j = 1,2,\ldots,J$ = jth level of duration of exposure;

$\hat{p}_{ij}$ = predicted joint probability of the ith level of pollutant concentration and jth level of duration of exposure; and

$\hat{P}_{ij}$ = predicted joint cumulative exceedance probability of the ith level of

pollutant concentration and jth level
of duration of exposure.

B. Toxicity Study

Results in a somewhat similar format could be developed for the incidence fraction of death or disability of organisms for different levels of pollutant concentration and duration of exposure. This type of toxicity study is similar to the development of a "pseudo" NOEL, suggested by Nelson (1984) and discussed previously in Chapter II. By systematically testing the fraction of deaths or disabilities of a sample of organisms at incremental levels of pollutant concentration and duration of exposure, a joint cumulative incidence fraction distribution corresponding to the joint cumulative exceedance probability distribution could be constructed. After statistically analyzing the data, a predictive mathematical equation could be estimated for the cumulative incidence fraction in a method similar to that for the cumulative exceedance probability, as reported in Chapter V. The predicted joint incidence fraction of any (i,j level) may be computed by the equation given below:

$$\hat{1d}_{ij} = \hat{LD}_{ij} + \hat{LD}_{i-1,j-1} - \hat{LD}_{i-1,j} - \hat{LD}_{i,j-1} \qquad \text{(Eq. VI-2)}$$

where,

$i = 1,2,\ldots,I$ = ith level of pollutant concentration;

$j = 1,2,\ldots,J$ = jth level of duration of exposure;

$\hat{ld}_{ij}$ = predicted joint incidence fraction of ith level of pollutant concentration and jth level of duration of exposure; and

$\hat{LD}_{ij}$ = predicted joint cumulative incidence fraction of the ith level of pollutant concentration and jth level of duration of exposure.

C. Intersection of Probability and Incidence Fraction Distributions

Figure VI-1 shows a simulated cross section view or slice of the joint probability distribution and joint incidence fraction distribution at a specified duration of exposure. For a selected pollutant concentration, both the joint probability and the joint incidence fractions may be identified. It should be noted that these two variables are accumulated in opposite directions. Cumulative exceedance probability approaches 1.0 as pollutant concentration and duration of exposure approach zero. Cumulative incidence fraction approaches 1.0 as pollutant concentration and duration of exposure increase in value.

The relative size of the product of these joint measures is a determining factor in estimating the potential benefits from cleaning up a groundwater contamination event. When both the joint probability and the joint incidence fraction are large, their product is relatively very large. When both are small, their product is relatively extremely small. The next section will describe the exact form of the benefits function.

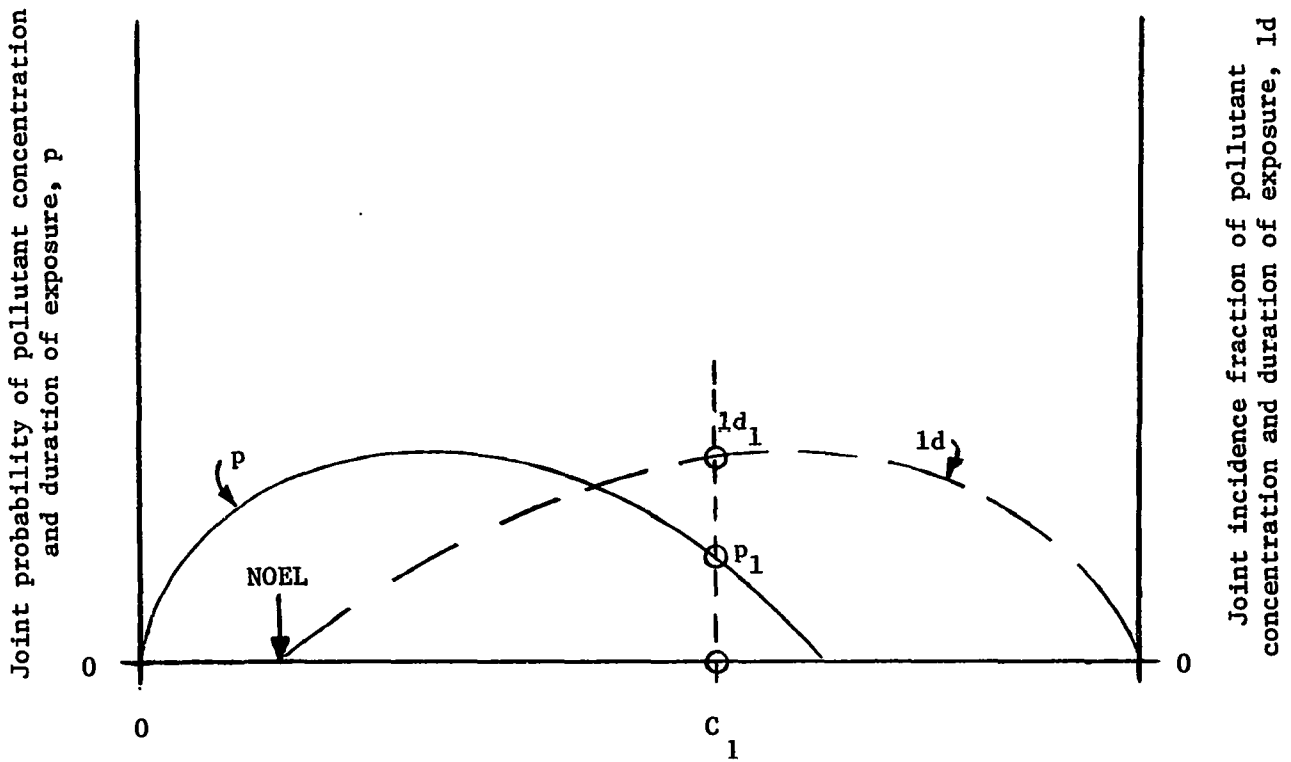

Figure VI-1. Joint probabilities and joint incidence fractions for various pollutant concentrations and a specified duration

D. Benefit-Cost Analysis

The potential benefit of cleaning up a groundwater contamination event may be computed using the joint probability and incidence fraction of pollutant concentration and duration of exposure levels, the number of organisms exposed to contamination and the assumed value of each organism. The mathematical equation for summing up the benefits is given below:

$$B = \sum_{i=1}^{I} \sum_{j=1}^{J} (p_{ij} \times ld_{ij}) (N_o \times \$_o) \qquad \text{(Eq. VI-3)}$$

where,

p_{ij} = predicted joint probability of level (i,j);

ld_{ij} = predicted incidence fraction of level (i,j);

N_o = number of exposed organisms;

$\$_o$ = value of one organism; and

B = benefits associated with groundwater contamination cleanup.

The benefit-cost analysis would be completed by estimating the cleanup cost of the contamination event and comparing it to the computed benefits. Normally, if benefits exceed costs, the cleanup would be considered cost effective. This procedure would also be applicable for situations where less than complete cleanup is contemplated. Benefits would accrue only for concentrations and duration of exposure larger than selected minimum values.

VII. CONCLUSIONS AND RECOMMENDATIONS

This investigation has succeeded in accomplishing the four objectives presented in Chapter I. First, a procedure has been developed which introduces probability into estimating the magnitude and duration of exposure of a pollutant. Second, the spatial variability of hydraulic conductivity has been incorporated into this procedure. Third, this procedure has been validated through its application to an observed and recorded pollutant disposal event under field conditions. Last, statistical analyses have been performed in order to systematically describe the results of the disposal event.

A. Conclusions

Several conclusions may be made based on the experience gained in this investigation:

1. The Turning Bands Method of generating spatially-varying, correlated hydraulic conductivity fields works quickly and inexpensively on the computer, but it does have some practical limitations. Either a transmissivity contour map or several borings for hydraulic conductivity testing are required to obtain good estimates of the mean, standard deviation and correlation function in the study area. Few aquifers in the country are as well-documented as the Snake River Plain aquifer. Additionally, the grid network for the TBM needs thousands of nodal points with a constant interval spacing in order to achieve a standard deviation for each realization comparable in size to the estimated

value. This characteristic will mean that the grid network for the TBM may have, in some portions of the study area, a smaller grid interval than the mass transport model. If the grid network for the TBM and mass transport model are not identical, transferring hydraulic conductivity values between programs would be site specific and could be cumbersome.

2. The shape of the pollutographs at an observation well is extremely sensitive to the hydraulic gradient of the aquifer. This sensitivity increases as an observation well becomes closer to the site of pollutant introduction into the aquifer. The large difference in concentrations between the recorded and synthetic disposal events is associated with differences in seepage velocities. Good documentation of the hydraulic gradient is essential to obtain accurate pollutographs. This conclusion is similar to statement of Smith and Schwartz (1981a) that accurate measurements of seepage velocities must be made in order to obtain accurate results.

The shape of the pollutograph at some location in the aquifer can also be highly sensitive to the hydraulic conductivity field realization. Large amounts of hydraulic conductivity data and/or a highly correlated hydraulic conductivity field are needed to significant decrease the uncertainty of pollutant movement.

3. Smith and Schwartz (1981a) also contended that dispersion in the field was due mainly to spatial variability in hydraulic conductivity, rather than a dispersion coefficient. The calibration of the recorded disposal event used longitudinal and transverse

dispersivities fifty times smaller than the previous USGS studies. Actual transmissivities at each node were used during the calibration, as opposed to using an average transmissivity value. There appears to be some validity in Smith and Schwartz's contention.

4. Smith and Schwartz (1981a) also observed that the arrival of the pollutant to an observed location tended to follow a non-normal pattern. Statistical tests on the modeled results in this investigation showed a similar pattern. Only in a few isolated instances was a normal distribution hypothesis accepted. In the majority of the cases where a normal distribution hypothesis was rejected, skews varied between large positive and large negative values. The maximum tritium concentration and maximum duration of exposure of the joint cumulative exceedance probability distribution is not independent of the pollutant loading pattern. In a comparison of the joint distribution of a recorded and synthetic disposal, the maximum pollutant concentration was extremely sensitive to the pollutant loading pattern. A synthetic disposal event caused the maximum tritium concentration to be quadrupled with only a doubling of the peak tritium load. The maximum duration of exposure increased less than the maximum tritium concentration, only about 25%. As the duration of the loading of the synthetic disposal event was decreased by about 75%, the smaller increase in duration of exposure was not unexpected.

5. Statistical descriptions of the modeled results varied in per cent error between the observed and predicted values for a specified

exceedance probability. In general, the time of arrival predictions had an error percentage less than 10. The conditional probability predictions for both tritium concentration and duration of exposure were also generally less than 10%. Marginal and joint probability predictions had much larger error percentages than the conditional probability distributions; in some instances the percent error reached 30. The accuracy of the time of arrival and conditional probability distributions, less than 10% error, is considered to be good by this investigator. The per cent error associated with the marginal and joint probability distributions is thought to be associated partly with the number of realizations used to generate the probabilities. This investigator believes that some of the erratic changes in the observed joint probability from cell to cell would be smoothed out as the number of realizations increased.

6. Executive Order 12291 requires the USEPA to regulate the quality of groundwater in a cost-effective manner. This investigation has indicated how a benefit-cost analysis could be undertaken for a groundwater contamination event. Joint probabilities for pollutant movement and death incidence fractions from toxicity studies at various levels of pollutant concentration and duration of exposure are predicted. This information is combined with an estimate of the number of organisms exposed and the value of each organism to compute the benefits associated with a cleanup effort, as shown in the equation below:

$$B = \sum_{i=1}^{I} \sum_{j=1}^{J} (p_{ij} \times ld_{ij}) (N_o \times \$_o) \qquad \text{(Eq. VI-6)}$$

where,

$i = 1,2,\ldots,I$ = ith level of pollutant concentration;

$j = 1,2,\ldots,J$ = jth level of duration of exposure;

p_{ij} = predicted joint probability of the ith level of pollutant concentration and jth level of duration of exposure;

ld_{ij} = predicted incidence fraction of death or disability of an organism with the ith level of pollutant concentration and the jth level of duration of exposure;

N_o = number of organisms exposed;

$\$_o$ = value of each organism; and

B = benefits associated with groundwater contamination cleanup.

B. Recommendations

This investigation should be considered only as a beginning in the development of a comprehensive procedure for incorporating probability in the exposure assessment step of a risk assessment for groundwater contamination. Several recommendations for further research on this topic are presented below:

1. Further analyses should be made under a variety of pollutant loading and flow rate patterns at the INEL site, in order to determine if any empirical relationships can be developed from the results. Special consideration should be given to constant, continuous loading patterns, similar to leakage from sanitary landfills.

2. Similar analyses should be conducted in different types of aquifers. The INEL site is located in a fractured basalt aquifer. Other potential aquifers include unconsolidated deposits with different grain size distributions and fractured limestone, dolomite or sandstone formations.

3. Additional research should be undertaken to better understand the effects of unsteady flow conditions on pollutant movement in aquifers.

4. A study comparing the results of this investigation with a similar investigation's results, but using a finite element analysis mass transport model instead of a finite difference model, should be made. An evaluation comparing the compatibility of both the finite element and finite difference models with the Turning Bands Method should also be made.

5. A study should be made of how semi-confined, layered or other complex geologic formations may affect the probability distributions of pollutant movement.

6. Additional research should be conducted in refining and expanding the methodology of benefit-cost analyses for groundwater contamination events.

VIII. BIBLIOGRAPHY

Anderson, Mary P. "Movement of Contaminants in Groundwater: Groundwater Transport-Advection and Dispersion." Studies in Geophysics: Groundwater Contamination. Washington, D. C.: National Academy Press, 1984, pp. 37-45.

Bakr, A. A. "Stochastic Analysis of the Effect of Spatial Variations in Hydraulic Conductivity on Groundwater Flow." Ph.D. dissertation, New Mexico Institute of Mining and Technology, Socorro, July, 1976.

Bakr, A. A., L. W. Gelhar, A. L. Gutjahr and J. R. MacMillan. "Stochastic Analysis of Spatial Variability in Subsurface Flows, 1, Comparison of One- and Three-Dimensional Flows." Water Resources Research, 14, No. 2 (1978), 263-271.

Brown, V. M. "Concepts and Outlook in Testing the Toxicity of Substances to Fish." Bioassay Techniques and Environmental Chemistry. Gary E. Glass, Editor. Ann Arbor, Michigan: Ann Arbor Science Publishers, Inc., 1973, pp. 73-95.

Brown, V. M. Acute Toxicity in Theory and Practice. Chichester, England: John Wiley & Sons, Inc., 1980.

Dagan, G. Comment on "A Stochastic-Conceptual Analysis of One-Dimensional Groundwater Flow in Nonuniform Homogeneous Media," by R. A. Freeze. Water Resources Research, 12, No. 5 (1976), 567.

Freeze, R. Allan. "A Stochastic-Conceptual Analysis of One-Dimensional Groundwater Flow in Nonuniform Homogeneous Media." Water Resources Research, 11, No. 5 (1975), 725-741.

Gelhar, L. W. "Effects of Hydraulic Conductivity Variations on Groundwater Flows." In Proceedings of the Second International IAHR Symposium on Stochastic Hydraulics. Lund, Sweden: International Association of Hydraulics Research, 1976.

Hoaglin, David C. "Direct Approximations for Chi-Squared Percentage Points." Journal of the American Statistical Association, 72, No. 35 (September, 1977), 508-515.

Hutt, Peter Barton. "Legal Considerations in Risk Assessment Under Federal Regulatory Statutes." Assessment and Management of Chemical Risks. Washington, D. C.: American Chemical Society, 1984, pp. 83-85.

Kadi, Aly I. and Wilfried Brutsaert. "Applicability of Effective Parameters for Unsteady Flow in Nonuniform Aquifers." Water Resources Research, 21, No. 2 (February, 1985), 183-198.

Lee, G. Fred, R. Anne Jones and Brooks W. Newbry. "Alternative Approach to Assessing Water Quality Impact of Wastewater Effluents." Journal WPCF, 54, No. 2 (February, 1982), 165-174.

Lewis, Barney D. and Flora J. Goldstein. "Evaluation of a Predictive Groundwater Solute-Transport Model at the Idaho National Engineering Laboratory, Idaho." Report No. USGS/WRI-82-25, March, 1982.

Linsley, Ray K., Jr., Max A. Kohler and Joseph L. H. Paulhus. Hydrology for Engineers. 3rd Edition. New York: McGraw-Hill Company, Inc., 1982.

Mantoglou, Aristotelis and John L. Wilson. "Simulation of Random Fields with the Turning Bands Methods." Report 264. Ralph M. Parsons Laboratory, Department of Civil Engineering, Massachusetts Institute of Technology, Cambridge, Massachusetts, July, 1981.

Mantoglou, Aristotelis and John L. Wilson. "The Turning Bands Method for Simulation of Random Fields Using Line Generation by a Spectral Method." Water Resources Research, 18, No. 5 (October, 1982), 1379-1394.

McMillan, W. D. "Theoretical Analysis of Groundwater Basin Operations." Water Resource Center Contribution No. 114. University of California, Berkeley, 1966.

Nelson, Norton. "Use of Toxicity Test Data in the Estimation of Risks to Human Health." Assessment and Management of Chemical Risks. Washington, D. C.: America Chemical Society, 1984, pp. 13-22.

Office of Technology Assessment, Congress of the United States. "Protecting the Nation's Groundwater from Contamination." Vol. II. Washington, D. C.: Author, 1984, Appendix A, pp. 243-247.

Prickett, T. A. and C. G. Longquist. "Selected Digital Computer Techniques for Groundwater Resource Evaluation." Bulletin 55. Illinois State Water Survey, Urbana, Illinois, 1971.

Prickett, T. A., Thomas G. Naymik and Carl G. Longquist. "A 'Random-Walk' Solute Transport Model for Selected Groundwater Quality Evaluations." Bulletin 65. Illinois State Water Survey, Champaign, Illinois, 1981.

Robertson, J. B. "Digital Modeling of Radioactive and Chemical Waste Transport in the Snake River Plain Aquifer at the National Reactor Testing Station, Idaho." USGS Open-File Report IDO-22054. May, 1974, 41 pages.

Rodericks, Joseph V. and Robert G. Tardiff. "Conceptual Basis for Risk Assessment." Assessment and Management of Chemical Risks. Washington, D. C.: American Chemical Society, 1984, pp. 3-12.

SAS Institute, Inc. "SAS User's Guide: Basics, 1982 Edition." Alice Allen Ray, Editor. Cary, North Carolina: SAS Institute, Inc., 1982a.

SAS Institute, Inc. "SAS User's Guide: Statistics, 1982 Edition." Alice Allen Ray, Editor. Cary, North Carolina: SAS Institute, Inc., 1982b.

Smith, Leslie and R. Allan Freeze. "Stochastic Analysis of Steady State Groundwater Flow in a Bounded Domain, 1, One-Dimensional Simulations." Water Resources Research, 15, No. 3 (1979a), 521-528.

Smith, Leslie and R. Allan Freeze. "Stochastic Analysis of Steady State Groundwater Flow in a Bounded Domain, 2, One-Dimensional Simulations." Water Resources Research, 15, No. 6 (1979b), 1543-1559.

Smith, Leslie and Franklin W. Schwarz. "Mass Transport, 1, A Stochastic Analysis of Macroscopic Dispersion." Water Resources Research, 16, No. 2 (1980), 303-313.

Smith, Leslie and Franklin W. Schwarz. "Mass Transport, 2, Analysis of Uncertainty in Prediction." Water Resources Research, 17, No. 2 (1981a), 351-369.

Smith, Leslie and Franklin W. Schwarz. "Mass Transport, 3, Role of Hydraulic Conductivity Data in Prediction." Water Resources Research, 17, No. 5 (1981b), 1463-1479.

Tukey, John W. Exploratory Data Analysis (Limited Preliminary Edition). Reading, Massachusetts: Addison-Wesley Publishing Company, 1970.

Warren, J. E. and H. S. Price. "Flow in Hetergeneous Porous Media." Society of Petroleum Engineers Journal, 1 (1961), 153-169.

Westinghouse Idaho Nuclear Company, Inc. "Revised ICCP Effluent Data 1976 through 1983." WINCO-1004. March, 1984.

Zentner, Rene D. "Chemical Industry Perspectives on Regulatory Input Analysis." Assessment and Management of Chemical Risks. Washington, D. C.: American Chemical Society, 1984, pp. 161-173.

IX. ACKNOWLEDGEMENTS

The author gratefully expresses his thanks to the Department of Civil Engineering, the Engineering Research Institute and the Water Resources Research Institute of Iowa State University for their financial support during this research. The author also expresses his gratitude to Barney Lewis, Chief Hydrologist, and the Idaho District of the United States Geological Survey for providing data used in the model calibration process. A special statement of thanks goes to Kevin Anderson and Brenda Ihle of the Department of Statistics for their advice in the development of the correlation function for the hydraulic conductivity fields and in fitting the joint probability distribution to a mathematical relationship.

A special statement of gratitude is given to Dr. E. R. Baumann, head of the Sanitary Section, and Dr. Carl Ekberg, former Head of the Department of Civil Engineering, for establishing an atmosphere conductive to free inquiry and independent thought. Last, the author deeply appreciates the advice, patience and encouragement of Dr. T. Al Austin, his major professor, during the author's graduate studies at Iowa State.

The author also recognizes his sons, Daniel and Mark, for their smiling faces and unconditional support at the beginning and end of each workday. Finally, this work is dedicated to Joyce Wolka, wife, mother, typist and co-participant throughout.

X. APPENDIX: PREDICTED JOINT CUMULATIVE EXCEEDANCE PROBABILITIES

Table X-1. Observed, predicted and residual joint cumulative exceedance probability values

Tritium Concentration (pCi/ml)	Observed Probability	Predicted Probability	Residual[a]
Duration of Exposure = 0 days			
0	0.996	0.943	0.053
50	0.925	0.900	0.025
100	0.780	0.832	-0.052
150	0.682	0.731	-0.049
200	0.588	0.598	-0.010
250	0.490	0.450	0.040
300	0.409	0.310	0.099
350	0.326	0.198	0.128
400	0.256	0.119	0.137
450	0.189	0.069	0.120
500	0.130	0.039	0.091
550	0.075	0.022	0.053
600	0.027	0.012	0.015
650	0.007	0.007	0.000
Duration of Exposure = 60 days			
0	0.974	0.900	0.074
50	0.913	0.832	0.081
100	0.760	0.731	0.029
150	0.662	0.599	0.063
200	0.568	0.450	0.118
250	0.470	0.310	0.160
300	0.389	0.198	0.191
350	0.306	0.119	0.187
400	0.237	0.069	0.168
450	0.170	0.039	0.131
500	0.113	0.022	0.091
550	0.061	0.012	0.049
600	0.019	0.007	0.012
650	0.005	0.004	0.001

[a]Rounded off to nearest .001.

Table X-1 (continued)

Duration of Exposure = 120 days		Observed Probability	Predicted Probability	Residual[a]
Tritium Concentration (pCi/ml)	0	0.848	0.832	0.016
	50	0.788	0.731	0.057
	100	0.637	0.599	0.038
	150	0.541	0.450	0.091
	200	0.447	0.310	0.137
	250	0.361	0.198	0.163
	300	0.280	0.119	0.161
	350	0.209	0.069	0.140
	400	0.150	0.039	0.111
	450	0.097	0.022	0.075
	500	0.055	0.012	0.043
	550	0.024	0.007	0.017
	600	0.007	0.004	0.003
	650	0.000	0.002	-0.002
Duration of Exposure = 180 days				
Tritium Concentration (pCi/ml)	0	0.661	0.731	-0.070
	50	0.601	0.599	0.002
	100	0.451	0.450	0.001
	150	0.356	0.310	0.046
	200	0.271	0.198	0.073
	250	0.200	0.119	0.081
	300	0.139	0.069	0.070
	350	0.089	0.039	0.050
	400	0.053	0.022	0.031
	450	0.027	0.012	0.015
	500	0.015	0.007	0.008
	550	0.006	0.004	0.002
	600	0.001	0.002	-0.001
	650	0.000	0.001	-0.001

Table X-1 (continued)

Duration of Exposure = 240 days		Observed Probability	Predicted Probability	Residual[a]
Tritium Concentration (pCi/ml)	0	0.486	0.599	-0.113
	50	0.427	0.450	-0.023
	100	0.279	0.310	-0.031
	150	0.192	0.198	-0.006
	200	0.127	0.119	0.008
	250	0.077	0.069	0.008
	300	0.041	0.039	0.002
	350	0.021	0.022	-0.001
	400	0.012	0.012	0.000
	450	0.005	0.007	-0.002
	500	0.000	0.004	-0.004
	550	0.000	0.002	-0.002
	600	0.000	0.001	-0.001
	650	0.000	0.001	-0.001
Duration of Exposure = 300 days				
Tritium Concentration (pCi/ml)	0	0.376	0.450	-0.074
	50	0.268	0.310	-0.042
	100	0.175	0.198	-0.023
	150	0.101	0.119	-0.018
	200	0.046	0.069	-0.023
	250	0.021	0.039	-0.018
	300	0.008	0.022	-0.014
	350	0.001	0.012	-0.011
	400	0.000	0.007	-0.007
	450	0.000	0.004	-0.004
	500	0.000	0.002	-0.002
	550	0.000	0.001	-0.001
	600	0.000	0.001	-0.001
	650	0.000	0.000	0.000

Table X-1 (continued)

Duration of Exposure = 360 days		Observed Probability	Predicted Probability	Residual[a]
Tritium Concentration (pCi/ml)	0	0.245	0.310	-0.065
	50	0.140	0.198	-0.058
	100	0.063	0.119	-0.056
	150	0.013	0.069	-0.056
	200	0.003	0.039	-0.036
	250	0.001	0.022	-0.021
	300	0.000	0.012	-0.012
	350	0.000	0.007	-0.007
	400	0.000	0.004	-0.004
	450	0.000	0.002	-0.002
	500	0.000	0.001	-0.001
	550	0.000	0.001	-0.001
	600	0.000	0.000	0.000
	650	0.000	0.000	0.000
Duration of Exposure = 420 days				
Tritium Concentration (pCi/ml)	0	0.162	0.198	-0.036
	50	0.065	0.119	-0.054
	100	0.009	0.069	-0.060
	150	0.001	0.039	-0.038
	200	0.000	0.022	-0.022
	250	0.000	0.012	-0.012
	300	0.000	0.007	-0.007
	350	0.000	0.004	-0.004
	400	0.000	0.002	-0.002
	450	0.000	0.001	-0.001
	500	0.000	0.001	-0.001
	550	0.000	0.000	0.000
	600	0.000	0.000	0.000
	650	0.000	0.000	0.000

Table X-1 (continued)

Duration of Exposure = 480 days		Observed Probability	Predicted Probability	Residual[a]
Tritium Concentration (pCi/ml)	0	0.138	0.119	0.019
	50	0.043	0.069	-0.026
	100	0.006	0.039	-0.033
	150	0.001	0.022	-0.020
	200	0.000	0.012	-0.012
	250	0.000	0.007	-0.007
	300	0.000	0.004	-0.004
	350	0.000	0.002	-0.002
	400	0.000	0.001	-0.001
	450	0.000	0.001	-0.001
	500	0.000	0.000	0.000
	550	0.000	0.000	0.000
	600	0.000	0.000	0.000
	650	0.000	0.000	0.000
Duration of Exposure = 540 days				
Tritium Concentration (pCi/ml)	0	0.119	0.069	0.050
	50	0.033	0.039	-0.006
	100	0.002	0.021	-0.019
	150	0.000	0.012	-0.012
	200	0.000	0.007	-0.007
	250	0.000	0.004	-0.004
	300	0.000	0.002	-0.002
	350	0.000	0.001	-0.001
	400	0.000	0.001	-0.001
	450	0.000	0.000	0.000
	500	0.000	0.000	0.000
	550	0.000	0.000	0.000
	600	0.000	0.000	0.000
	650	0.000	0.000	0.000

Table X-1 (continued)

Duration of Exposure = 600 days		Observed Probability	Predicted Probability	Residual[a]
Tritium Concentration (pCi/ml)	0	0.087	0.039	0.049
	50	0.010	0.022	-0.012
	100	0.000	0.012	-0.012
	150	0.000	0.007	-0.007
	200	0.000	0.004	-0.004
	250	0.000	0.002	-0.002
	300	0.000	0.001	-0.001
	350	0.000	0.001	-0.001
	400	0.000	0.000	0.000
	450	0.000	0.000	0.000
	500	0.000	0.000	0.000
	550	0.000	0.000	0.000
	600	0.000	0.000	0.000
	650	0.000	0.000	0.000
Duration of Exposure = 660 days				
Tritium Concentration (pCi/ml)	0	0.050	0.022	0.028
	50	0.001	0.012	-0.011
	100	0.000	0.007	-0.007
	150	0.000	0.004	-0.004
	200	0.000	0.002	-0.002
	250	0.000	0.001	-0.001
	300	0.000	0.001	-0.001
	350	0.000	0.000	0.000
	400	0.000	0.000	0.000
	450	0.000	0.000	0.000
	500	0.000	0.000	0.000
	550	0.000	0.000	0.000
	600	0.000	0.000	0.000
	650	0.000	0.000	0.000

Table X-1 (continued)

Duration of Exposure = 720 days		Observed Probability	Predicted Probability	Residual[a]
Tritium Concentration (pCi/ml)	0	0.027	0.012	0.015
	50	0.000	0.007	-0.007
	100	0.000	0.004	-0.004
	150	0.000	0.002	-0.002
	200	0.000	0.001	-0.001
	250	0.000	0.001	-0.001
	300	0.000	0.000	0.000
	350	0.000	0.000	0.000
	400	0.000	0.000	0.000
	450	0.000	0.000	0.000
	500	0.000	0.000	0.000
	550	0.000	0.000	0.000
	600	0.000	0.000	0.000
	650	0.000	0.000	0.000
Duration of Exposure = 780 days				
Tritium Concentration (pCi/ml)	0	0.019	0.007	0.012
	50	0.000	0.004	-0.004
	100	0.000	0.002	-0.002
	150	0.000	0.001	-0.001
	200	0.000	0.001	-0.001
	250	0.000	0.000	0.000
	300	0.000	0.000	0.000
	350	0.000	0.000	0.000
	400	0.000	0.000	0.000
	450	0.000	0.000	0.000
	500	0.000	0.000	0.000
	550	0.000	0.000	0.000
	600	0.000	0.000	0.000
	650	0.000	0.000	0.000

Table X-1 (continued)

Duration of Exposure = 840 days		Observed Probability	Predicted Probability	Residual[a]
Tritium Concentration (pCi/ml)	0	0.014	0.004	0.010
	50	0.000	0.002	-0.002
	100	0.000	0.001	-0.001
	150	0.000	0.001	-0.001
	200	0.000	0.000	0.000
	250	0.000	0.000	0.000
	300	0.000	0.000	0.000
	350	0.000	0.000	0.000
	400	0.000	0.000	0.000
	450	0.000	0.000	0.000
	500	0.000	0.000	0.000
	550	0.000	0.000	0.000
	600	0.000	0.000	0.000
	650	0.000	0.000	0.000
Duration of Exposure = 900 days				
Tritium Concentration (pCi/ml)	0	0.007	0.002	0.005
	50	0.000	0.001	-0.001
	100	0.000	0.001	-0.001
	150	0.000	0.000	0.000
	200	0.000	0.000	0.000
	250	0.000	0.000	0.000
	300	0.000	0.000	0.000
	350	0.000	0.000	0.000
	400	0.000	0.000	0.000
	450	0.000	0.000	0.000
	500	0.000	0.000	0.000
	550	0.000	0.000	0.000
	600	0.000	0.000	0.000
	650	0.000	0.000	0.000